



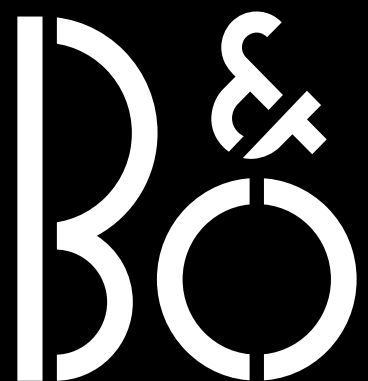
High quality laser cutting in aluminium

Master Thesis

By:
Jacob Erik Stadel Petersen
&
Henrik Dahl Jensen

In collaboration with

BANG & OLUFSEN



Synopsis:

Title: High quality laser cutting in aluminium

Theme: Master's Thesis

Project period:

1. February 2012 - 13. June 2012

Project group: 13-82 - 4. semester
Manufacturing Technology

Group members:

Henrik Dahl Jensen

Jacob Erik Stadel Petersen

Supervisors:

Morten Kristiansen
Ewa Kolakowska

Number of copies: 6

Report: 97 pages

Appendix: 13 pages

Handled in: 13. June 2012

This master thesis is based on a collaboration with the danish manufacturer of high-end audio and video products; B&O. Through this thesis it is investigated if an existing drilling process, at B&O can be replaced with a laser cutting process. A speaker grill with holes of 1.8mm in diameter and a thickness of 2.0mm is used as case. From the case a definition of high quality holes is made, which includes the quality parametes: dross, melting of top edge, heat affected zone (in this thesis defined as change in color in the workpiece), kerf width, kerf taper, and hole roundness.

From laser cutting experiments with an 380W Nd:YAG laser it is found, that the intensity of the beam spot diameter is desicive in order to cut in aluminium. A 400 W single mode fiber laser is used to conduct 36 laser cutting experiments in 0.5, 0.7 and 1.0mm thick aluminium sheets. It is concluded, that it is possible to satisfy the defined quality parameters from the case, when using a sheet thickness of 0.7mm.

The effects from the control variables; focal point and cutting speed are concluded to have a significant influence on the kerf width and kerf taper. Indications of influence on the experiments from sheet thickness and stand-off distance is observed but not analyzed. The effects from the control variables, on dross and melting of top edge is incunclusive. The heat affected zone do not ouccur in any of the experiments.

It is concluded, that the single mode fiber laser have a great potential in relation to high quality laser cutting at B&O. Despite of this, the results of the experiments cannot be applied directly on the B&O case. That is because the results are affected by noise and too few sheet thickness' are used to be able to predict the results in 2mm thick aluminium sheets. In order to anwser this, more experiments must be conducted.

Based on conclusions and know how obtained in this thesis and during the project period recomendations to B&O, regarding what to be aware in relation to the quality of the workpieces when using a laser cutting process, are presented.

sponsible for the content as well as keeping any confidential information secret. The report may not be passed on without permission from the group.

Foreword

This report is a Master Thesis done on the Master Programme of Manufacturing Technology at Aalborg University, at the Department of Mechanical and Manufacturing Engineering in the period from 1. February til 13. June 2012.

The main experiments described in this thesis were performed at IPU on the 10th of May.

There are 14 chapters and 3 appendixes. For chapters, where it is relevant, an introduction in italic text describes the purpose of the chapters. Tables, formulas, figures (graphs, pictures and diagrams) are given a number in relation to their respective chapters. An appendix-DVD is found in the back of the report with the project and supplementary information on it.

References are made using the Chicago-method, where the text is shown either as (author, year) or (author, year)[side]. If a reference is used for a whole chapter, it is written in the introduction of the respective chapter or section. If there is no reference in the introduction the reference in the text apply to the specific part or line. In the bibliography the references are given as: Author, Year, *Titel*. URL / ISBN. When referring to a file on the appendix-DVD the following method is used: "chapter/folder/file". When referring to a folder: "chapter/folder"

The report contains a list of nomenclature in chapter ??.

The group would like to thank the following people for their help during the project: Klaus Schütt Hansen (IPU) for assistance with experiments and Mekoprint A/S for the specially made front- and backpages.

Table of contents

Foreword	v
Table of contents	vii
1 Introduction	1
1.1 Industrial laser cutting applications	2
2 B&O and laser cutting	5
2.1 Manufacturing processes at B&O	8
3 Laser cutting processing	13
3.1 Control variables	14
3.2 Equipment parameters	15
3.3 Workpiece parameters	18
3.4 Quality parameters	19
3.5 Summary	26
4 Case study	29
4.1 Definition of high quality holes	29
4.2 Requirement specification	34
5 Problem formulation	35
5.1 Cutting quality	35
6 Approach to solution	37
6.1 Analytical approach	37
6.2 Empirical knowledge	38
6.3 Solution method in this thesis	39
7 Laser setup	41
7.1 Laser machine	41
7.2 Cutting head	43
7.3 Beam quality values	44
7.4 Laser beam caustic	47
7.5 Summary	52
8 Experiments with AAU setup	55
8.1 Operating power at workpiece	55
8.2 Cutting in aluminium sheets	56
8.3 Conclusion	59

9 Experiment description	61
9.1 Cutting quality experiments	61
9.2 Assumptions	66
10 Cutting quality experiments - Results	69
10.1 Dross	70
10.2 Melting of top edge	73
10.3 Heat affected zone	75
10.4 Kerf width	76
10.5 Kerf taper	87
10.6 Overview	89
10.7 Summary	90
11 High quality laser cutting at B&O	91
11.1 Quality parameters	91
11.2 Assist gas pressure and stand-off distance	93
11.3 Manufacturing considerations	93
12 Conclusion	95
13 Discussion	97
14 Nomenclature & Abbreviations	99
Bibliography	101
I Appendix	105
Appendix A Vision Builder Measurements	107
A.1 Dross and MTE	107
A.2 Kerf width	109
A.3 Holes and beam spot diameter	111
Appendix B Laser cut sheets	113
B.1 Aluminium sheets used in section 9.1	113
Appendix C Analysis of variance	115
C.1 Residual analysis	117
Dansk resumé	121

This thesis deals with the manufacturing process - laser cutting. Laser cutting is a thermal cutting process where it is made use of the physical fact that laser light is absorbed in materials. The process is used for many materials (primarily metals) in the manufacturing industry. A laser cutting setup could be like this, when not considering safety and control systems; A laser machine, an optical fiber, Cutting gas, a cutting head and an xy-table, see figure 1.1. In such a setup the laser machine is generating a laser beam which is transferred to the cutting head via an optical fiber. The cutting head is designed so that the laser beam becomes focused at one spot on a workpiece. In this spot the laser light contains so much energy, that the material melts or evaporates. From the cutting head also a jet of gas is lead out. The gas is used to either push out the material from the cut zone (inactive gas) or also to add more energy to the cut zone while pushing the molten material out (active gas). In traditional laser cutting the workpiece is very close, $2\pm 0.5\text{mm}$, to the cutting head (Narendra B. Dahotre, 2008). Further explanation of the laser cutting process will be given in chapter 3.

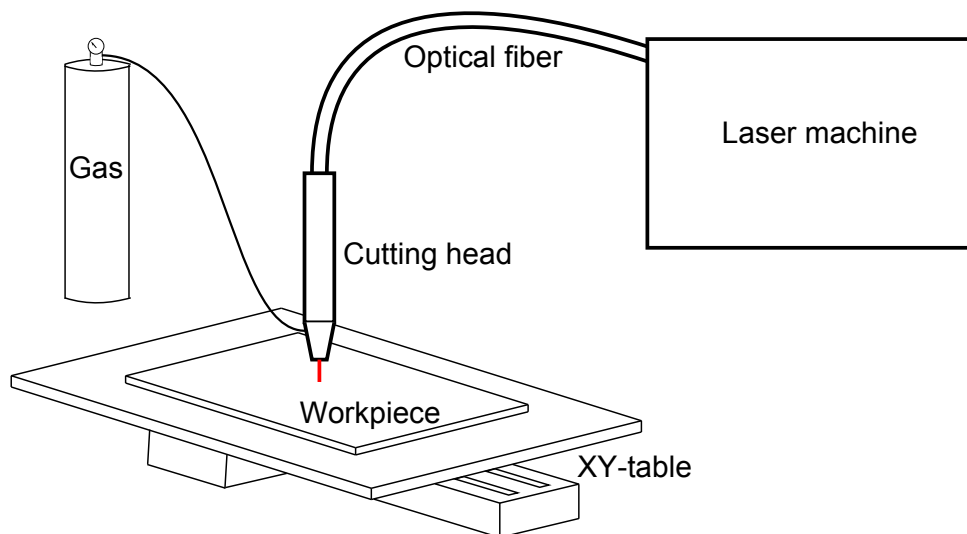


Figure 1.1: Example of a laser cutting setup consisting of a laser machine, optical fiber, cutting head, gas, workpiece and an xy-table.

The first laser was invented in 1960. It was an optical pumped laser using a ruby crystal as gain medium. Since then the technology have been in constant development. In 1967 laser cutting was demonstrated for the first time. This was done using a focused CO_2 laser and an assist gas jet. (Wandera, 2010) It wasn't until 1978 that the first flatbed laser cutting machine was introduced for commercial use. This machine was actually a punch/laser cutting machine, where the cutting head was a stationary unit and the workpiece could be moved in the x-y directions using numerical controls. The year after (1979) Trumpf (German laser machine manufacturer) introduced a 500-700 W CO_2 laser cutting machine (Trumpf, 2012).

Through the years the power and the beam quality of laser cutting machines have increased continuously where the CO₂ lasers have dominated the market with recently (2011) a market share of 67 % of all industrial lasers, used for metal processing (Belforte, 2012).

In 2005 IPG Photonics introduced the worlds first high-power (>1kW) fiber laser. The fiber laser is capable of having nearly the best beam quality achievable compared to what in theory should be possible (Paschotta, 2012). For instance can the single-mode fiber lasers be be focused ten times better than CO₂ lasers (Olsen, 2010). The power output range for fiber lasers are capable of reaching up to 50kW (Photonics, 2012a) which allows cutting speeds and penetration depth never before achieved and expands the application of laser processing (Shiner, 2012).

The increasing laser beam quality and laser power is of high interest for the manufacturing industry, since these factors are highly influencing the obtainable quality of the workpiece and allowable material thickness. On figure 1.2 a comparison of some of the most popular industrial high-power lasers can be seen. It can be seen how the fiber laser is superior to the other lases used for industrial purposes for all the shown process considerations.

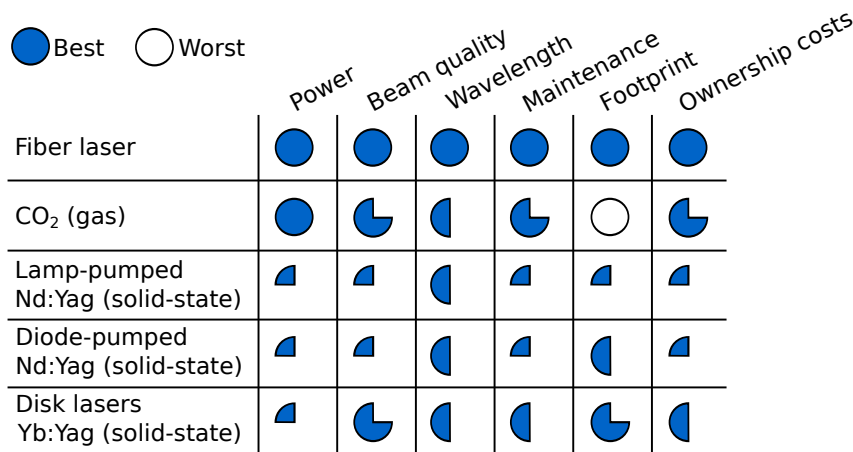


Figure 1.2: Comparison of some of the most popular industrial high-power laser types with respect to process considerations (Shiner, 2012).

In the near future lasers are expected to be capable of cutting from a further distance to a workpiece than it has previously been possible, called Remote Laser Cutting (RLC). This is made possible due to the introduction of single-mode fiber laser with the necessary power and laser beam quality (A. Pihlava, 2011). The RLC technology is currently being developed at the Fraunhofer Institute IWS Dresden. The technology is still limited to cutting in thin sheets (less than one mm steel). Also in Denmark a project is running on creating RLC. The project, called ROBOCUT, started in 2010 and will be running until 2015 where it is expected that demonstrations of RLC with the ROBOCUT technology will be finished. (Olsen, 2010)

1.1 Industrial laser cutting applications

In the industry the users of the laser cutting process stretches far, from big companies down to small shops creating products where the company can utilize the advantages of the laser cutting process. It could be companies that specializes in the laser cutting process but also companies that uses the process as a means of being able to create products without being specialists in the laser cutting process.

Laser cutting in metal is today the most used laser processing process in the industry with over 40% of the laser processing market shares (Caristan, 2004). The process is used for processing various products/parts in various industry areas, see table 1.1 for a brief example of application areas.

Area	Product example wherein laser cutting is used
Aerospace	Turbine blades
Automobile	Doors
Multimedia	TV
Medical	Implants
Etc.	-

Table 1.1: Examples of areas where laser cutting is used along with examples of products made with laser cutting.

The market for laser cutting is still increasing as it have been for many years as laser cutting machines have become better and better and new applications where laser cutting can be used are found. This can also be seen from figure 1.3. High power fiber lasers were introduced on the commercial market in 2005 (Olsen, 2010).

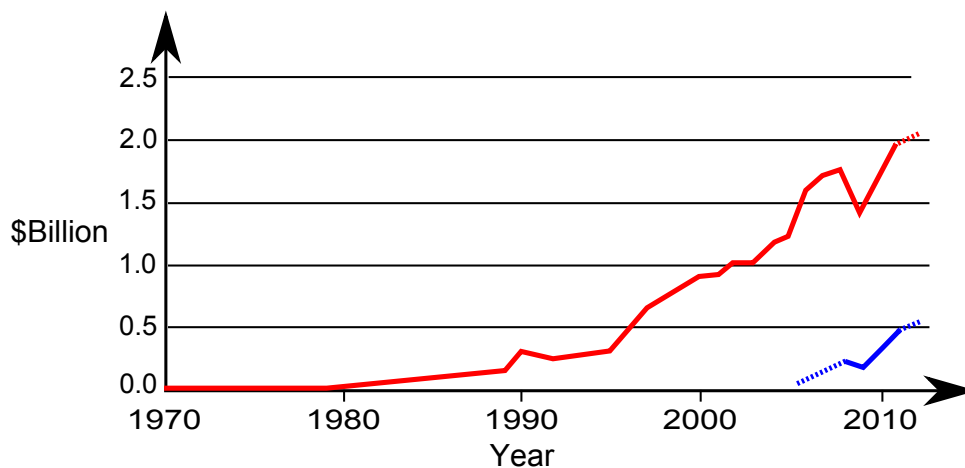


Figure 1.3: Industrial laser revenue 1970-2011 (Belforte, 2012). Red is total, blue is fiber lasers. The stippled lines indicates estimations.

In relation to the increase in the use of laser cutting in the manufacturing industry and the increase in the beam quality of the laser cutting process, Bang & Olufsen A/S has shown an interest in laser cutting, which will be elaborated further in the following chapter.

B&O and laser cutting 2

In this chapter an introduction to B&O and their products, their vision and how they differentiate their products, from other products in the same category, is presented. An example of a product and how it is manufactured is presented in order to investigate if there is advantages/disadvantages in using laser cutting instead of a currently used process.

Bang & Olufsen A/S is a company known around the world for their design and high-end multimedia products. The company was established in 1925 in Struer, Denmark. Today (2012) they have production in Struer and in Kopřivnice, Czech Republic. B&O employ more than 2.000 employees and had a revenue on 2787 million DKK in the financial year of 2010/2011 (a/s, 2011a).

B&O sell their products from approximately 1000 (>50% in Europe) local stores all around the world that are dedicated to selling B&O products (a/s, 2011b). According to (K. T. Mortensen, 2009) B&O's customers are mainly those who has a good job position and a high income. The age of the customers are 25-54 years and they appreciate design, quality and the functionality of the B&O products. B&O's competences are: picture, sound, design, system integration, moving mechanics, user interaction, finish of materials and quality.

On figure 2.1 two of B&O's products are seen. A list of their current (2012) product series includes:

- Video: Five TV series in plasma/LCD in the range of 32-103 inches.
- Automotive: Speaker/sound systems for four car brands (BMW, Audi, Aston Martin and Mercedes-AMG).
- Audio: Sound systems/home integration.
- Loudspeakers: 16 different series (floor standing, sub-woofers, built-in and compact).
- Spare parts, accessories etc.
- Phones.



(a) B&O sound system, BeoSound 5. (a/s, 2012)



(b) B&O speaker grill for the BMW 6 series. (a/s, 2012)

Figure 2.1: Examples of B&O audio and video products.

B&O vision

A vision for a company can be said to be its state of mind. It withholds the company's values, purpose and goals (James C. Collins, 1996). The vision for B&O have been formulated in the statement: *Courage to constantly question the ordinary in search of surprising, long-lasting experiences.*

Their vision is expressed through four values:

- Excellence
- Synthesis
- Originality
- Passion

The B&O vision demands a high level of innovation since the market constantly changes. This applies both to their products and their production. The four values helps them to maintain and develop competences that sets the direction of innovation in relation to their vision (a/s, 2011a).

2.0.1 Differentiation from competitors

Compared to the mainstream multimedia market B&O generally stands out in relation to product quality, both their technical ability and their design etc. Their description of quality is:

"Bang & Olufsen products are designed to be not only aesthetically pleasing but also essentially functional and easy to use. The expectations raised by a strikingly individual appearance must be completely fulfilled in terms of high quality performance in all areas when the system is switched on. Therefore, our excellence in providing the consumer with the highest pleasure in both ownership and use rests on "high quality" as the common denominator of all activities and competence areas."(a/s, 2012)

To give an overview of how B&O differentiates from the majority of multimedia companies, different dimensions of quality is described. According to (Montgomery, 2005b) there are eight dimensions of the term quality:

- Performance - Will the product do the intended job?

-
- Reliability - How often does the product fail?
 - Durability - How long does the product last?
 - Serviceability - How easy is it to repair the product?
 - Aesthetics - What does the product look like?
 - Features - What does the product do?
 - Perceived Quality - What is the reputation of the company or its products?
 - Conformance to standards - Is the product made exactly as the designer intended?

In order for B&O to consider laser cutting as a process in their portfolio of processing techniques, laser cutting must not compromise these quality dimensions in their products.

2.0.2 Aluminium

In the 1960's B&O began to use aluminium in their audio receivers and it has been their most used metal since. Since the 1990's they have also used it for loudspeaker cabinets and from the 2000's as speaker grills in cars. Examples of the use of aluminium can be seen on figure 2.1b.

Aluminium has been important for many years for B&O and they now have developed skills with aluminium surface treatment to the point where they are unparalleled in the industry. This is one of the reasons why they have been able to differentiate themselves from their competitors. Technologies they master (or have developed) in relation to working with aluminium is among others: Alucoat on casts, aludisplays, protective coating in anodizing, electrochemical machining, selective grinding, black laser marking etc.

Design aspects in using aluminium

The design aspects consists of the atmosphere the material entails. Credibility and authentic appearance is some of the most important features of the material and therefore the products. When a user interacts with the material, it must feel right (as is looks) and give the user a convincing experience. Beautiful surface finish, in many different colors, can be obtained through anodizing and/or polishing processes.

Technical advantages using aluminium

The technical advantages is among others: Light weight (with a relative high stiffness), able to be anodized in many different colors giving a hard and durable surface, easy to process/form, causes no distortion of sound since it is a "dead" material, recyclable etc.

The mechanical properties of aluminium is relevant, for example for an automotive speaker grill which is often mounted in the side of a car door. In a car, the speaker grill may very well be exposed to a foot banging on it or something lying against it. It must therefore be resistant to impact and getting scratches.

2.1 Manufacturing processes at B&O

As an example, of which processes a product goes through in the production at B&O in Struer, Denmark, a speaker grill in aluminium is used, see figure 2.2. Since this product is not yet introduced on the market, not all information about it is known. This example will primarily introduce the concept of producing speaker grills.



Figure 2.2: Speaker grill for an unknown car. The level of completion is up until the shaping process according to figure 2.3. The width of the grill is approx. 40cm.

The sequence in which the speaker grill is processed can be seen on figure 2.3 and is described through eight processes:

- Stamping/mechanical cutting: First aluminium sheets delivered from B&O's supplier are stamped/cut into smaller sheets to make handling of the sheets easier and to make the sheets fit into the next machines that they must go through.
- Welding of mounting poles: On the stamped/cut sheets 13 mounting poles on the backside of the grill is welded on.
- Circumference processing: Afterwards the circumference is milled to a round and smooth edge which is curved.
- Hole drilling: When the edge is processed several hundred holes are drilled in the grill (in some of the other speakers grills that B&O produce the holes are stamped out).
- Shaping: In the shaping process the speaker grill is formed making it double curved.
- Anodizing: When all the mechanical processing is done, the speaker grill goes through the electro-chemical process, anodizing, which creates a hard surface, protecting the speaker grill from scratches etc., and colours it.
- Laser engraving: A laser engraving machine engraves the company logo in the surface of the speaker grill.
- Packaging: Lastly the speaker grill is packed and sent off to the buyer.

On figure 2.3 the process of interest further in this thesis is marked with a red square.

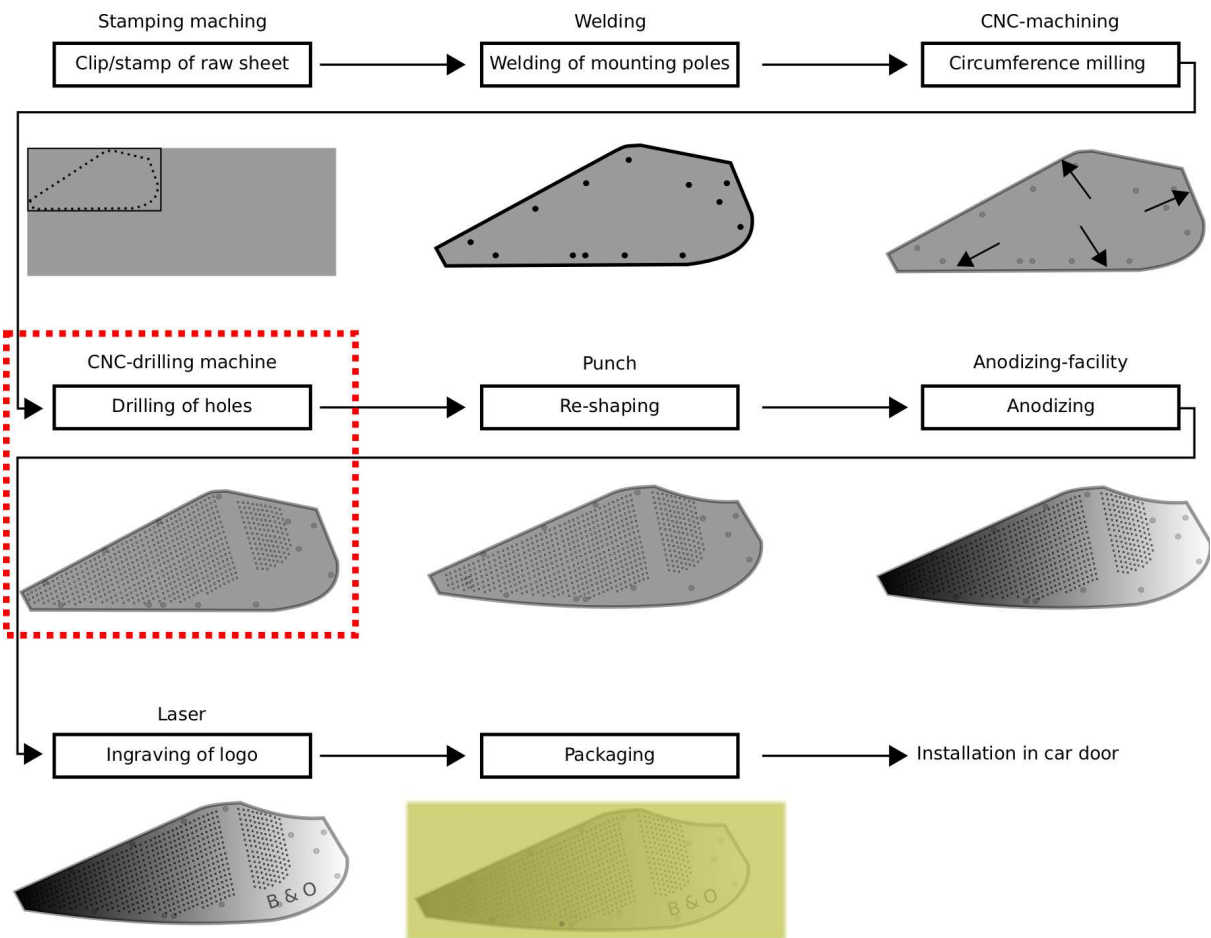


Figure 2.3: Manufacturing processes at B&O for a car speaker grill. The area marked in red is the process of interest in this thesis. The black boxes refer to the process, the text above the used machine.

2.1.1 Hole processing

The processes used at B&O, for making holes in different speaker grills, is drilling and stamping. It is a very important process for the performance and aesthetics quality of the speaker grills. This is since the performance of the loudspeaker depends on the number and form of the holes (has to do with how much air the speaker can "breathe") and the aesthetics appearance depends on the design of the pattern of the holes.

On figure 2.4 a speaker grill for an Audi is seen. Compared to the grill on figure 2.2 it has a lot more holes. This grill is made with a stamping tool, which stamp out the holes in three steps.

The reason why some of the holes are made through the stamping process and some through drilling depends of the lot size of the specific workpiece and the complexity of it. Only when the lot size is big enough is it cost-effective to invest in an often expensive stamping tool.

An alternative to using drilling or stamping for processing the holes in the speaker grills could be laser cutting. B&O currently doesn't use laser cutting in their manufacturing of any of their products. Mainly due to the reason that they don't have much knowledge about the process and how it will perform in relation to their products.

In order to make an assessment of whether or not laser cutting can satisfy B&O's process requirements when making holes, criterias which are important when making holes at B&O are set up. These criterias will then be used for a comparison with the currently used processes. The criterias are:

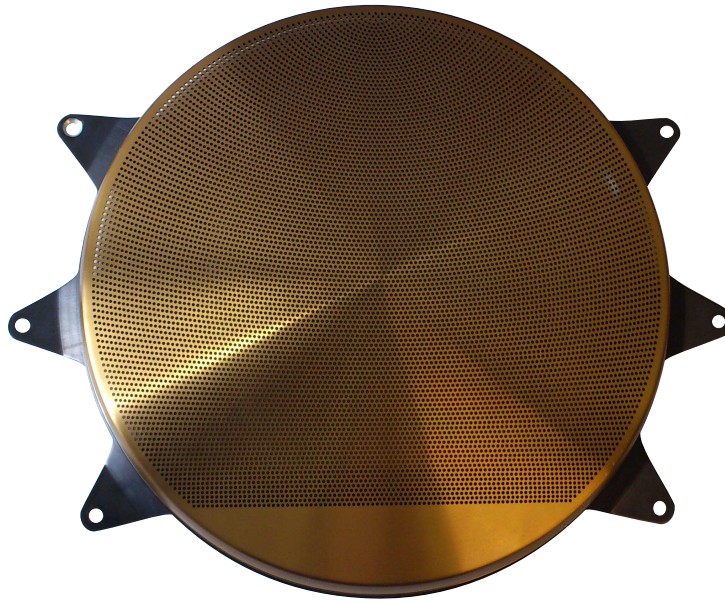


Figure 2.4: Speaker grill for a speaker to an Audi. The number of holes is above 3000. The holes in this speaker grill is stamped out in three steps. The width of the grill is approx. 25cm.

- Setup time in changeovers: The setup time between making other types of holes or workpieces with different designs.
- Repeatability: To which degree it is possible to continuously recreate the same result of the cut holes.
- Reliability: Reliability in relation to breakdowns and maintenance.
- Design sensitivity: Sensitivity to design changes after launching a production of a workpiece.
- Hole versatility: The complexity in hole design which is possible to be created with the process.
- Dimensional tolerance: The dimensional tolerance of the cut holes.
- Production rate: The rate at which holes can be cut.
- Tool wear: The amount of tool wear there is from process.
- Capital investment: The amount of money needed to buy a machine for the specific process.
- Tooling price: The price of the tools for the process.

The criterias may have different weights of importance for B&O, which is not included in the comparison, see table 2.1.

From table 2.1 it can be seen that laser cutting is superior to the drilling and stamping processes in the following criterias; setup time in changeovers, design sensitivity and hole versatility. This can be taken advantage of especially in small lot sizes and give more freedom regarding the design of the hole pattern in a workpiece. This corresponds well with the kind of production that B&O has for some of their products, such as limited edition automotive speaker grills.

There is formed a basis for further studying the laser cutting process in relation to hole processing. The

Process Criteria	Drilling	Stamping	Laser cutting
Setup time in changeovers	Medium	Very high	Very low
Repeatability	Very high	Very high	Very high
Reliability	Very high	Very high	Very high
Design sensitivity	Medium	Very high	Very low
Hole versatility	Low	High	Very high
Processing tolerances	High	Very high	High
Production rate	Low	Very high	Medium
Tool wear	Low	Low	Very low
Capital investment	Low	Medium	High
Tooling price	Low	High	Low

Table 2.1: Relative comparison of drilling, stamping and the laser cutting process for use in hole processing in aluminium at B&O. The comparison is inspired by (laser Division, 2012), (GROUP, 1998) and (Narendra B. Dahotre, 2008).

question that needs to be answered is, if the quality of the laser cut, that B&O require, can be obtained by the use of the laser cutting process. The general objective for this thesis is therefore:

To which extent can laser cutting be used for hole processing of high quality workpieces in aluminium at B&O?

Laser cutting processing 3

The purpose of this chapter is to give an overview and understanding of the laser cutting process. For this purpose a process model is introduced. The process model will relate the quality of cuts made with a laser machine with the factors that influence them.

The laser cutting process works in principle by focusing a laser beam on a workpiece that needs processing, see figure 3.1. Due to the focused laser beam the workpiece is heated up in the small area around it. This causes melting of the material. The molten material is ejected through the bottom of the workpiece due to the pressure of a cutting assist gas. The area from where the material is removed, is called the cut kerf.

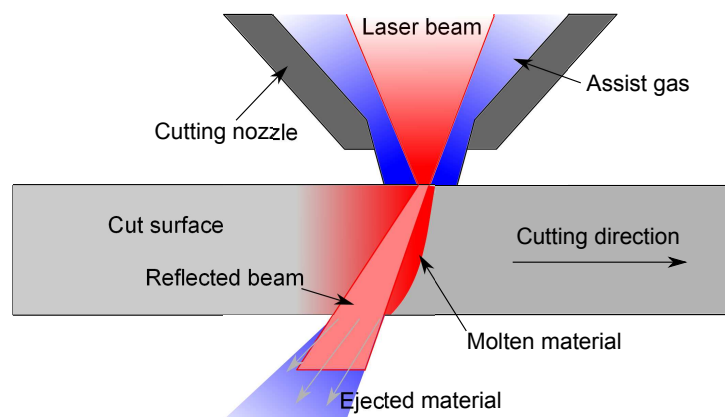


Figure 3.1: Principle of how the laser cutting process works.

The cut surface inside the cut kerf, that is created when cutting with a laser, may have different quality depending on how the laser cutting process is controlled.

A process model is set up in order to describe and analyze the relations between the parameters and variables of the process. On figure 3.2 a general model of a process is seen. It can be seen that both controllable and uncontrollable parameters have an effect on the output of the process. This also applies to the laser cutting process, where uncontrollable parameters includes specific properties of the laser cutting setup. By using the general process model it is possible to describe what affects the quality of the cut. In this thesis it is defined, that the inputs to the model, is in form of control variables, the uncontrollable parameters are equipment parameters, the controllable parameters are workpiece parameters and the output is the quality of the cut described through quality parameters.

Through this thesis the definition of the inputs, controllable/uncontrollable parameters and output for the process model is:

- **Control variables** are characterized as being the variables that are changeable in the process.

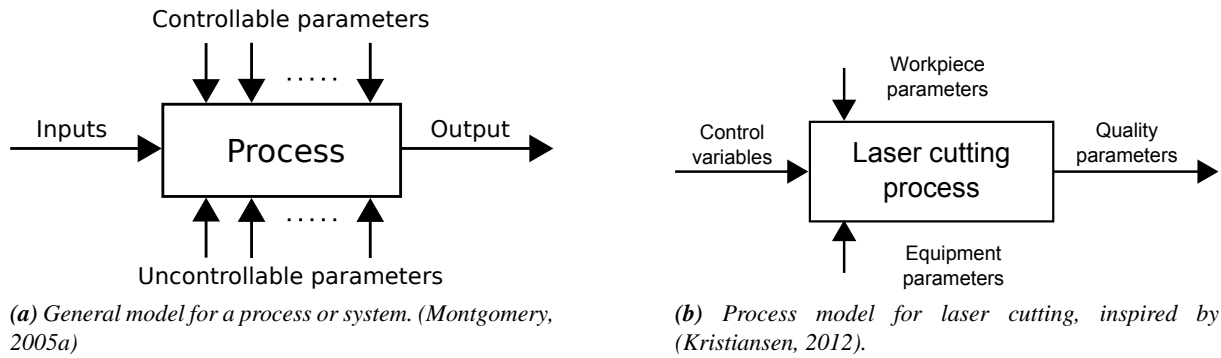


Figure 3.2: General process model and laser cutting process model.

- **Equipment parameters** are fixed according to the specific equipment used. In theory the equipment parameters are changeable because parts of the equipment that is used can be changed.
- **Workpiece parameters** are in this thesis controllable because it is possible to replace the used workpiece.
- **Quality parameters** denotes the quality to be achieved from process execution.

3.1 Control variables

The changeable variables depends on the specific laser cutting system. The control variables for the laser cutting process in this thesis are:

- Cutting speed

Is the relative speed between the workpiece and the laser beam during cutting.
- Focal point

Is the offset from a defined plane to the point along the laser beam, where it has the smallest spot diameter, see figure 3.3. In this thesis the plane which the focal point is an offset from is the bottom surface of the workpiece.
- Operating laser power

Is the power the laser operates with in the workpiece during cutting.
- Assist gas pressure

Is the pressure of the assist gas during laser cutting. The gas pressure is measured before it enters the cutting head.
- Stand-off distance

Is the distance from the tip of the cutting nozzle to the workpiece, see figure 3.4

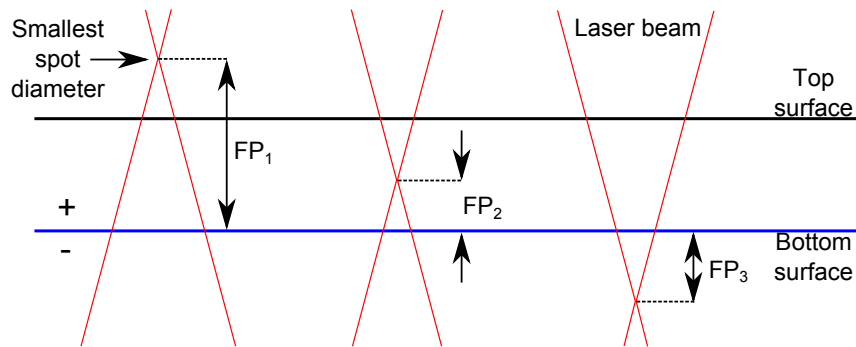


Figure 3.3: Examples of three different focal points (FP). The blue line indicates the reference plane which in this thesis is the bottom surface of the workpiece. If a FP is below the blue line it will have a negative value. If the FP is above the blue line it will have a positive value. The first and second FP on the figure therefore have positive values and the third FP a negative value.

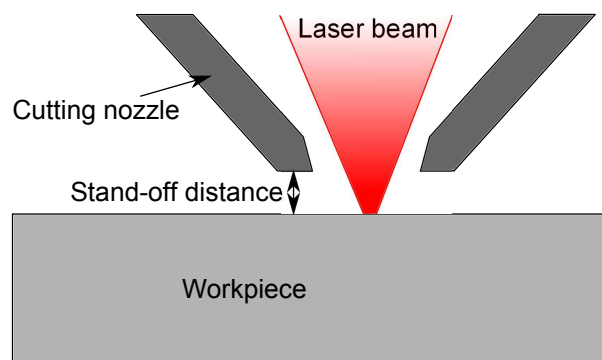


Figure 3.4: Graphical definition of stand-off distance.

3.2 Equipment parameters

The characteristics and capacity of a laser cutting system is decisive for the laser cutting process and the obtained result. In the following, equipment parameters that influence geometric and metallurgic quality of the cuts made with a laser, are presented and explained. The parameters are categorized into the following five sections:

- Laser type
- Optical system
- Maximum laser power
- Nozzle parameters
- Assist gas type

3.2.1 Laser type

In this thesis two lasers both of the type; continuous wave solid state lasers, are used.

The used lasers are a Nd:YAG laser and a single mode fiber laser. These are both solid state lasers, which means that the gain medium which is used to create the laser beam is in a solid state. There also

exist laser machine where the gain medium used to create the laser is of another form than a solid state form, for example gas. A common laser using a gas as gain medium is a CO₂ laser.

Solid state and gas lasers have different wavelengths, depending on the gain medium which the laser is based. The shorter the wavelength, the better the laser beam is absorbed by the material. This happens because the more energetic photons from the laser beam is absorbed by a greater number of bound electrons in the workpiece (William M. Steen, 2010). This entails that more of the energy in the laser beam will generate heat in the workpiece. When cutting in materials, that have a high value of reflectivity and thermal conductivity, such as aluminium, it is therefore better to use a laser with low wavelength.

The approximate wavelength of the three lasers mentioned before are as follows:

- Fiber laser: 1.06 μ m
- Nd:YAG laser: 1.06 μ m
- CO₂ laser: 10.6 μ m

It can be seen, that the fiber laser and the Nd:YAG laser both have a ten times lower wavelength compared to the CO₂ laser. Based on the wavelength, the best laser type to use, is either a fiber laser or an Nd:YAG laser, when cutting in aluminium.

As it was described in the beginning of this section this thesis only deals with continuous wave lasers. A continuous wave laser is a laser that emits a laser beam continuously. In contrast to a continuous wave laser there also exist pulsed lasers that emits a laser light in short pulses. Many different types of pulsed lasers exist. These are not described in this thesis. The main differences between the two types of lasers are that a continuous wave laser delivers a high average powered beam and a pulsed laser delivers short pulses of very high power and a low average power (Hansen, 2012).

3.2.2 Optical system

The optical system which in this thesis is defined as the collimation lens, focal lens and optical fiber, see figure 3.5 are highly important in relation to achieving a high quality cut. The role of the collimation lens is to limit the angle at which the laser light spreads out (diverges). The focal lens' role is to focus the beam, so obtains a high enough intensity in the smallest beam spot, to cut in a workpiece. The optical fiber delivers the laser light from the laser machine to the cutting head in which the collimation lens and focal lens are placed. The reason why the collimation lens, focal lens and optical fiber are so important in relation to the quality of the cut is because the ratio between them are decisive in relation to how small a beam spot diameter can be achieved, see equation 3.1, (GmbH, 2004).

$$d_{0f} = \frac{f}{f_c} \cdot d_k \quad (3.1)$$

Where f is the focal length of the focal lens which is the distance from the focal lens to where the minimum spot diameter is located, d_{0f} , see figure 3.5. f_c is the collimation length of the collimation lens which is the distance from the optical fiber to the collimation lens. d_k is the core diameter of the optical fiber.

The smaller the beam spot diameter, with a given amount of laser power, the higher the intensity of the laser light is. The intensity is important since it determines what materials, how fast and how thick workpieces can be cut with the laser. It is in this relation important to be aware that the beam cannot be made infinitely small in order to achieve a high intensity. This is because the beam diameter at some point will become so small that the molten material cannot be ejected out of the bottom of the workpiece by the assist gas. If the beam diameter is too small, there is a high risk for the molten material only to flow around the beam and re-solidify on the backside of the beam (Kristiansen, 2012).

It is in this relation important to remember that the highly reflective materials such as aluminium doesn't absorb as much energy as materials which aren't highly reflective. Therefore a higher intensity is needed for cutting two materials with the same thickness where one is aluminium and one is regular steel, presuming that it is cut with the same laser cutting system.

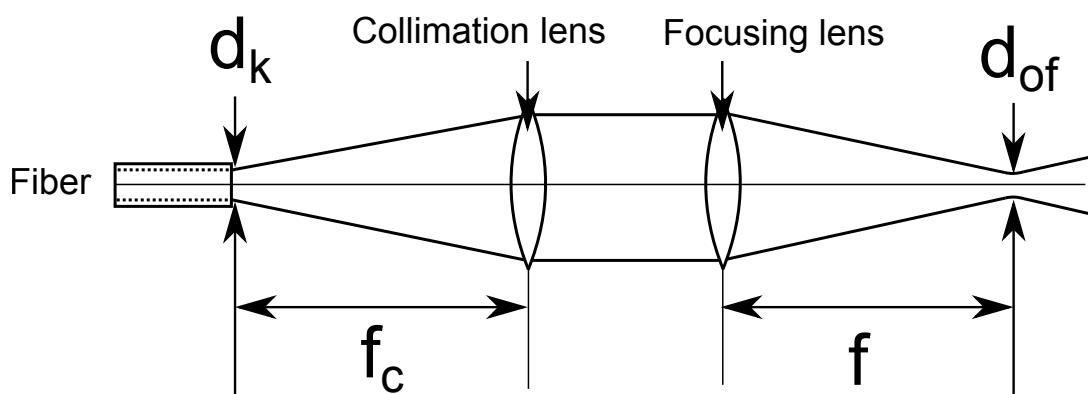


Figure 3.5: Principle of collimating and focusing a laser beam. f is the focal length, f_c is the collimation length, d_k is the core diameter of the optical fiber and d_{of} is the smallest beam spot diameter. (GmbH, 2004)

3.2.3 Maximum laser power

Because power and smallest beam spot diameter are decisive for how high an intensity that can be achieved in the smallest beam spot diameter, the maximum power is critical in relation to achieving an intensity which is high enough to cut in a specific material. In this case aluminium.

3.2.4 Nozzle parameters

Considerations with respect to nozzle parameters are important in order to obtain an effective removal of the molten material from the cutting kerf. By optimizing the removal of the molten material it is possible to obtain higher cutting speeds and better cut quality (Narendra B. Dahotre, 2008). Two of the important nozzle parameters are:

- Nozzle design
- Nozzle diameter

Several nozzle designs developed based on gas dynamics exist. The different nozzle designs each have their drawbacks and advantages. Some designs improve cutting speed and some the capability to cut thicker materials. For more information about nozzle designs see (Narendra B. Dahotre, 2008). The nozzle

diameter is mainly governed by the thickness of the workpiece. Thick workpieces are often cut with larger nozzle diameters ($>1.5\text{mm}$) than thin workpieces. A large diameter of the cutting nozzle is less sensitive to misalignment of the laser but also introduces a larger consumption of assist gas compared to a small nozzle diameter. (Narendra B. Dahotre, 2008) Due to assist gas costs, it is desirable to keep to pressure as low as possible, without compromising the cut quality.

3.2.5 Assist gas type

In relation to making high quality cuts with a laser the assist gas type is of great importance. Several gases are used in laser cutting and can be categorized as:

- Pure reactive gasses
- Pure inert gasses
- Neutral gasses

The reactive gasses such as oxygen and hydrogen, apart from ejecting the molten material, provides extra energy to the cut zone because the gas reacts with the laser generating more heat. This enables the possibility to for example cut thicker workpieces. The downside is that reactive cutting gasses provides a lower cut quality compared to a non-reactive gas. (Narendra B. Dahotre, 2008)(Caristan, 2004) A reactive gas may therefore not be able to create a high enough cut quality for the purpose of this thesis.

A Pure inert gas such as argon is the best solution when concerning high cut qualities. The downside is that inert gasses compared to other types are more expensive. (Narendra B. Dahotre, 2008)

Neutral gasses such as nitrogen will in most cases not react with the cutting process. The results in cut quality are not as good as pure inert gasses but is instead cheaper and therefore often better to use instead of a pure inert gas. (Caristan, 2004)

3.3 Workpiece parameters

In laser cutting the workpiece parameters influence the cutting process. Two workpiece parameters are:

- Specific material properties
- Material thickness

Specific material properties

The thermal properties of the material which shall be cut has a great influence on the laser cutting process. Some of the most important properties for metals in relation to laser cutting is the thermal conductivity and the reflectivity of the surface (Wollenberger, 2012). Aluminium is for example a very thermal conductive and reflective material compared to steel. Aluminiums higher thermal conductivity and reflectivity entails that less energy is absorbed by the material. The energy that is absorbed is dispersed faster in aluminium compared to steel making it more difficult to obtain a high temperature in the cut zone.

Material thickness

The thickness has a significant impact on the cutting process in relation to e.g. laser power and cutting speed. It also affects gas pressure as a deeper cut kerf may require a higher gas pressure to be able to eject the molten material at the bottom of the workpiece.

3.4 Quality parameters

This section refers to a literature study, that is based on scientific papers. The used papers can be found on the appendix-DVD in the folder "Chapter 3/Papers".

According to (Association, 2002) the quality of the cut surface can be described by the following characteristics:

- Perpendicularity or angularity tolerance (PAT)
- Mean height of the profile (MHP)
- Melting of top edge (MTE)
- Dross

Furthermore other characteristics can help determine the quality of the cut, these are:

- Heat affected zone (HAZ)
- Kerf width (KW)
- Kerf taper (KT)

3.4.1 Perpendicularity and angularity tolerance

The perpendicularity and angularity tolerance, u , is defined as the distance between the highest and the lowest point (not taking thickness reduction Δa into account) of the cut surface when seen in profile, see figure 3.6.

The control variables and/or workpiece parameters which affect the perpendicularity and angularity tolerance is unknown since this quality parameter haven't been described elsewhere in the studied literature, than in (Association, 2002).

The way that the perpendicularity or angularity tolerance is measured is by using a guide device, for example a pickup, in the thickness direction. The guide device has to be perpendicular to the intended cut angle and has to have a stylus point radius of maximum 0.1mm (Association, 2002).

3.4.2 Mean height of the profile

The mean height of the profile relates to the surface roughness of the workpiece. The mean height of the profile, R_z5 , (calculated as in equation 3.2) is defined as the mean of 5 roughness samples measuring the highest and the lowest point, see figure 3.7a.

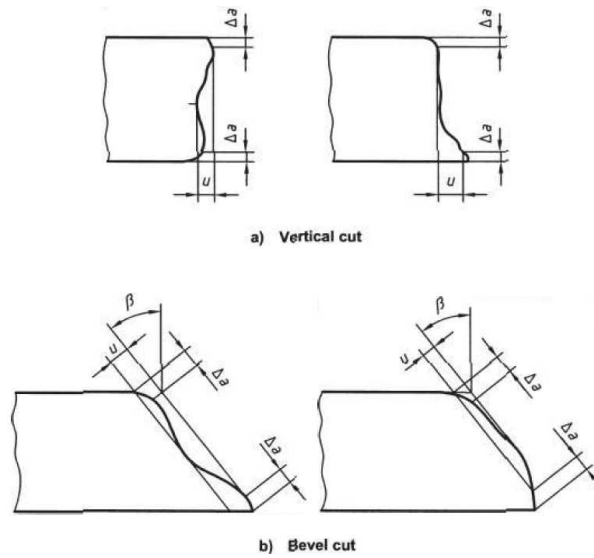
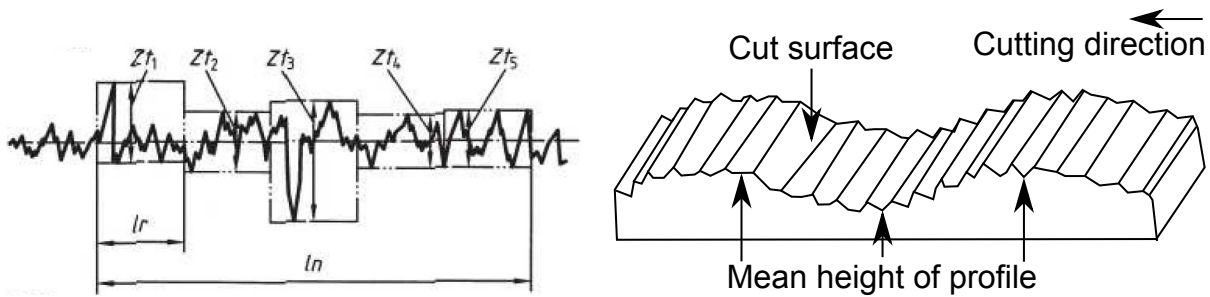


Figure 3.6: Graphical definition of the perpendicularity and angularity tolerance. Where u is the distance between the highest and lowest point of the cut surface when seen from the side, Δa is the thickness reduction and β is the angle of the cut compared to the vertical direction. (Association, 2002)



(a) Graphical definition of the mean height of the profile. Where Zt_1 to Zt_5 is the distance between the highest and lowest point in each sample. ln is the evaluation length and lr is the sampling length which shall be $1/5$ of ln . (Association, 2002)

(b) Illustration of mean height of profile on the cut surface.

Figure 3.7: Mean height of the profile from two viewing angles.

$$R_{z5} = \frac{Zt_1 + Zt_2 + Zt_3 + Zt_4 + Zt_5}{5} \quad (3.2)$$

When high quality cuts is needed the lower the value of the mean height of the profile the better. If the mean high of the profile has a high value, it can be visible on the cut surface on the workpieces, which must be avoided on the high quality workpieces from B&O.

According to the information found from the litterature study, control variables and equipment parameters that affect the mean height of the profile significantly are:

- Cutting speed

In order to obtain a low value of the mean height of the profile the cutting speed should have a moderate value.

- Focal Point

For aluminium, dross is reduced when the focal point is placed in the bottom of the workpiece. Placing the FP above the workpiece can entail dross (Caristan, 2004).

- Operating laser power

In order to obtain a low value of the mean height of the profile the operating laser power should have a moderate value.

- Assist gas pressure

In order to obtain a low value of the mean height of the profile the assist gas pressure should have a moderate value. The assist gas pressure interacts with the assist gas type for this quality characteristic.

- Assist gas type

In order to obtain a low value of the mean height of the profile the assist gas type should be inert.

The mean height of the profile can be measured using a precise measuring instrument such as an electric contact stylus instrument (Association, 2002). It is important to notice that the measurement is done on the cut surface in either the cutting direction or opposite of the cutting direction.

3.4.3 Melting of top edge

During cutting the top edge of the cut may become rounded off due to melting of the top edge. A measure of how much the edge is rounded off is the radius, r , of the rounded edge, see figure 3.8.

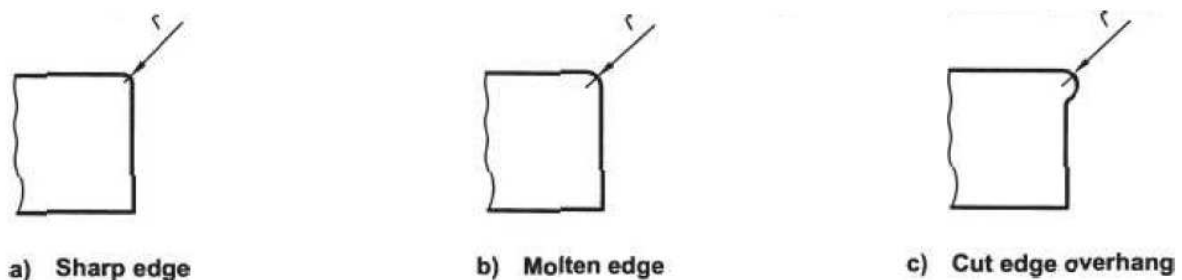


Figure 3.8: Graphical definition of the melting of the top edge. Where r is the radius of the rounded off edge. (Association, 2002)

It is unknown what control variables and/or workpiece parameters affects melting of top edge because the phenomenon isn't described in the studied literature. A reasonable guess would be that the cutting speed and the operating laser power influences it, because it affects how much energy goes into the material, thereby how large the for melting the top edge becomes.

In relation to processing high quality holes with laser cutting melting of top edge needs to be controllable because it influences the appearance of the holes. It is noticeable, that a radius on zero is not realistic. According to (Association, 2002) melting of the top edge can be measured using a radius gauge.

3.4.4 Dross

Dross is material which haven't been fully expelled in the cutting process by the assist gas and as a result of this have resolidified on the bottom of the cut edge, see figure 3.9. The higher thermal conductivity of aluminium entails, that is resolidifies faster than eg. steel.

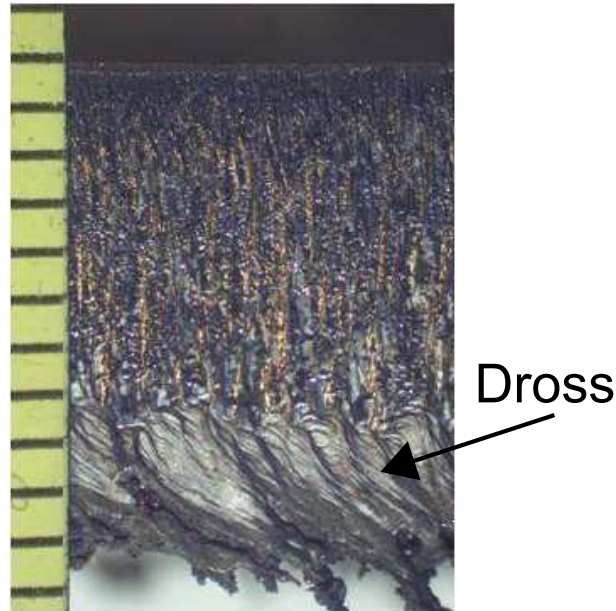


Figure 3.9: Illustration of dross on a cut edge.(Wandera, 2010)

According to the information found from the litterature study, control variables and equipment parameters that affect dross significantly are:

- Cutting speed

In order to obtain a low value of dross the cutting speed should have a high value.

- Operating laser power

In order to obtain a low value of dross the operating laser power should have a high value.

- Assist gas pressure

In order to obtain a low value of dross the assist gas pressure should have a high value. The assist gas pressure interacts with the assist gas type for this quality characteristic.

- Assist gas type

In order to obtain a low value of dross the assist gas type should be inert.

Often dross is unwanted because it gives a rough bottom surface of the workpiece that has to be removed by machining the workpiece. Another reason that dross is unwanted on a workpiece is that it can become a hazard to customers and/or workers who shall handle the workpiece. This is due to the fact that dross can be very sharp.

According to (Association, 2002) there is no standard of how dross is measured.

3.4.5 Heat affected zone

The Heat Affected Zone (HAZ) is the area which is affected by the heat developed when the laser cuts in the workpiece. An example on the HAZ can be seen in figure 3.10.

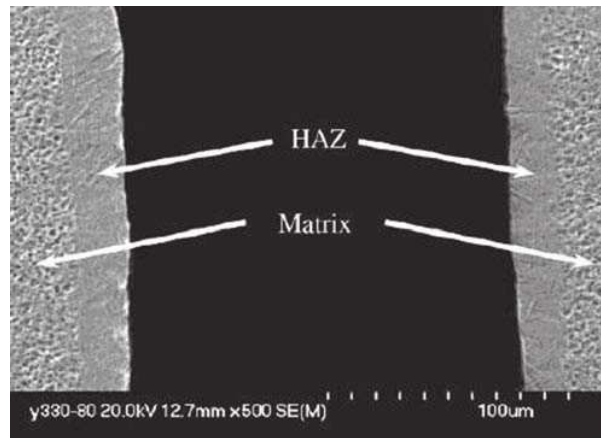


Figure 3.10: Heat affected zone of a laser cut of a titanium-alloy. (Narendra B. Dahotre, 2008)

According to the information found from the literature study, control variables and workpiece parameters that affect the HAZ significantly are:

- Cutting speed

In order to obtain a low value of the HAZ the cutting speed should have a high value. The cutting speed interacts with the operating laser power for this quality characteristic.

- Operating laser power

In order to obtain a low value of the HAZ the operating laser power should have a low value.

- Assist gas pressure

In order to obtain a low value of the HAZ the more the assist gas pressure the better.

- Material thickness

In order to obtain a low value of the HAZ the material thickness should be thin.

In the HAZ the mechanical properties of the material changes which may be unwanted. It is also possible that the heated up material changes color which one may have to avoid if the workpiece is going to be used as a visual component in a product like for example is the case with many of the aluminium workpieces in B&O products.

The HAZ is often investigated using an optical microscope or a scanning electron microscope often referred to as SEM.

3.4.6 Kerf width

The kerf width (KW) is the width of the cut kerf created by the laser an example of a kerf width is seen in figure 3.11. The width represents the removed material.

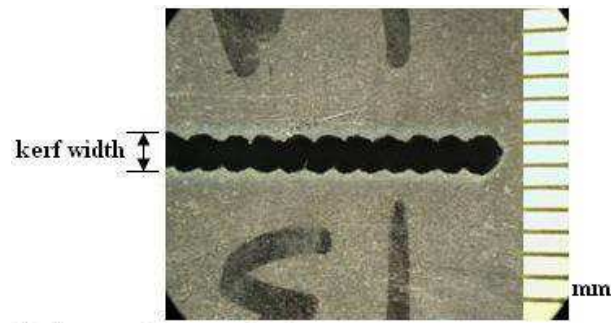


Figure 3.11: Cut kerf with varying kerf width. This kerf is made with a pulsed laser beam, which entails the large KW variation. (Wandera, 2010)

According to (Caristan, 2004), (Wandera, 2010) and (A. Stournaras, 2009), control variables and work-piece parameters that affect the KW significantly are:

- Cutting speed
The lower the cutting speed, the larger the KW becomes.
- Focal point
- The focal point affects the beam spot diameter in the workpiece, which affects the size of the KW.
- Operating laser power
- For higher values of the operating laser power, the KW will increase.
- Assist gas pressure
- A high assist gas pressure will remove the molten material more effectively, which entails a larger KW.
- Specific material properties

In general materials with high heat conductivity cause wider kerfs.

The KW in itself is not unwanted but the variation in it often is, especially if the variation is visible to the naked eye. Large variations in the KW entail that cuts that should be straight or round will not be so. In the case of cutting holes as is the objective of this thesis large variations in KW is therefore unwanted.

According to (Association, 2002) there is no standard of how to measure the KW but in (Avanish Kumar Dubey, 2007b) the KW is measured using a microscope.

3.4.7 Kerf taper

The kerf taper is a parameter that describes the angle between the top and bottom of cut, compared to what is intended. Kerf tapering occurs because the laser beam is focused on a specific spot and diverges afterwards. Kerf tapering is especially seen when cutting thick workpieces. On figure 3.12 kerf tapering can be seen.

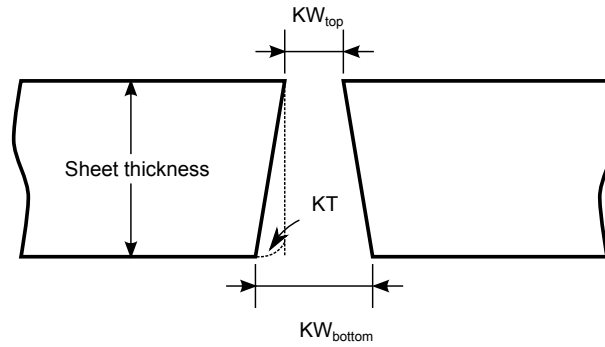


Figure 3.12: Example of a tapered cut kerf and the measurements needed for calculating the kerf taper.

The tapering angle is calculated as in equation 3.3 (G. Thawari, 2005).

$$\text{Taper angle} = \tan^{-1} \left(\frac{KW_{top} - KW_{bottom}}{\text{sheet thickness}} \right) \quad (3.3)$$

Where KW_{top} and KW_{bottom} is the width of the top of the kerf and the bottom of the kerf respectively.

From the information found in the literature study, control variables and workpiece parameters that affect the kerf taper significantly are:

- Cutting speed

In order to obtain a low value of the kerf taper the cutting speed should have a high value. The cutting speed interacts with the pulse frequency for this quality characteristic.

- Focal point

In order to obtain a low value of the kerf taper the focal point should be above the work surface. This focal point interacts with the material thickness for this quality characteristic.

- Operating laser power

In order to obtain a low value of the kerf taper the operating laser power should have a low value. The operating laser power interacts with the material thickness for this quality characteristic.

- Material thickness

In order to obtain a low value of the kerf taper the thinner the material thickness the less the influence is from this factor.

Kerf tapering is as many of the other quality parameters wished kept at a minimum because the workpieces will have to be machined afterwards to remove the tapering if the tapering angle is too far away from the wanted result. Kerf tapering might though also be possible to use as a design feature, if the process can be controlled. The most desirable KT angle is zero.

Kerf tapering is measured using a measuring microscope. The top and bottom kerf width is measured and a kerf tapering angle is calculated.

3.5 Summary

Through this chapter the laser cutting process have been introduced and a process model used for describing the various variables/parameters in laser cutting has been presented. In table 3.1 the control variables/workpiece parameters that influences the quality parameters is summed up. Also a value, low to high, is given for each control variable/workpiece parameter as an indication of how to get an optimum setting for the specific quality parameter. In the table question marks can be seen at some of the quality parameters. This is due to not being able to find any documentation on what influences these parameters. In table 3.2 the equipment that can be/are used for determining the value of the quality parameters is given.

Quality parameter	Settings of the CV, EP and WP affecting the quality parameters	Settings of the CV, EP and WP to get the bestresult for the specific quality parameter
Perpendicularity and angularity tolerance	?	?
Mean height of the profile	Cutting speed Operating laser power Assist gas pressure Assist gas type	Moderate Moderate Moderate Inert
Melting of top edge	?	?
Dross	Cutting speed Operating laser power Assist gas pressure Assist gas type	High High High Inert
Heat affected zone	Cutting speed Operating laser power Assist gas pressure Material thickness	High Low More Low
Kerf width	Cutting speed Focal point Operating laser power Assist gas pressure Specific material properties	? ? ? ? Low heat conductivity
Kerf taper	Cutting speed Focal point Operating laser power Material thickness	High Above the work surface Low More

Table 3.1: Control variables (CV), equipment parameters (EP) and workpiece parameters (WP) influencing the quality parameters significantly. The table is inspired by (Avanish Kr. Dubey, 2007).

Quality parameter	Measurement equipment	Measurement unit
Perpendicularity/angularity tolerance	Pickup	height
Mean height of the profile	Electric contact stylus	height
Melting of top edge	Radius gauge	radius size
Dross	Measuring microscope	height
Heat affected zone	SEM/Optical microscope	length
Kerf width	Measuring microscope	width
Kerf taper	Measuring microscope	angle

Table 3.2: An overview of what equipment can be/are used for determining the value of the quality parameters.

Case study 4

In this chapter the workpiece, which is used as reference in this thesis, is presented and measured. A definition of a high quality workpiece from B&O is given from determining the values of the quality parameters on the reference workpiece.

It has not been possible to get a clear definition of how laser cut holes can be declared high quality from B&O. Therefore a definition of high quality processed holes is made in this thesis from measuring and inspecting a workpiece. The holes are assessed with respect to the quality parameters previously described (chapter 3).

In order to set up the requirements for high quality laser cut holes, a workpiece with drilled holes, currently being manufactured by B&O is used as reference, see figure 4.1.

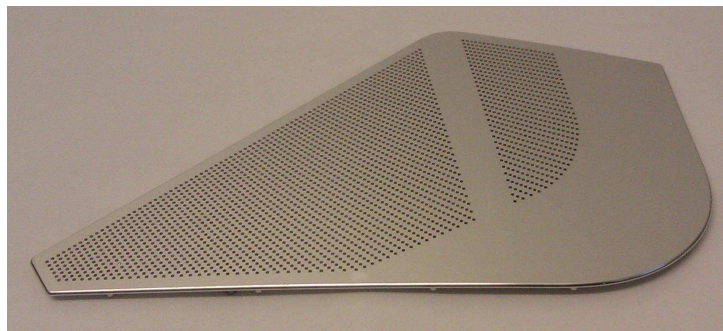


Figure 4.1: B&O speaker grill for an unknown automobile. The width is approx. 40cm.

4.1 Definition of high quality holes

The method used to define high quality laser cut holes, is through the quality parameters previously introduced (chapter 3). The quality parameters includes PAT, MHP, MTE, dross, HAZ, KW and KT.

The quality parameters and dimensional tolerances are measured from pictures of the top and bottom side of the workpiece and a picture taken of the holes in profile, see figure 4.2, using the method described in appendix A. The method may not be the optimum method for measuring all the quality parameters, but is used due to a lack of resources in time and measuring equipment. Because of this, the quality parameters PAT and MHP are not measured and therefore not included in the requirement specification. Throughout this thesis PAT and MHP are therefore not evaluated for the laser cut workpieces.

The individual quality parameters are evaluated from the following pictures:

- Picture of top surface: KW, KT, HAZ.
- Picture of the profile of a hole: MTE, dross.

- Picture of bottom surface: KW, KT, HAZ.

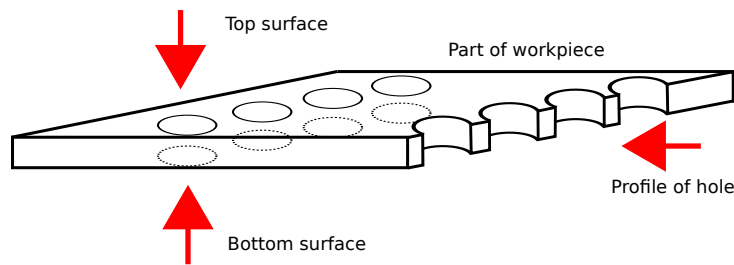


Figure 4.2: The views the pictures are taken from.

4.1.1 Quality parameters

Through measuring and visual inspection of holes in the speaker grill workpiece, the quality parameters are evaluated. The quality parameters MTE and dross are evaluated from two holes, whereas the quality parameters HAZ, KW and KT are evaluated from 10 holes.

MTE

From figure 4.3 it can be seen that the drilling process does not leave an MTE phenomenon because it isn't a thermal process. Even though the current process doesn't leave an MTE phenomenon it still creates a rounded edge which instead will be used to set up the reference for MTE. MTE is described as either a sharp edge, molten edge or an edge with overhang as in figure 3.8.

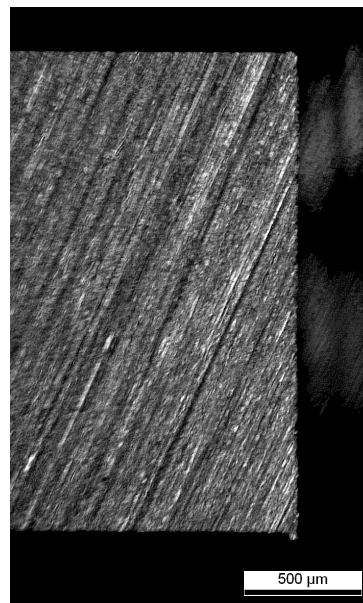
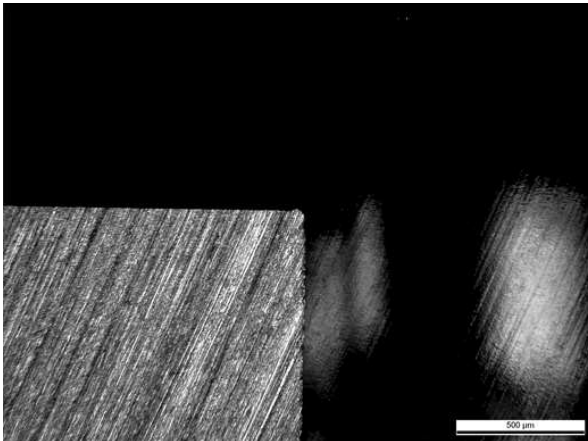


Figure 4.3: Stereo microscope (Wild M8 Heerbrugg) picture of the profile of a hole in the drilled workpiece, zoom 25.

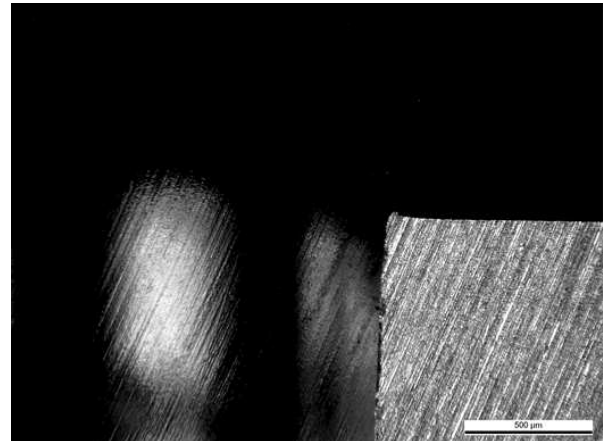
In order to describe whether an edge is sharp, molten or with overhang, a definition is to be made. In this thesis this is done by measuring the radius of the edges of the drilled holes, see figure 4.4 and 4.5. In table 4.1 the results of measuring the top edges are seen. The top edges of the holes for the speaker grill

are defined as sharp edges. A distinction between sharp and molten edges based on the results is made as follows along with edges with overhang:

- Sharp edge: $r \leq 35 \mu\text{m}$
- Molten edge: $r > 35 \mu\text{m}$
- Edge with overhang: melt is attached to the inner side of the kerf.

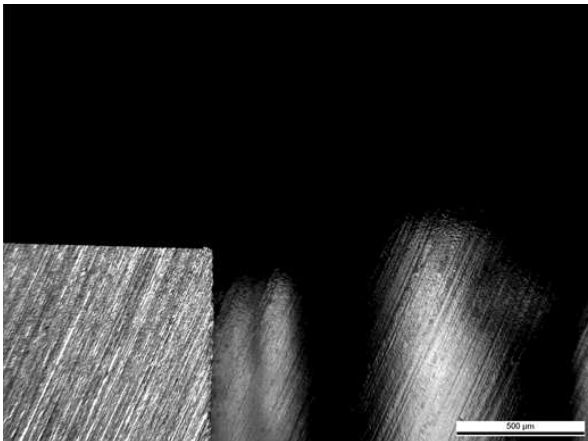


(a) Top left edge of hole 1 - defined as sharp edge.

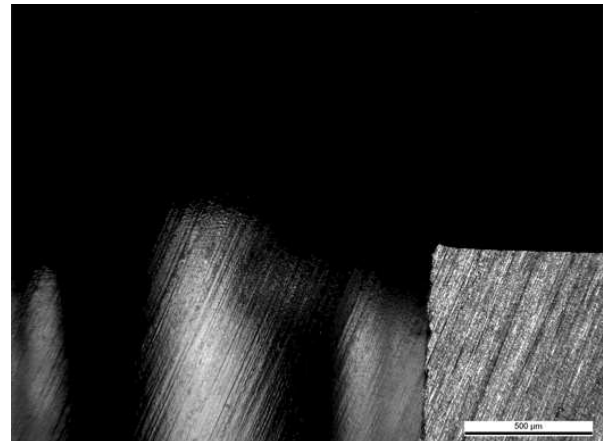


(b) Top right edge of hole 1 - defined as sharp edge.

Figure 4.4: Pictures of the top edges of hole 1 in profile, taken with a Wild M8 Heerbrugg stereo microscope with zoom 50.



(a) Top left edge of hole 2 - defined as sharp edge.



(b) Top right edge of hole 2 - defined as sharp edge.

Figure 4.5: Pictures of the top edges of hole 2 in profile, taken with a Wild M8 Heerbrugg stereo microscope with zoom 50.

Dross

In a drilling process burr may occur at the bottom edge of the drilled workpiece, see figure 4.3. The quality parameter directly relating to burr, in a laser cutting process, is dross. On picture 4.3 the height of the burr of the drilled holes can be seen. The burr is only visible when looking on the hole profile through

a microscope. The height of the burr is measured to have an average height of approximately $24 \mu\text{m}$, see table 4.1. The maximum burr height is $44 \mu\text{m}$ and is used as a reference for allowable dross from laser cut workpieces.

Hole no.	MTE [μm]	Dross [μm]
1(left)	35	30
1(right)	31	10
2(left)	28	11
2(right)	33	44
Allowable MTE and dross	≤ 35	≤ 44

Table 4.1: Measurements of quality parameters for obtaining a reference of high quality laser cut holes in aluminium.

HAZ

HAZ is for the workpiece defined as change in color/nuance of the surfaces and not metallurgical changes. The reason for this is that the mechanical properties in the material isn't of interest as the workpieces aren't influenced by large external forces. This entails that mechanical properties, such as hardness or Young's module is not dealt with during this thesis. As there isn't a color change on the surfaces of the reference workpiece, see figure 4.6, there may not be a color change visible to the eye on the laser cut workpieces due to heating of the workpiece material.

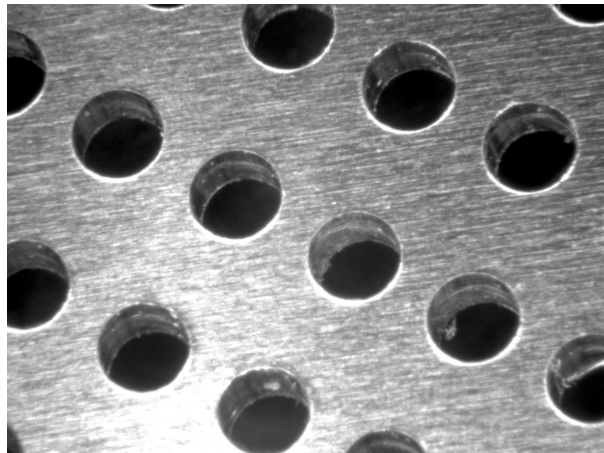


Figure 4.6: Top surface of the speaker grill with zoom 10, taken with the Wild M8 Heerbrugg stereomicroscope. No color change is visible.

KW

The quality parameter kerf width cannot be identified for the reference workpiece since it doesn't directly relate to anything in the process of drilling holes. The kerf width will instead in this thesis relate to the diameter and roundness of the holes, see figure 4.7. Where the roundness is defined as in (Nielsen, 2010). If the kerf width has a large variation, either due to thermal effects or inaccuracy of the XY-table, the roundness of a hole will vary, which is undesirable in a high quality laser cut hole. In order to set up a requirement of how much the diameter and the roundness of a hole is allowed to vary, the diameter and the roundness of the drilled holes are measured and calculated respectively. In order to calculate the

roundness of the holes minimum and maximum diameters fitted to the top and bottom of the holes are measured. In figure 4.7 it can be seen how the minimum and maximum diameter is found on a drilled hole. The roundness is found using equation 4.1. The results of measuring minimum and maximum diameters and calculating the roundness are seen in table 4.2.

$$Roundness = \frac{d_{Max} - d_{Min}}{2} \quad (4.1)$$

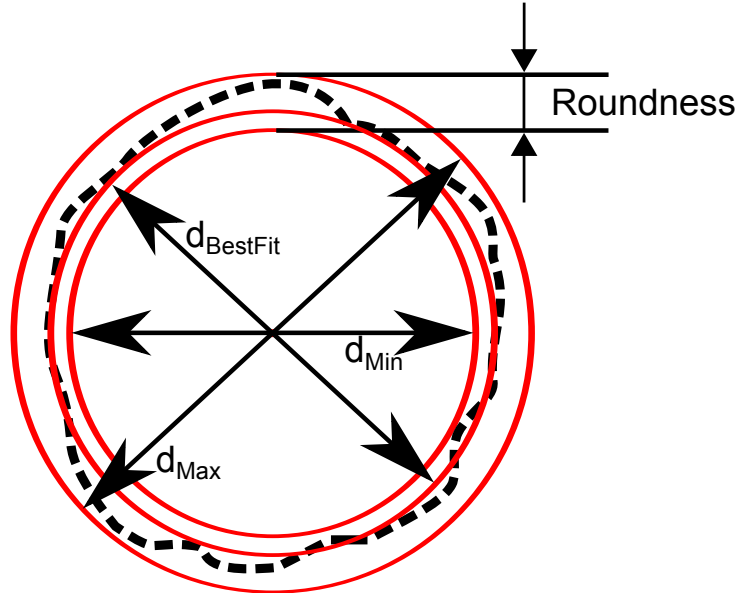


Figure 4.7: Graphical illustration of how the three different diameters and roundness of a hole is defined. The two diameters d_{Min} and d_{Max} are used for calculating the roundness. The diameter $d_{BestFit}$ is the best fit diameter used in calculating the kerf taper angle.

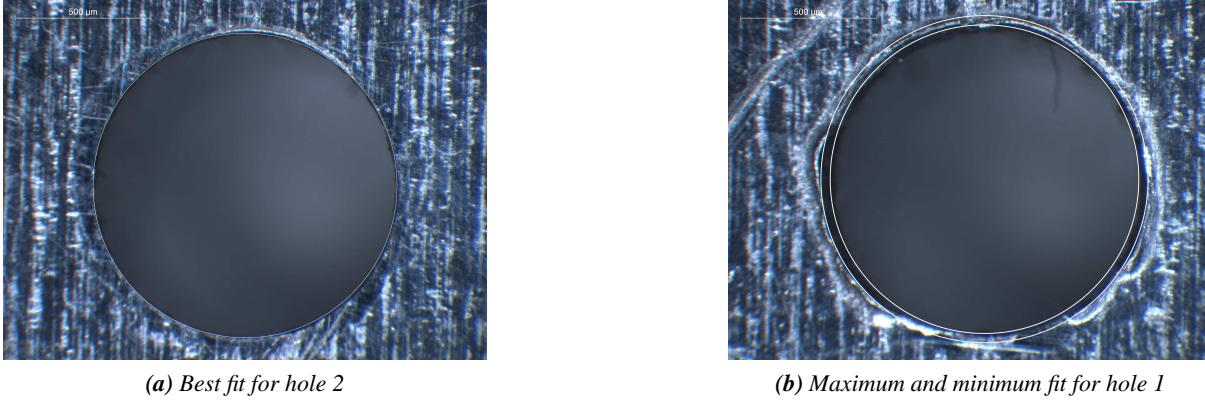
KT

Because the drill used to process the holes has the same diameter along its length, kerf tapering should theoretically not exist for the holes. The KT angle is calculated using trigonometri. A best fit diameter of the top and bottom of a hole is measured for this purpose, because the minimum and maximum radius is not representative for calculating the KT. In figure 4.7 it can be seen how the best fit diameter is found on a drilled hole. The angle is found using equation 4.2.

$$KT = \tan^{-1} \left(\frac{\frac{|d_{BestFitTop} - d_{BestFitBottom}|}{2}}{\text{sheet thickness}} \right) \quad (4.2)$$

Where $d_{BestFitTop}$ and $d_{BestFitBottom}$ is the best fit of the top and bottom diameter of the hole respectively. This equation assumes that the KT angle in the drilled hole is symmetric. Figure 4.8a shows a best fit for a hole, figure 4.8b shows maximum and minimum fitted diameters of an other hole.

From measuring the best fit diameter of 10 holes in the top and bottom the mean tapering angle is found along with a standard deviation, see table 4.2.



(a) Best fit for hole 2

(b) Maximum and minimum fit for hole 1

Figure 4.8: The white circle is the fitted diameters for a hole from the speaker grill.

Hole no.	HAZ	Top diameter [μm]			Bottom diameter [μm]			Roundness [μm]		KT [$^\circ$]
		Min.	Max.	Best fit	Min.	Max.	Best fit	Top	Bottom	
1	no	1783	1899	1783	1779	1981	1831	58	101	-0.7
2	no	1813	1834	1817	1771	1817	1797	11	23	0.3
3	no	1806	1830	1811	1782	1796	1791	12	7	0.3
4	no	1810	1825	1813	1759	1792	1778	8	17	0.5
5	no	1805	1830	1811	1777	1805	1779	13	14	0.5
6	no	1798	1835	1808	1778	1792	1779	19	7	0.4
7	no	1805	1820	1820	1770	1799	1785	8	15	0.5
8	no	1795	1847	1804	1777	1797	1780	26	10	0.3
9	no	1801	1821	1800	1770	1791	1781	10	11	0.3
10	no	1801	1824	1811	1775	1791	1782	12	8	0.4
Mean	-	1804	1830	1808	1773	1798	1788	18	21	0.3
Std. dev.	-	-	-	-	-	-	-	-	-	0.4

Table 4.2: Measurements of the diameters, roundness and KT of the holes in the top and bottom surface along with a visual assessment of whether there is a color change (HAZ) around the holes. Pictures of the holes used to create this table can be seen on the appendix-DVD under the folder "Chapter 4/Case Holes".

4.2 Requirement specification

From evaluating all the quality parameters a requirement specification for the holes in the speaker grill is set up, see table 4.3. This requirement specification will henceforth, in this thesis, serve as reference of high quality laser cut holes.

	Reference
Maximum MTE, [μm]	30
Maximum Dross, [μm]	44
Diameter _{Top} , [μm]	1808
Diameter _{Bottom} , [μm]	1788
Roundness _{Top} , [μm]	18
Roundness _{Bottom} , [μm]	21
KT, [$^\circ$]	0.2 \pm 0.4

Table 4.3: Requirement specification for the holes in the B & O speaker grill.

Problem formulation 5

Based on the previous chapters the problem formulation is presented.

Since B&O have never used laser cutting before the general objective of this thesis is to gather the necessary knowledge that can answer the general objective of this thesis, which is: *To which extent can laser cutting be used for hole processing of high quality workpieces in aluminium at B&O?*

Together with the general objective, the description of the manufacturing processes used at B&O (described in chapter 2) and the speaker grill case (described in chapter 4), a problem in relation to high quality laser cutting at B&O can be defined:

- Cutting quality: Can the desired cutting quality, of the holes in the speaker grill, be obtained through laser cutting?

5.1 Cutting quality

The definition of high quality aluminium workpieces have been defined in chapter 4 based on a speaker grill currently produced at B&O. This will be the reference for high quality aluminium workpieces during this thesis.

To investigate if it is possible to obtain the specified quality, laser cutting of straight lines is performed. This is done with the assumption that results from stright cutting is comparable with laser cutting of holes. This entail the following problem:

- Which settings of the equipment parameters and control variables result in quality parameters that satisfies the requirements for the quality parameters for the B&O case workpiece?

Approach to solution 6

In this chapter two different approaches for solving the problem formulation in this thesis is presented. From a description of the two approaches in relation to laser cutting an empirical approach is chosen.

There are two approaches of solving an engineering problem. Either by the use of analytical or empirical approach. These are in the following two section described.

6.1 Analytical approach

There are generally two types of analytical approaches in science, these are:

- Analytical knowledge

This type of analytical approach uses very well defined and approved equations and rules etc. found in literature (Kristiansen, 2007).

- Numerical simulations.

This type of analytical approach uses computer software to simulate real world problems and is based on analytical knowledge.

Numerical simulations makes is possible to use modern computers and perform large scale simulations e.g. the Finite Element Method (FEM). By the use of this approach, problems based on approved analytical knowledge can be solved with a high credibility and accuracy. This includes both simple and very complex problems in both static and dynamic problems. Numerical simulations are powerful when dealing with a situation where it is difficult to observe the process and/or obtain measurements. This applies in situations where the execution time is very short e.g. metal stamping, crash tests, explosions etc. Simulations can also be necessary because certain physical effects occur e.g. at very high temperatures, at microscopic process level, at high speeds, fatigue, etc.

Analytical knowledge in laser cutting

Several papers demonstrates good results by the use and construction of analytical models for the laser cutting process. Stand alone simulations of the thermo mechanical process in laser cutting are already state of the art (Andreas Ottoa, 2010).

Noticeable papers that deals with analytical optimization of quality parameters is among others: (Yilbas, 2004), (R. Aloke, 1996), (B.S. Yilbas, 2011) and (Jun Hu, 2010). Generally these papers deal with one quality parameter at a time and not how the laser cutting process affects all the quality parameters defined in chapter 4 and thereby not the overall appearance of the workpiece.

The complexity of the laser cutting process entails that it is very difficult to describe the whole process with analytical knowledge and with a sufficient accuracy for predictions etc. (Andreas Otto, 2010) have developed a "Universal Numerical Simulation Model for Laser Material Processing" and concluded, that there is a lot of work ahead before such a model is practically applicable.

Interdisciplinary knowledge of several branches of physics, that are coupled with each other, are a part of laser cutting, some of these are given below: (Narendra B. Dahotre, 2008):

- Thermo-physical effects: Heating, melting, vaporization and plasma formation
- Material properties: Absorptivity, thermal conductivity, specific heat, density and latent heats
- Electromagnetic radiation effects: Intensity, wavelength, spatial and temporal coherence, angle of incidence, polarization, illumination time, refraction and reflection

From the requirement specification in chapter 4 it is found, that the the measure for high quality is in the range of \pm few μm . Even if a good laser cutting simulation can be obtained, it will be very difficult to predict quality parameters, with a precision on a few μm .

6.2 Empirical knowledge

Empirical knowledge in science is generally used for two scenarios:

- Verification of analytical models/results.

This can be used as a part of statistical hypothesis testing in e.g. the medical industry or to fit a computer simulation to results obtained through experiments.

- Obtain new knowledge through experiments.

It can be necessary to gather empirical knowledge through experiments when the analytical knowledge is insufficient or doesn't exist.

Based only on empirical knowledge from experiments, it is possible to construct a process model. This is often desired since such a model may be able to predict the output of a setting which haven't been tested through experiments.

Empirical knowledge in laser cutting

Empirical knowledge from experiments are used to a high degree and approved for laser cutting. Papers that deals with the optimization of quality parameters from laser cutting have shown good results for many different system setups (different lasers and materials) and with different optimization methods e.g. ANOVA, fuzzy-expert-system, artificial neural network, taguchi method, design of experiments, etc. These papers are e.g. (Amit Sharma, 2011), (Avanish Kumar Dubey, 2007a), (Chong Zhian Syn, 2010) (Avanish Kumar Dubey, 2007c) and (B. Adelman, 2011).

The papers demonstrate that both single and multi objective optimization for quality parameters in laser cutting can be obtained through experiments.

Advantages/disadvantages of the analytical/empirical approaches

An overview of the advantages and disadvantages of the analytical and empirical approaches is seen in table 6.1 and 6.2. In relation to laser cutting the advantages/disadvantages are only presented in relation to numerical simulations and physical experiments.

Numerical simulations	
Main advantages	Main disadvantages
Cost savings (time and money) Easy to perform "what-if" analysis Study system without building it	Interpretation of results can be very difficult Expensive software/hardware High process understanding and information necessary Implementation of results is not straight forward Calculation errors due to simplification of the real world

Tabel 6.1: Main advantages and disadvantages of numerical simulations.

Physical experiments	
Main advantages	Main disadvantages
Gather process insight for unknown systems Cause-effects can be observed Better practical understanding	Noise can disturb results Valid results demands high repeatability Results can be interpreted differently High cost (time and money)

Tabel 6.2: Main advantages and disadvantages of physical experiments.

6.3 Solution method in this thesis

Because of the insufficiency in precision, and incompleteness of analytical models, an empirical approach in the form of experiments will be the source of knowledge in this thesis. In this thesis empirical knowledge is defined as measurements from laser cutting experiments. Laser cutting experiments with different settings of control variables and workpiece parameters are conducted and the quality parameters, from the case study (chapter 4), are evaluated through the measurements. The measured workpieces are further on analyzed and an analysis/conclusion of the results is given.

Laser setup 7

In this chapter the setups, used in all of the experiments that are conducted, is presented. First the system setup, along with specifications of it is presented. Calculations of laser beam quality values are calculated and evaluated through experiments. A summary compares the two setups.

In this chapter two system setups are presented. Two setups are presented because experiments with both are conducted, with significantly different results. During experiments with the AAU setup, it is concluded, that it is not possible to cut 1mm aluminium sheets with it. An analysis of these experiences are presented in chapter chapter 8.

During this chapter the two setups are compared and analyzed in order to understand the differences of the used systems. The two system setups are:

- AAU laser system setup
- IPU laser system setup

Common for both setups is that they consist of the following equipment:

1. Laser machine
2. Cutting head
3. Laser transmission (from laser machine to cutting head)
4. PC control
5. Laser beam monitoring
6. XY-table
7. Assist gas (Nitrogen)

In this chapter focus is on the laser machine, laser transmission, and cutting head. Because of this the other pieces of equipment will not be further described. The setup at IPU is experimental, and do not include surveillance and high level security as the AAU setup does.

7.1 Laser machine

In this section the laser machines for the system setup at AAU and IPU will be presented. Specifications of the lasers, given by the manufacturer is presented, and verified through experiments in section 7.4, to validate the values. The specifications described in this section, is explained in section 7.3.

7.1.1 AAU setup

In the system setup at the Department of Mechanical and Manufacturing Engineering at AAU the laser machine is a Trumpf HL 383 D. It is a continuous wave lamp pumped Nd:YAG laser. The smallest core diameter of the fiber that can be mounted to the laser machine is 300 μm . Figure 7.1 shows an illustration of the setup, where it is seen, that the laser cutting process is conducted in a laser cell and the XY-table and laser machine have individual PC controls. The laser cell has an integrated security system with surveillance. From the laser machine's manual the following specifications are found (laser GMBH, 2006):

- Operating power output: up to 380W
- Beam parameter product (BPP): 12mm·mrad
- Wavelength (λ): 1064nm

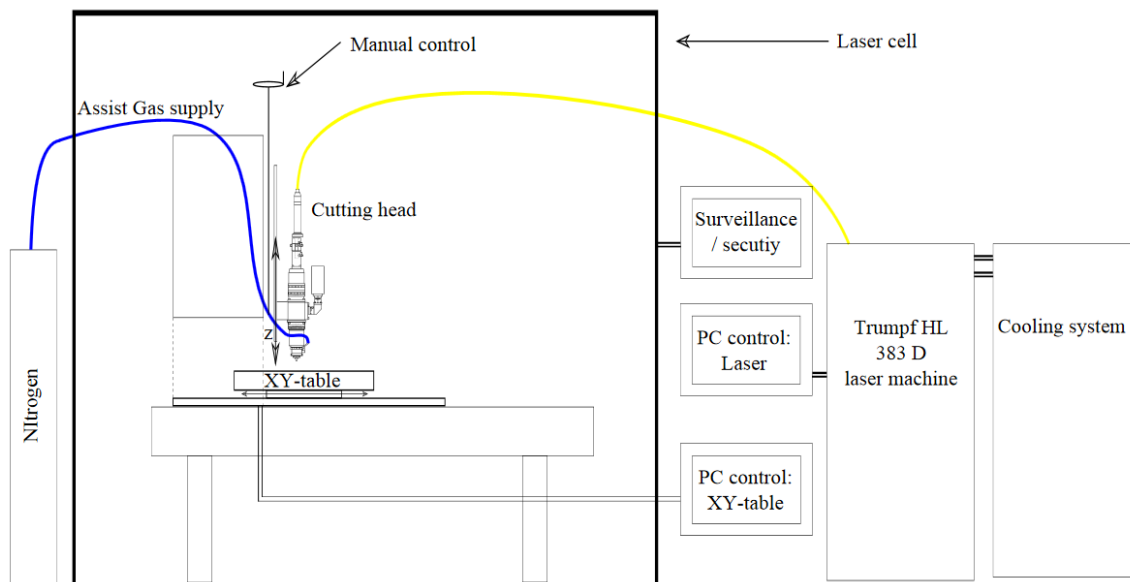


Figure 7.1: The AAU setup. The laser machine is placed outside the laser cell.

7.1.2 IPU setup

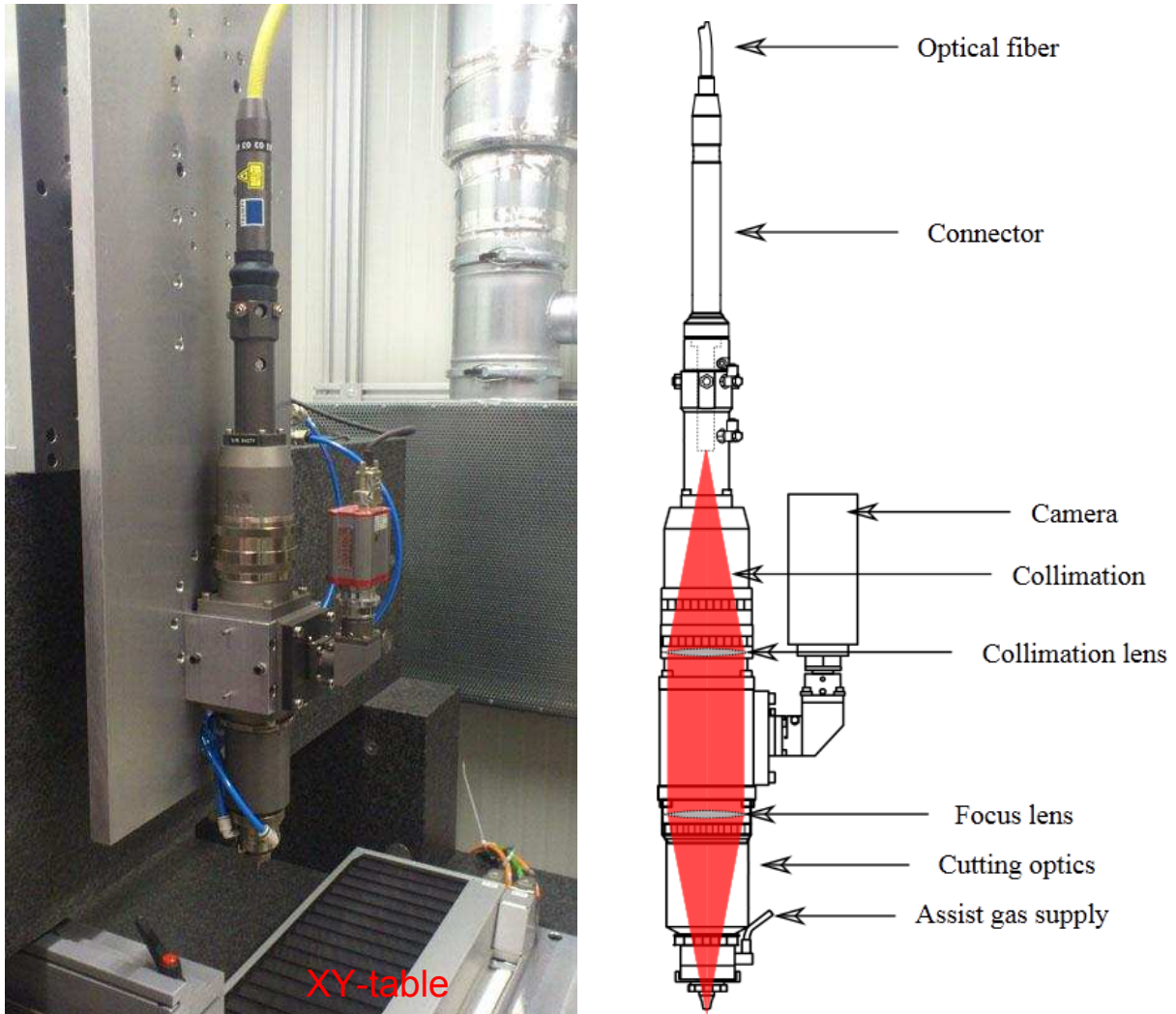
In the system setup at IPU the laser machine is an IPG YLR-400-SM-WC. The laser is of the type; single mode fiber laser which operates in continuous wave mode. An illustration of the IPU setup is shown in figure 7.3. From the laser machine's manual the following specifications are found (Hansen, 2012):

- Power output: up to 400W
- M^2 : 1.05-1.1
- Wavelength (λ): 1065-1075nm

7.2 Cutting head

7.2.1 AAU setup

The cutting head in the AAU system setup consist of a Trumpf D70 laser optic mounted with a cutting head, see figure 7.2.



(a) Picture of Trumpf D70 laser cutting head above the XY-table

(b) Illustration of Trumpf D70 laser cutting head. (GmbH, 2004)

Figure 7.2: Trumpf D70 cutting head

On the cutting head a videocamera (monitor) is mounted, figure 7.2. The function of the videocamera is to assist the adjustment of the laser beam in the XY-direction inside the cutting head. The images from the videocamera are projected onto a monitor. This is done in order to assure, that the laser beam is placed in the center of the nozzle. This is done because it is important to know precise where the laser beam is placed on the workpiece. If the laser beam is not in the center of the nozzle, a systematic error will occur when moving the XY-table, with the workpiece on it, relative to the center of the nozzle.

From the cutting heads operator's manual, (GmbH, 2004) the following specifications are found:

- Collimation length, $f_c = 200\text{mm}$

- Focal length of lens, $f = 150\text{mm}$
- Nozzle design, Conical
- Nozzle diameter, 1.0 mm

7.2.2 IPU setup

The cutting head in the IPU setup is custom built and the setup of it can be seen on figure 7.3.

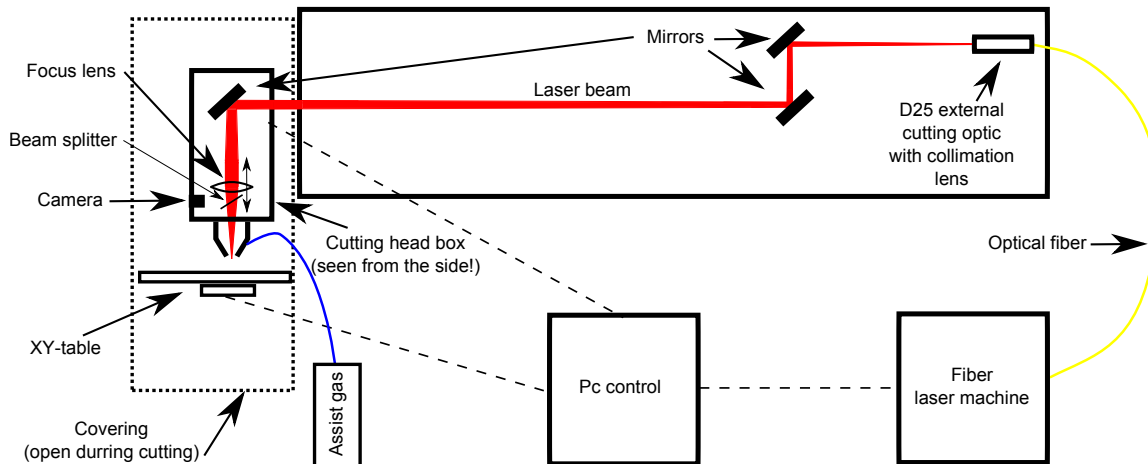


Figure 7.3: The cutting head sketched as it is setup at IPU. The setup is seen from the top except the cutting head box which is seen from the side.

As it is seen in figure 7.3 the setup at IPU consist of a fiber laser machine and an optical fiber which leads the laser source to a D25 optoskand external optic with collimation lens. From the D25 the collimated laser beam is transmitted to several mirrors guiding the laser beam down to the cutting head box over a distance of approximately 4 m. In the cutting head box the collimated beam is focused through a focusing lens, see figure 7.3. The collimation lens, focal lens and the nozzle has the following specifications (Hansen, 2012):

- Collimation length, $f_c = 356\text{mm}$
- Focal length of lens, $f = 100\text{ mm}$
- Nozzle design, Conical
- Nozzle diamter, 2.0 mm

7.3 Beam quality values

Based on the specifications it is possible to calculate laser beam values which are of interest in relation to the beam quality. The main assumption for the following beam value calculations is, that the laser beam has a gaussian intensity distubrtion (William M. Steen, 2010). This assumption is evaluated in section 7.5.

7.3.1 Smallest beam spot diameter, d_{0f}

The spot diameter is important since a decrease in spot diameter will increase the average power intensity for constant operating power. A higher power intensity entails that it is possible to cut in thicker materials or faster in a material with a specific thickness. On figure 7.4 is it shown how, the diameter of the laser spot is defined, by 86% of the maximum intensity. The figure shows a Gaussian intensity distribution, which is the ideal for a laser beam.

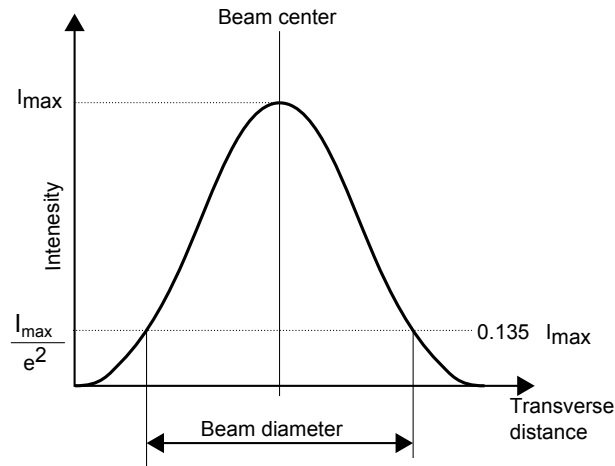


Figure 7.4: Gaussian laser beam with a circular cross section (symmetric). (point group, 2012), (Paschotta, 2012)

In relation to high quality laser cutting it is desirable to obtain a very small beam spot diameter and thereby a small KW. There is a limitation which is influenced by the cut kerf being large enough to allow the assist gas to access the cut kerf and eject the molten material. This limit is not known, but is function of material, laser beam, assist gas, stand-off, etc.

7.3.2 Beam intensity

In equation 7.1 is shown how the average beam intensity is calculated. In equation 7.2 the relationship between the maximum and average intensity is shown. d_z is the beam diameter at a given distance, z , along the laser beam. (Paschotta, 2012)

$$I_{avg} = \frac{\text{Operating power}}{(d_z/2)^2 \pi} \quad (7.1)$$

$$I_{max} = \frac{\text{Operating power}}{\frac{(d_z/2)^2 \pi}{2}} \iff 2 \cdot I_{avg} \quad (7.2)$$

7.3.3 Beam quality factor, M^2

The M^2 factor of the laser beam defines how far from an ideal gaussian beam it is, see figure 7.5. The M^2 factor is the ratio between the full beam divergence angle of a ideal gaussian laser beam, θ and the real laser beam, Θ , equation 7.3.

$$M^2 = \frac{\Theta}{\theta} \quad (7.3)$$

The M^2 factor of a laser beam is commonly used as the measure for its quality. (Paschotta, 2012).

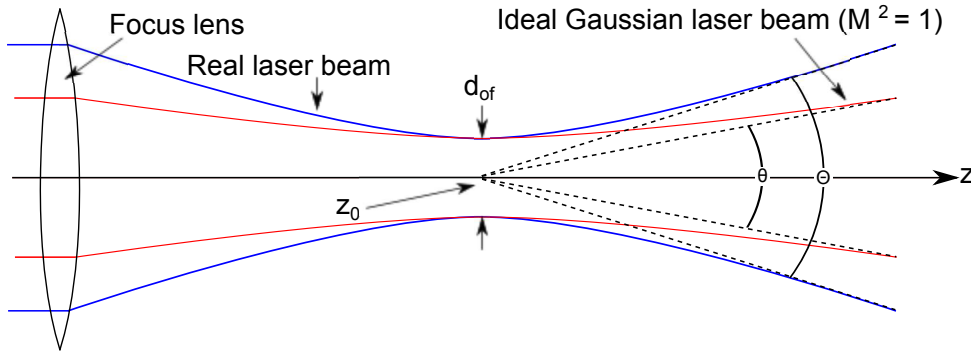


Figure 7.5: M^2 definition, equation 7.3. (Coherent, 2012).

To calculate M^2 , the beam spot diameter at different distances, z , on the laser beam must be known. The M^2 value can then be found from equation 7.4 (William M. Steen, 2010) when several spot diameters are known, see section 7.4.

$$d_z = d_{0f} \left[1 + \left(\frac{4M^2 \lambda z}{\pi d_{0f}^2} \right)^2 \right]^{\frac{1}{2}} \quad (7.4)$$

The theoretical M^2 value can be calculated using equation 7.5 if the BPP is known. BPP is the beam parameter product and is defined as the product of the minimum beam radius and the half beam divergence angle. (Paschotta, 2012).

$$M^2 = \frac{\pi \cdot BPP}{\lambda} \quad (7.5)$$

7.3.4 Depth of focus, DOF

DOF is the distance, z , where the focused laser beam has approximately constant intensity distribution. DOF is defined as z -distance where the beam spot diameter changes $\pm 5\%$. To obtain the optimum cutting quality it is desired that the depth of focus equals the workpiece thickness or is greater, in order to obtain equal kerf width in top and bottom. From equation 7.6 the DOF can be calculated (William M. Steen, 2010). On figure 7.6 the DOF is visualised on a laser beam in a workpiece.

$$DOF = \pm 0.08 \pi \frac{d_{0f}^2}{M^2 \lambda} \quad (7.6)$$

7.3.5 Rayleigh length, z_R

The Rayleigh length is another measure of the depth of focus. The Rayleigh length is defined as the distance, z , over which the beam spot diameter increases by: $\sqrt{2} \cdot d_{0f}$. The Rayleigh length can be found using equation 7.7 and is seen on figure 7.6.

Based on the information on DOF and Rayleigh length, the KW for a cut would theoretically be equal in top and bottom, when the focal point is placed in the middle of a given sheet. It is from (William M. Steen, 2010) unknown which value, is most relevant to use in connection with high quality laser cutting. In the summary, of the results of the experiments, these values are evaluated, section 10.7.

$$R = \frac{\pi d_{0f}^2}{4M^2 \lambda} \quad (7.7)$$

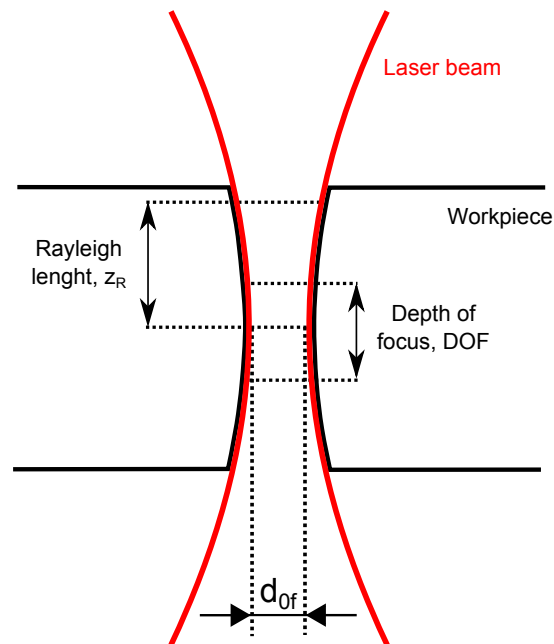


Figure 7.6: Smallest beam spot diameter, d_{of} , of a laser beam, depth of focus and Rayleigh length, of a laser beam in relation to a workpiece.

7.4 Laser beam caustic

In this section the caustic of the laser beam from the AAU setup and IPU setup is analysed through experiments. The purpose of the experiments is to be able to describe the characteristics of the laser beam in order to measure and calculate the actual beam values of the different setups. This is done in order to understand the beam quality values' influence on laser cutting in aluminium.

7.4.1 AAU caustic

For the AAU experiment the following materials and equipment have been used:

- A 1mm thick black anodized aluminium sheet 100x100mm
- A 2mm thick piece of cardboard 80x200mm
- Nd:YAG laser system setup (7.1.1).
- Leitz Metallovert inverted metallurgical microscope with zoom 100x
- Measuring tape
- Spindle on which the cutting head is mounted. One full rotation of it will result in either lifting or lowering the cutting head by 2mm.

On figure 7.1 a sketch of the system setup is seen. The black anodized aluminium sheet is fixated on the XY-table below the cutting head. In the experiment, the cutting optics is removed in order to be able to move the cutting head down without conflicting with the XY-table, figure 7.7.

The spot diameter is defined as 86 % if the beam intensity, 7.3.1. To assure, that the measured spot diameter only is made from 86 % of the beam intensity, experiments with different operating power,

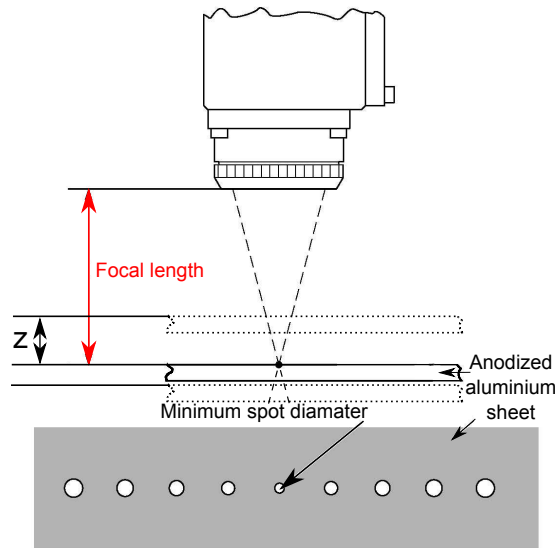


Figure 7.7: Cutting head without nozzle and different spot diameters in anodized aluminium sheet, (GmbH, 2004).

laser on-time and materials are performed. If the laser transfers too much energy ($Power \cdot laser\ on\ time = Joule$) to the material, it is burned or melted and the spot represents more than the 86%. On figure 7.8 it is seen how the beam spot diameter is highly depending on the amount of energy transferred to the aluminium sheet or cardboard.

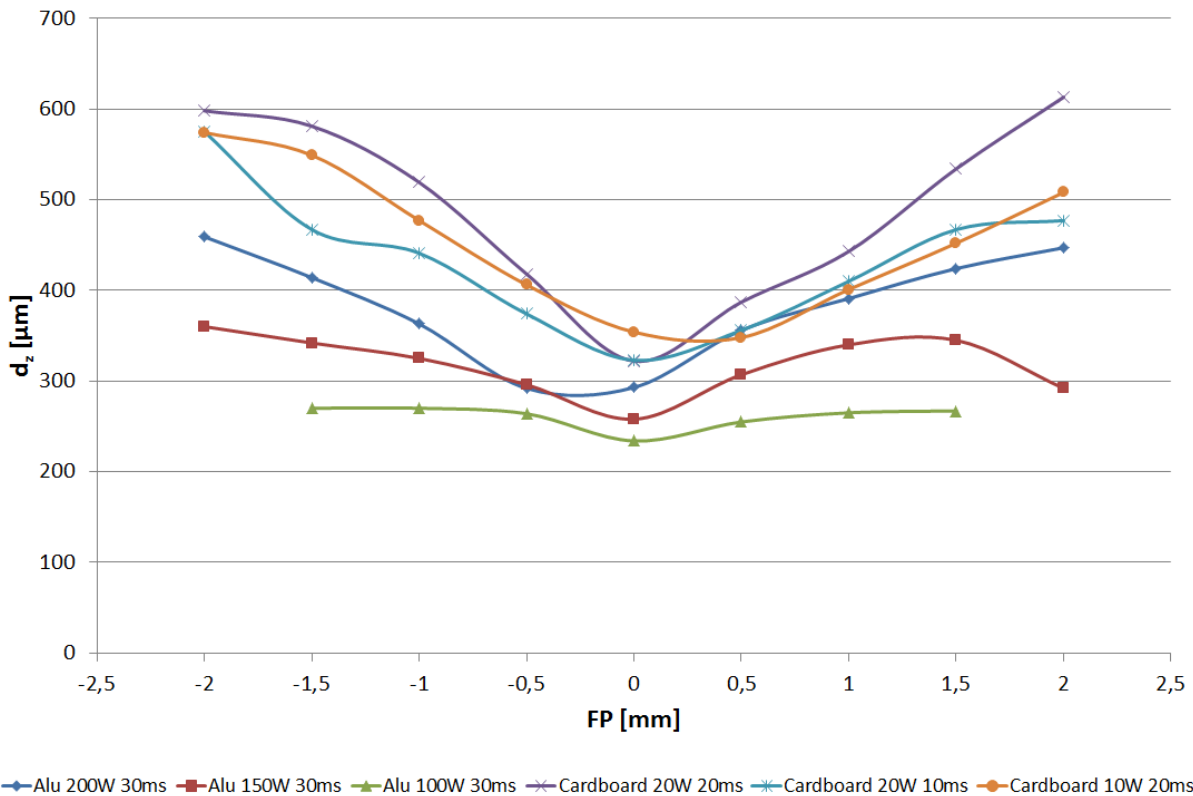


Figure 7.8: Different beam spot diameters as a function of the FP for an anodized aluminium sheet and cardboard with different energy levels. Caustics with slopes far from the average is the most incorrect, and will entail a high error in M^2 value.

The caustic from using 200W in 20ms on the aluminium sheet, is closest to the cardboards caustics and has not been melted in its surface, which happens for 300W in 20ms, see figure 7.9. The experiment with 200 W in 20 ms is therefore used for the caustic. All the experiments are conducted as follows:

The cutting head is adjusted, using a measuring tape, so that the length from the top surface of the aluminium sheet to the focal lens, $z = 150\text{mm}$, figure 7.7. 150mm is the lens' focal length, and should in theory be where the smallest spot diameter is. 9 spots in intervals of 0.5mm are made, when the cutting head is raised and lowered 2.0 mm. This is the same as moving the focal point $\pm 2.0\text{mm}$.

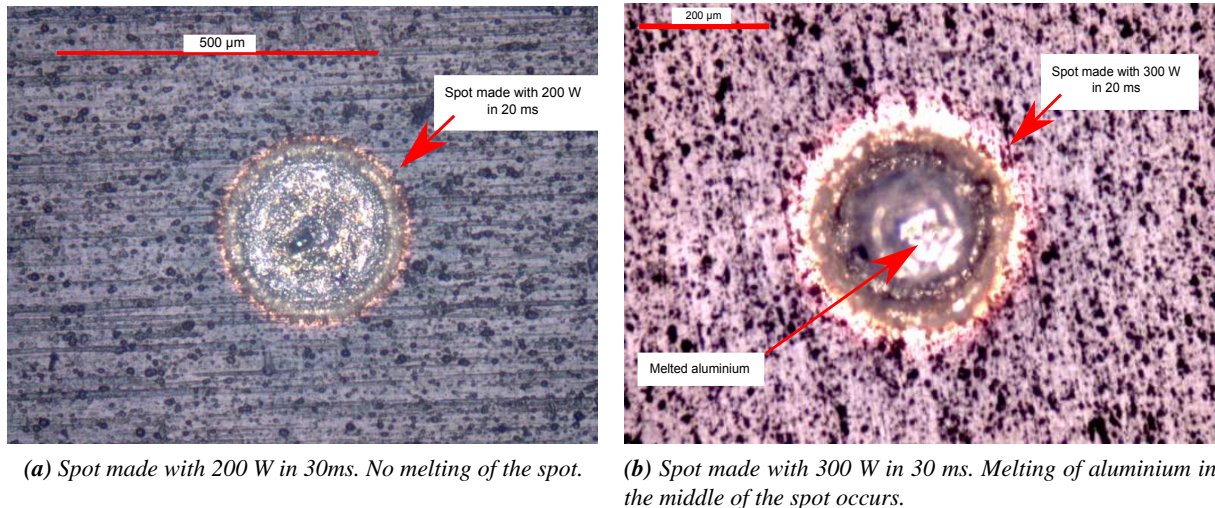


Figure 7.9: Different spot diameters made with the Nd:YAG laser in a black anodized aluminium sheet, $z=150\text{mm}$ ($FP=0.0\text{mm}$). The pictures are taken using a Leitz Metallovert inverted metallurgical microscope with 100x zoom.

From the experiment the following spot diameters are found, see table 7.1. The table suggest that the smallest spot diameter is located in +0.5 mm.

FP [mm]	Spot diameter [μm]
+2.0	459
+1.5	414
+1.0	363
+0.5	292
0.0	293
-0.5	356
-1.0	391
-1.5	424
-2.0	447

Table 7.1: Spot diameters created with different focal points in the anodized aluminium. The spots are measured using a Leitz Metallovert inverted metallurgical microscope with zoom 100x, see appendix A

From the results of the experiments shown in table 7.1 it can be concluded that a smallest beam spot diameter can be found among the measurements. This is due to the fact that the spot diameter increases when the focal point is changed from +0.5mm. The smallest beam spot diameter is 150.5mm from the focal lens to the workpiece which does not corresponds to theory. This is due to an measuring error, when using the measuring tape. Furthermore it can be concluded that the smallest spot diameter is actually

approximately $292 \mu\text{m}$ instead of $225 \mu\text{m}$ as it is found in table 7.4 through theoretical calculations. From picture 7.9 it can be concluded that the Nd:YAG laser beam can be approximated as a gaussian intensity distribution, because more of the aluminium surface is burned (melted) in the middle of the spots. In order to measure the correct intensity distribution beam analysis equipment must be used. The main error for the measurements of the Nd:YAG beam spot diameter, that it cannot be known if 86 % of the beam intensity is represented by the spots in the aluminium. The spots being larger, indicates, that more than 86% of the intensity have burned away the oxide layer in the aluminium. The amount of energy necessary to burn away the oxide layer is not known.

7.4.2 IPU caustic

For the IPU experiment the following materials and equipment have been used:

- IPG YLR-400-SM-WC 7.3.
- PC software, Spiricon
- PC control system
- Laser beam monitoring camera

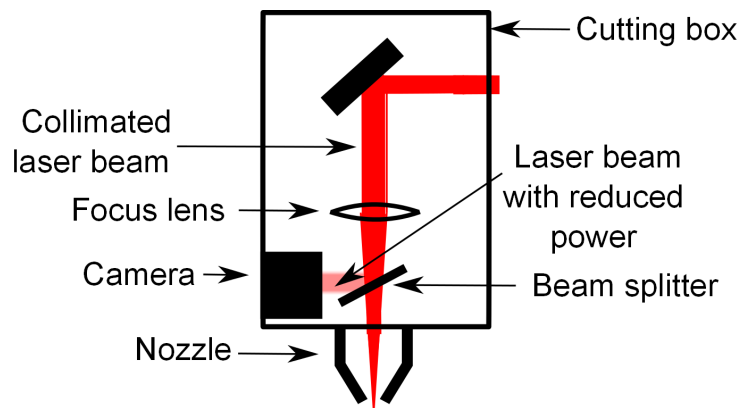


Figure 7.10: Illustration of the camera measuring the beam intensity. The beam splitter lets in a few percent of the laser beam into the camera's chip.

The beam spot diameter is, in the IPU setup, defined as the diameter of the spot wherein 86% of the power exists.

The spot diameter is measured at 48 lengths, z , along the beam. This is done by moving the focus lens from, -5.50mm - 6.25mm , in intervals of 0.25 mm . For each z value, the spot diameter is measured by a camera (monitor), that measures the beam intensity. PC software calculates the spot diameters based on 86 % of the intensity, see figure 7.11. For each spot diameter an operator defines an area, which the software calculations are based on, white circle on figure 7.11. The whole routine is executed through the PC control seen on figure 7.3, which controls the equipment. The 48 measurements of the beam spot diameters are listed in table 7.2.

An error for the experiments is present, by the influence from the operator defining the area wherein the software is capturing the intensity. This entails noise in the picture. The magnitude of this error is

FP [mm]	6.25	6.00	5.75	5.50	5.25	5.00	4.75	4.50	4.25	4.00
Spot, d_z [μm]	228	222	217	205	196	176	170	164	156	150
FP [mm]	3.75	3.50	3.25	3.00	2.75	2.50	2.25	2.00	1.75	1.50
Spot, d_z [μm]	140	134	128	116	110	100	92	85	79	73
FP [mm]	1.25	1.00	0.75	0.50	0.25	0.00	-0.25	-0.50	-0.75	-1.00
Spot, d_z [μm]	66	59	54	50	46	45	45	47	50	55
FP [mm]	-1.25	-1.50	-1.75	-2.00	-2.25	-2.50	-2.75	-3.00	-3.25	-3.50
Spot, d_z [μm]	62	68	75	82	90	98	107	116	123	130
FP [mm]	-3.75	-4.00	-4.25	-4.50	-4.75	-5.00	-5.25	-5.50		
Spot, d_z [μm]	142	151	160	168	177	188	200	212		

Table 7.2: Beam spot diameter for FP = -5.5 - 6.25 mm for the single mode fiber laser at IPU.

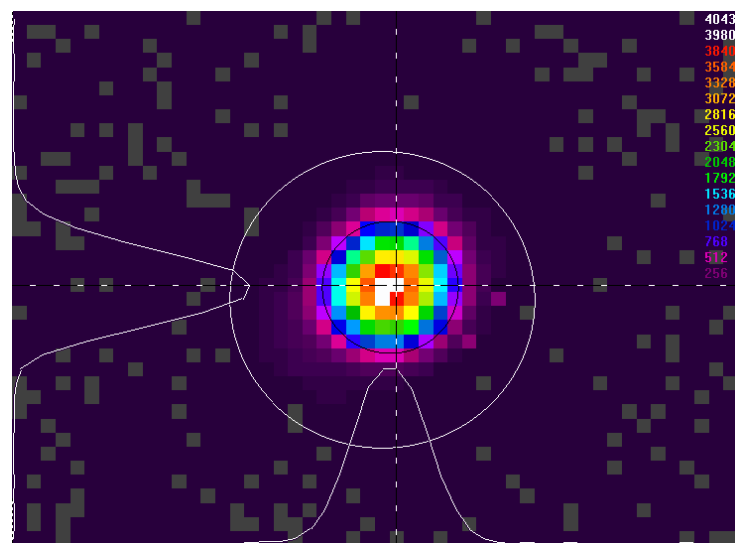


Figure 7.11: The figure shows how the camera captures the beam intensity. 86 % is calculated from the bit values seen on the scale, and the beam spot is identified (black circle). The intensity distribution on the figure is gaussian.

not known, but is considered relatively small because the values found in table 7.4 are very close to the specifications from IPG.

7.4.3 Comparison of laser caustics

In figure 7.12 the caustic of both the Nd:YAG (AAU setup) and the fiber (IPU setup) laser is shown. The influence from using two different measuring methods is very different. The fit for the fiber laser beam is with very small errors, since all the measured, d_z , lies on the fitted line. The fit for the Nd:YAG beam is influenced by noise, because the amount of energy necessary to burn the aluminium surface can vary due to impurity and measuring errors, see A.

Because the fiber laser has a much smaller beam spot diameter than the Nd:YAG laser it is able to reach a much higher average and maximum beam spot intensity, see table 7.4 and thereby be able to cut faster or through thicker materials. From figure 7.12 it can be seen, that the fiber laser beam has a smaller divergence angle, which entails a smaller (better) M^2 value.

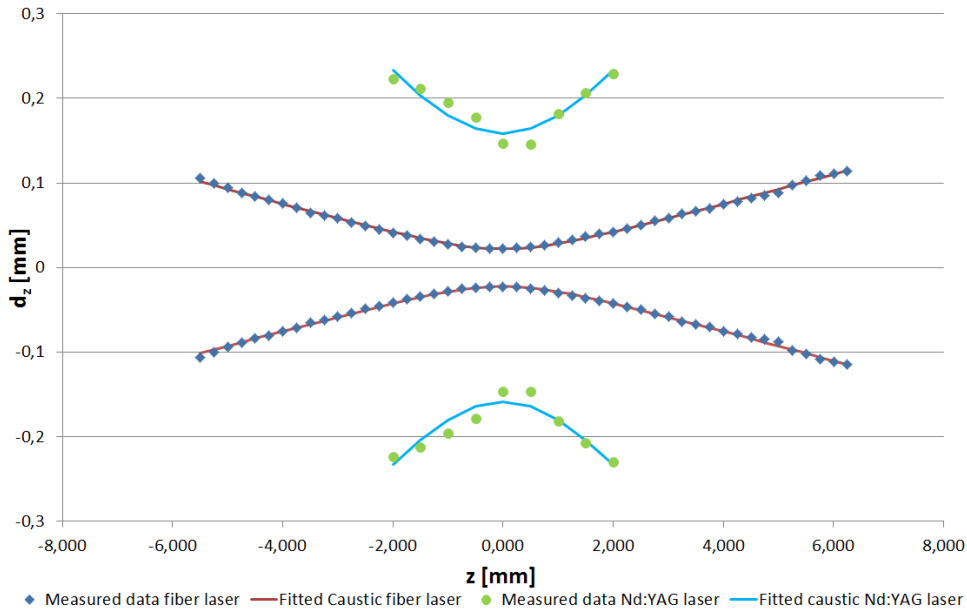


Figure 7.12: The graph shows the measured and fitted caustic of the Nd:YAG (AAU setup) and fiber (IPU setup) laser.

7.5 Summary

In this chapter the system setup along with the material used for experiments in this thesis have been described. In table 7.3 and 7.4 the setup along with specifications on it are shown.

	Specification	Symbol	Value	Unit
Nd:YAG laser machine	Power output		5-380	W
	Beam parameter product	BPP	12	mm·mrad
	Beam quality factor	M^2	35	
	Wavelength	λ	1064	nm
Fiber laser machine	Power output		?-400	W
	Beam parameter product	BPP	0.36-0.38	mm·mrad
	Beam quality factor	M^2	1.05-1.1	
	Wavelength	λ	1065-1075	nm
Nd:YAG laser cutting head	Focal length of collimation unit	f_c	200	mm
	Focal length of lens	f	150	mm
Fiber laser cutting head	Focal length of collimation unit	f_c	100	mm
	Focal length of lens	f	356	mm
Material	Thickness		1	mm

Table 7.3: Summation of specification values found in the laser machines manuals for the Nd:YAG laser (AAU setup) and the fiber laser (IPU setup).

As it is seen from table 7.3 especially the beam quality factor, M^2 , is very different for the setups. An ideal laser beam has an M^2 value of 1. The fiber laser therefore has a near perfect beam quality. The power for the Nd:YAG laser is from table 8.1. The smallest beam spot diameters, the DOF and Rayleigh length is influenced by the laser machine and the collimation and focus optics.

From table 7.4 it is seen that the theoretical value of the Nd:YAG's smallest beam spot diameter is approximately 1.3 times smaller than the measured value. This means that the average power intensity of the Nd:YAG laser becomes approximately 1.8 times lower because the spot area decreases with $\left(\frac{d_{0f}}{2}\right)^2$.

	Specification	Symbol	Nd:YAG laser	Fiber laser	Unit
Beam values (Theoretical)	Smallest beam spot diameter	d_{0f}	225	-	μm
	Average power intensity	I_{avg}	9500	-	$\frac{W}{mm^2}$
	Maximum power intensity	I_{max}	19000		$\frac{W}{mm^2}$
	Beam quality factor	M^2	35	1.05-1.1	
	Depth of focus	DOF	± 0.34	-	mm
	Rayleigh length	z_R	1.1	-	mm
	Specification	Symbol	Nd:YAG laser	Fiber laser	Unit
Beam values (Actual)	Smallest beam spot diameter	d_{0f}	292 (317)	45	μm
	Average power intensity	I_{avg}	5150(4400)	276300	$\frac{W}{mm^2}$
	Maximum power intensity	I_{max}	10300(8800)	552000	$\frac{W}{mm^2}$
	Beam quality factor	M^2	40	1.17	
	Depth of focus	DOF	± 0.59	± 0.41	mm
	Rayleigh length	z_R	1.9	1.2	mm

Table 7.4: Theoretical and actual beam values for both the Nd:YAG (AAU setup) laser and the fiber laser (IPU setup). The smallest beam spot diameter is given as the measured and the fitted diameter is given in brackets. The average beam intensity is in the same way given as the calculated from the measured and the calculated from the fitted inside brackets. The fitted beam spot diameter for the Nd:YAG laser is used to calculate the beam quality values.

The actual M^2 value of the Nd:YAG laser is higher than the anticipated. This along with the actual average power intensity means that the Nd:YAG lasers cutting potential weakens. Because actual smallest beam spot diameter is larger than the theoretical, the beam obtains higher values of the DOF, Rayleigh length. That entails that the average power intensity of the beam decreases less than in theory when moving the focal point. The deviation in the beam values of the Nd:YAG laser is influenced by measuring errors of the beam spot diameters.

Comparing the beam values of the single mode fiber laser and the Nd:YAG laser makes it clear that the fiber laser has a much bigger potential of creating very small cut kerfs or cut much faster due to its small beam spot diameter and its high power intensity.

It is noticeable that the values of the fibers DOF and Rayleigh length are lower than the Nd:YAG laser's. This means that the Nd:YAG laser, if it had enough power, has the potential to cut thicker sheets with less kerf tapering than the fiber laser. It is therefore important to take all of the beam values into account in relation to the relevant cutting task.

Experiments with AAU setup

8

In this chapter a presentation of experiments as well as results/experiences with the Nd:YAG laser previously described (chapter 7) is presented. It is concluded, that it is not possible to cut through an aluminium sheet with a thickness of 1mm with the present setup. The main reasons causing this is analysed in this chapter.

With the Nd:YAG laser the following experiments are conducted:

- Locate the smallest beam spot diameter using an anodized aluminium sheet (chapter 7).
- Measure laser output power after the optics.

The

- Test cutting in 1mm aluminium sheet.

8.1 Operating power at workpiece

The purpose of this experiment is to investigate if the laser machine delivers the expected operating power at the workpiece (after the cutting head) and not just at the laser machine.

In the experiment the following equipment is used:

- Nd:YAG laser system setup (chapter 7) without assist gas
- Ophir Vega power meter
- Ophir 5000W-LP power sensor
- PC control of Nd:YAG laser

A sketch of the setup used in the experiment is seen in figure 8.1.

In the following the procedure used in the experiment is described.

The power sensor is placed underneath the cutting head. The Power sensor is connected to water hoses so that it is cooled during measurement of the laser power. The power meter is connected to the power sensor so that it is possible to manually log the power output shown on the power meter. The cutting head is moved upwards so that the distance between the focal lens to the power sensor is 190mm. By doing this the laser beam is defocused, making a spot with a diameter of approximately 8mm, so that it will not destroy the power sensor. The Nd:Yag laser is turned on at 9 different power levels, see table 8.1, which are adjusted on the pc control, controlling the laser. The power output is logged manually at the 9 different power levels.

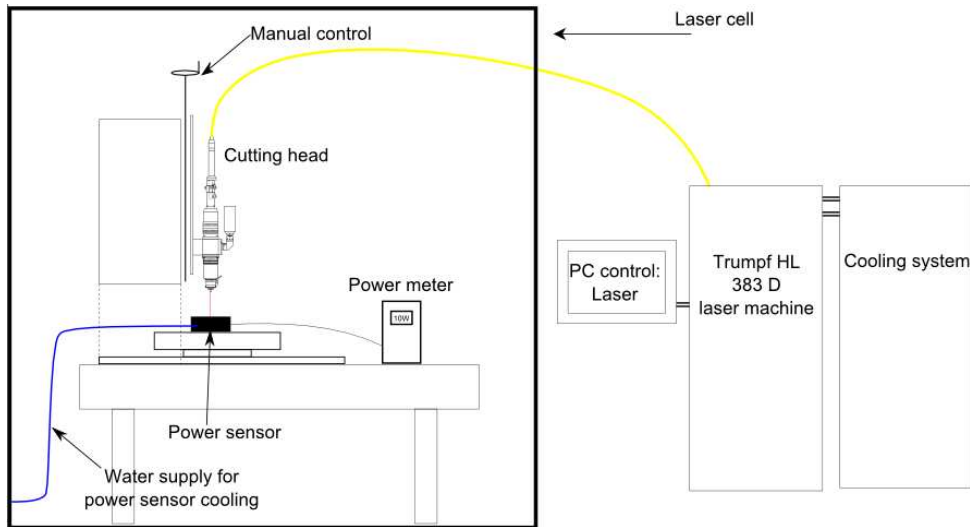


Figure 8.1: Experiment setup for measuring power output of laser.

From the experiment the following results are found, see table 8.1

Laser output [W]	5	50	100	150	200	250	300	350	380
Measured output [W]	2	40	82	132	177	225	269	319	345
Deviation [%]	60	20	18	12	12	10	10	9	9

Table 8.1: Power output measurements, measured using an Ophir 5000W-LP power sensor and an Ophir Vega power meter. The deviation of the measured output compared to the laser output is furtherly shown.

The sources of error in this experiment are:

- Inaccuracy in the power sensor and power meter

From table 8.1 it is seen that the operating power after the optics is approximately 10 percent lower than it should be if only the higher power levels (from 150-380W) are taken into account. From looking at the deviation percentages in table 8.1 it is also seen that the lower the operating power is the more the measured output deviates from the laser output.

The deviation in measured output compared to laser output may be explained by the fact that the power sensor has an inaccuracy of $\pm 5\%$ (Photonics, 2012b). That taken into account the laser power at the workpiece is up to 362W ($345W \cdot 1.05$). Furthermore the deviation in laser output at the workpiece from the laser output at the machine shall be approximately 5% according to (laser GMBH, 2006). The potentially 362W measured output will then become 380W ($362W \cdot 1.05$) at the laser machine. The measured outputs may therefore not be incorrect.

8.2 Cutting in aluminium sheets

The purpose of this experiment is to investigate if the laser in the AAU setup is able to cut through 1mm thick aluminium sheets.

In the experiment the following materials and equipment is used:

- 1mm thick EN-AW 1050A aluminium sheets (chapter 7)
- Nd:YAG laser system setup (chapter 7).
- Nitrogen assist gas
- Measuring tape

On figure 7.1 a sketch of the system setup is seen. The 1mm thick aluminium sheets are fixated on the XY-table. Three attempts of cutting through the 1mm aluminium sheet are made. In each attempt nitrogen assist gas is used at 8bar pressure and with the focal point in the top surface of the sheet. The focal point is adjusted using a measuring tape. In the first attempt the laser is turned on for 1 second at maximum operating laser power (345W). An observation is made that the laser does not cut through the aluminium sheet. In the two last attempts the laser is turned on for 5 and 20 seconds respectively both at maximum operating laser power and from these attempts the same results are experienced.

In this experiment the source of error may be that the focal point used in the experiment (found in section 7.4.1) is not the smallest spot diameter which can be obtained. This error can occur since 0.5mm intervals have been used in order to find the minimum spot diameter and the minimum spot diameter may actually lie in between one of the 0.5mm intervals.

The conclusion on the experiment is that it is not possible to cut through 1mm thick aluminium sheets using the system setup at AAU. The reason for this is due to the following reasons:

- High reflectivity of aluminium compared to steel.
- High thermal conductivity of aluminium compared to steel
- Too low power intensity in the focal point, see table 7.4

Reflectivity

Because the reflectivity for aluminum is high, it entails that less energy from the laser beam is absorbed into the sheet and converted into heat.

The reflectivity of various metals is shown in figure 8.2. The figure shows that the rate of absorption is highly depending in the wavelength of the laser as well as the material. The reflectivity for aluminium with the used Nd:YAG laser is found in equation 8.1 which describes the relationship between the absorption rate and the reflectivity. The rate of absorption for aluminium with an Nd:YAG laser is 5% (Joachim Berkmanns, 2003).

$$Reflectivity = 1 - absorptivity \Rightarrow Reflectivity = 1 - 0.05\% = 95\% \quad (8.1)$$

Because of the reflectivity the operating power, that is converted into heat in the aluminium sheet, is approximately 17 W ($345W \cdot 0.05$) instead of 345 W.

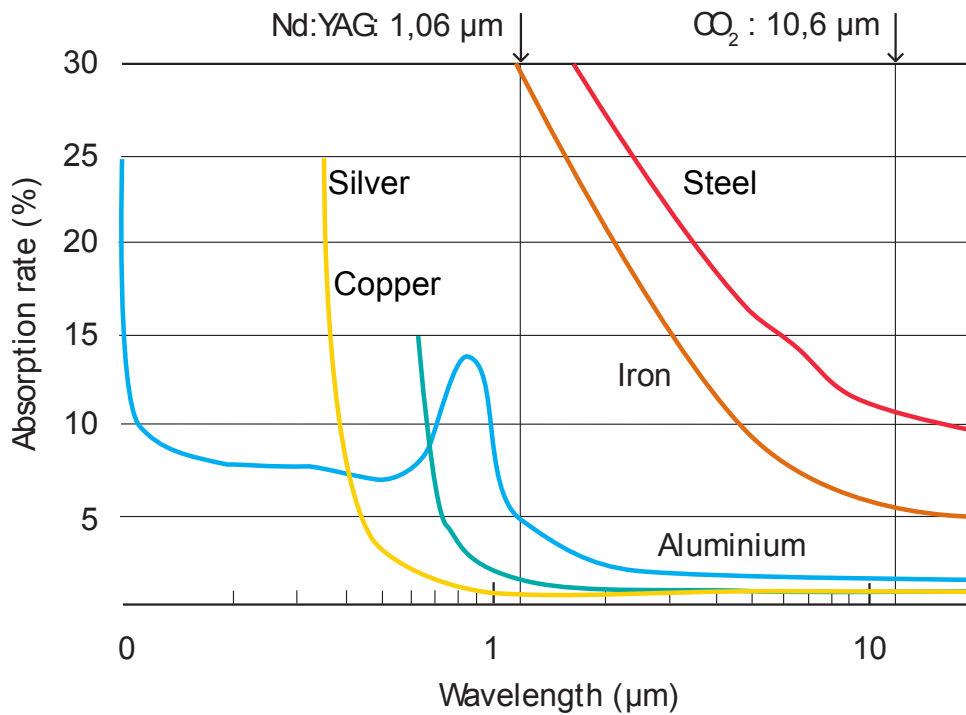


Figure 8.2: The rate of absorption for various metals and two different wavelengths (Joachim Berkmanns, 2003).

Thermal conductivity

The problem with thermal conductivity is related to the mechanisms of transient heat transfer. The same moment energy from the laser beam is transferred onto a single point on the aluminium sheet, the generated heat is conducted away from the cutting kerf and into the whole sheet, see figure 8.3. The higher the thermal conductivity is, the faster the heat is conducted away from the cutting kerf.

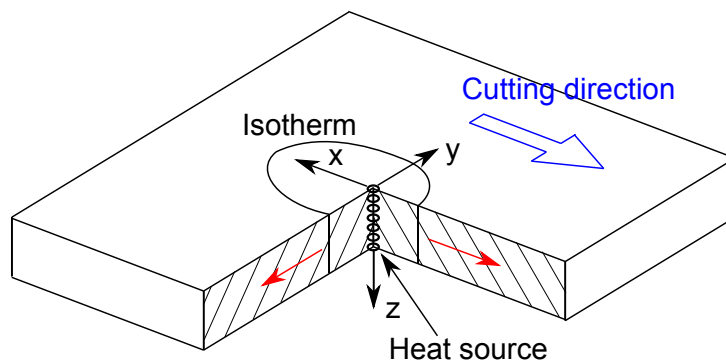


Figure 8.3: The figure shows how thermal conduction distributes heat, generated from a moving laser beam, into the aluminium sheet. The red arrows indicate heat distribution.

To emphasise how much influence thermal conductivity have when cutting in aluminium compared to e.g. stainless steel, Rosenthals equations for 2D heat conduction are used in an example showing how fast heat is conducted in Aluminium 1050A compared to Stainless steel 316. In the example the following assumptions are made, (K. Poorhaydari, 2005):

- Heat is conducted instantaneously through the thickness of the sheets
- A moving heat source is used

- There are no cooling effects, such as assist gas cooling the material.
- Heat transfer from the surface of the workpiece is neglected
- Physical coefficients are independent of temperature

Using Equation 8.2 the time, t , at which the temperature reaches its maximum temperature rise in a given distance from the heat source is calculated (Kristiansen, 2006).

$$t = \frac{\rho \cdot c \cdot y^2}{2 \cdot \lambda_{rc}} \quad (8.2)$$

Where c is the specific heat capacity of the material, ρ is the density of the material, λ_{rc} is the thermal conductivity and y is the distance from the heat source.

Using the thermal properties and physical properties of aluminium 1050A and stainless steel 316 from table 8.2 the time at which the temperature has risen to its maximum in a given distance, y , is found, see table 8.3.

	c [J/kg · K]	λ [W/m · K]	ρ [kg/m ³]
Aluminium 1050A	900	227	2705
Stainless steel 316	500	16.2	8000

Table 8.2: Thermal and physical properties of aluminium 1050A and stainless steel 316 (MATWEB, 2012).

Distance from source(y) [mm]	Time till max. temp. [s]
Aluminium 1050A	
0.1	$5.4 \cdot 10^{-5}$
20	2.1
Stainless steel 316	
0.1	$1.2 \cdot 10^{-3}$
20	49

Table 8.3: Example of calculating the time at which the temperature has risen to its maximum value at the distance, y , from the heat source using Rosenthals 2D heat conductivity equations.

As it is seen in table 8.3 heat is conducted much faster in aluminium compared to stainless steel, in this case approximately 23 times faster. This example makes it clear that thermal conductivity has a role in why it isn't possible to cut in 1mm aluminium sheets with the AAU system setup.

8.3 Conclusion

From the experiments with the Nd:YAG laser it can be concluded that one of the reasons that it is not possible to cut in 1mm thick aluminium sheets is due to the thermal properties of aluminium. Another reason is that a higher power intensity is needed than can be obtained with the Nd:YAG laser with the current system setup.

Experiment description 9

In this chapter the purpose of the laser cutting experiments is be described. The chapter is divided into two sections. The first section presents the experiment used to analyse the effects of control variable and workpiece parameters on the quality parameters. The second section presents assumptions that applies for all the experiments . For all the executed experiments, the system setup at IPU is used, chapter 7.

9.1 Cutting quality experiments

Using the approach described in chapter 6, experiments will be conducted in order analyze the effects from CV and WP on the quality parameters on aluminium sheets, from the laser cutting proces. From these experiments it will be possible to investigate if it is possible to satisfy the requirements from chapter 4.

9.1.1 Experiments theory

For identifying the process window two methods can be used (Kristiansen, 2007):

- Stochastic search

The stochastic search method is a trial error based method. Experiments are conducted without previously a decided plan and instead conducted iteratively in such a way, that the operator gains knowledge from previous experiments.

- Systematic search

The systematic search method is carried out after a pattern which the operator decides. With this method the operator has more control over the experiments than with the stochastic search method.

For the quality experiment a systematic search method is used because of its advantage in having more control over the experiments. The pattern used through systematic search is obtained by using a two-factor factorial design. The factorial design is used when the effects of two or more factors are desired to study. The methodology used in factorial designs (for two CV's) is to combine control variable A, with a settings, with CV B with b settings. The total number of unique experiments becomes $a \cdot b$. The used factorial design is called a fixed effect model, because the settings for each experiment are known beforehand. (Montgomery, 2005a)

In figure 9.1a, a general systematic method for searching for the process window is shown. Figure 9.1b, shows a systematic search by the use of a factorial design. Each setting of CV A and B are combined, executed and evaluated in relation to the requirements for the process window.

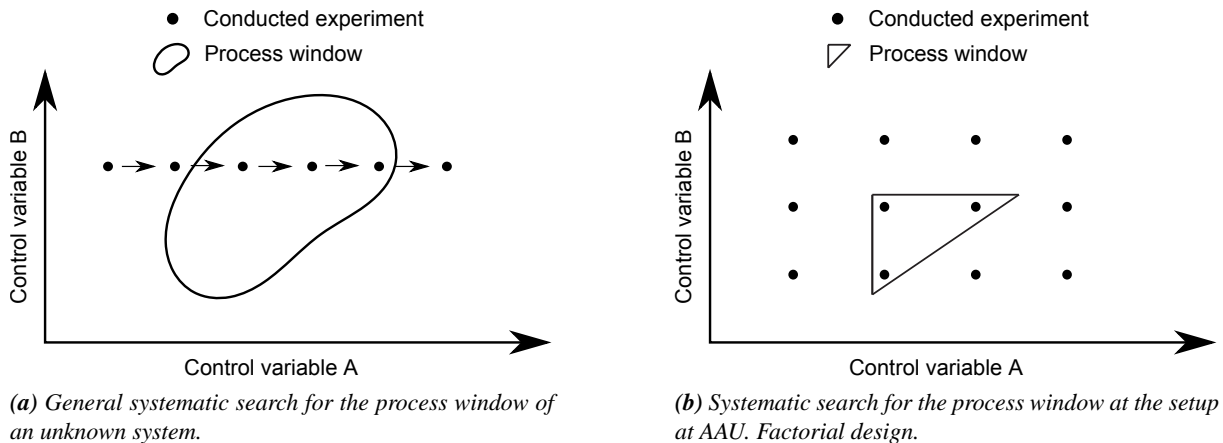


Figure 9.1: Two systematic search methods for the process window.

9.1.2 Selection of control variable and workpiece parameter

From chapter 3 five control variables and two workpiece parameters are defined. If factorial experiments with all combinations of the control variables and workpiece parameters are conducted, the amount of experiments becomes immense. Because of this two different control variables and one workpiece parameter are singled out for conducting experiments:

1. Control variables

- Focal point

From (Caristan, 2004) it is known that the position of the FP is important for high quality laser cutting. More specifically the FP shall be placed close to the bottom of the sheet in order to minimize dross. It is also known, that the focal point affects the cutting speed. Specific knowledge on the effect from using a single mode fiber laser is not known and is therefore desirable to investigate.

- Cutting speed

During initial experiments, it is found that it is necessary to use maximum operating power in order to cut through 1 mm aluminium sheets with the fiber laser. Because it is known that the quality of the cut is dependent on the energy input over time (chapter 3), the cutting speed is changed instead of operating power.

2. Workpiece parameter

- Sheet thickness

Because the laser machines, used for experiments in this thesis, aren't powerful enough to cut through 2mm aluminium sheets as is the case for the speaker grill, (chapter 4), it is chosen to use smaller thicknesses. By doing this, the effects of workpiece thickness on the quality parameters can be analysed.

Three control variables are not investigated during this thesis:

- Operation laser power. This CV is deselected because initial experiments shows, that it is necessary to use the maximum OLP on 420 W, to cut through 1mm aluminium with the desired cutting speeds.
- Assist gas pressure is deselected in order to reduce the number of control variables and to simplify the experiments.
- Stand-off distance. The stand-off distance is not investigated since experience indicates, that the optimum stand-off distance is in the interval of 0.4-1.0mm. (Hansen, 2012).

One workpiece parameter is deselected:

- Specific material properties. This WP is deselected, since a material as close as possible to the alloy B&O uses, is more desirable to use. This way the results from experiments can, to a higher degree, be applied on B&O's case.

9.1.3 Experimental procedure

Two types of experiments are used for the two control variables and single workpiece parameter. This is done to reduce the number of experiments and errors.

- Focal position vs cutting speed (FP vs CS). The sheet thickness is constant for this experiment. $ST = 0.7 \text{ mm}$
- Sheet thickness vs cutting speed (ST vs CS). The focal point is constant for this experiment. $FP = 0.0 \text{ mm}$

On figure 9.2 an illustration is shown of the experimental setup from the side. On figure 9.3 a picture of parts of the setup is shown. The experiments are conducted by first setting up the CV and WP for each experiment in the control software of the system setup or by changing the sheets. Straight cut are used, with the assumption in section 9.2.1.

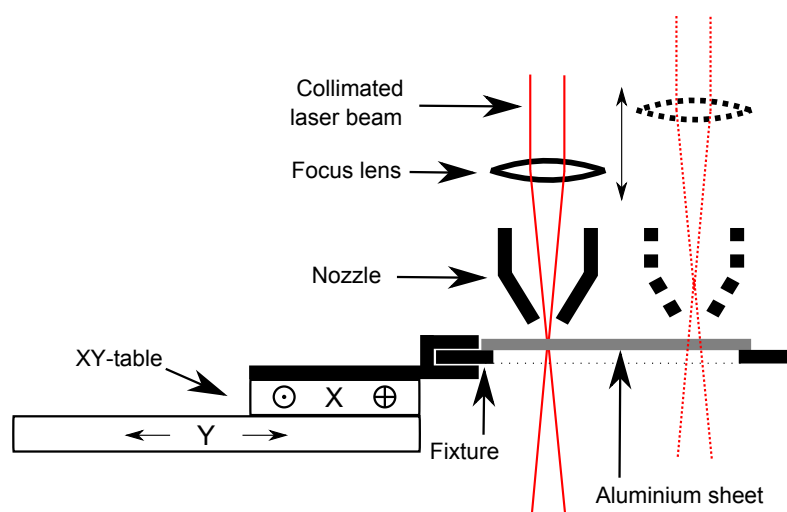


Figure 9.2: Illustration of the experiments conducted at IPU. The dotted lines illustrates a situation where the FP is moved by moving the focus lens. The nozzle is stationary.

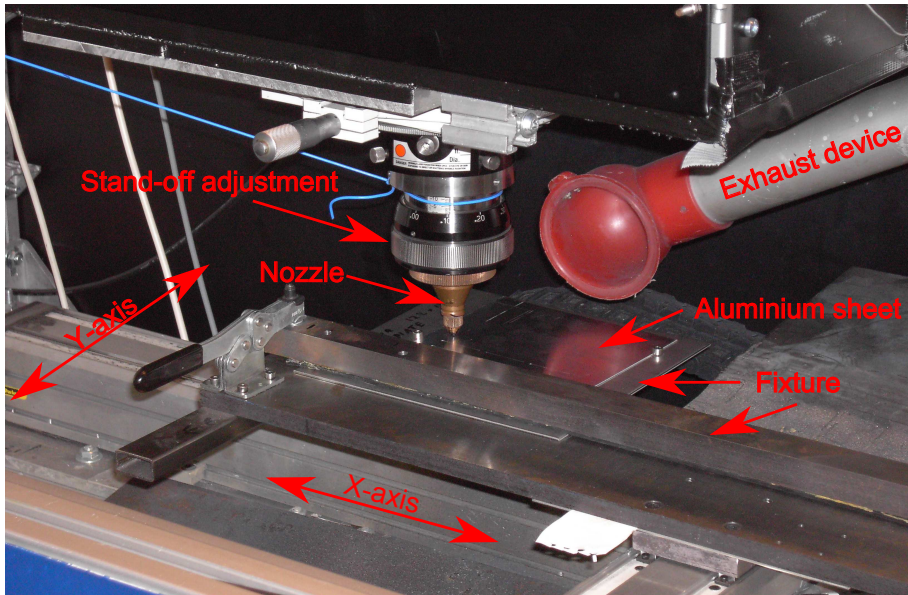


Figure 9.3: Picture of the IPU experiment setup, the viewing angle is slanting in relation to figure 9.2.

Three cuts of 30 mm in length, separated by 5 mm, are cut in an aluminium sheet by letting the PC control move the XY-table in its X-direction, see figure 9.4. The assist gas is turned on before the first cut is made, and turned off after the third. Three cuts are made with constant Y-position. After three cuts are made the Y-position is moved 15mm manually by approximately, before a new line with three cuts is executed from the PC control. All the cut lines begin in the same side of the sheet. Each cut in a line is cut with different settings, that are held constant throughout a specific cut. Each cut is initialized by piercing a hole in the sheet. This is done by turning on the laser for 1 second (420W), to ensure that the starting point for the line is cut through. A piercing time of 1 second is far too long, for both sheets of 0.5, 0.7 and 1 mm in thickness, but is not optimized due to lack of time.

The amount of cuts made in each aluminium sheet along with the placement of the cut varies due to the CVs and STs. In Appendix B figures showing the placement of the cuts on each aluminium sheet can be seen.

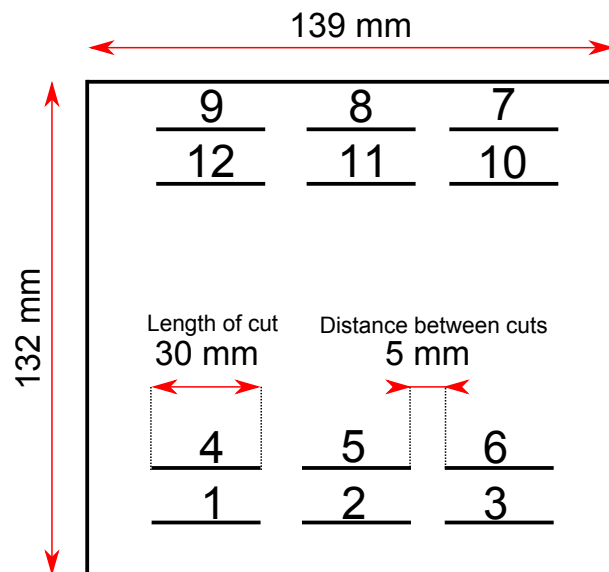


Figure 9.4: Example of straight cuts distributed over an aluminium sheet. The numbers is the experiment ID

Focal point vs cutting speed

In the FP vs CS experiment the position of the focal point and the cutting speed is changed. Six settings of the FP and four for the CS are executed through 24 experiments. The settings used in the experiment can be seen in table 9.1. FP is changed in intervals of 1.0 mm, because it from section 7.4 is concluded, that the spot diameter changes little when the FP is changed. The interval for CS is chosen to be 10 mm/s, to ensure that an effect can be observed and is inspired by (B. Adelman, 2011). STO for experiment 1-24 is set to 0.8mm.

Experiment ID \ CV/WP	CS [mm/s]	FP [mm]	ST [mm]	STO [mm]	OPL [W]	AGP [bar]
1	60	-2.0	0,7	0.8	420	20
2	70	-2.0	0,7	0.8	420	20
3	80	-2.0	0,7	0.8	420	20
4	90	-2.0	0,7	0.8	420	20
5	60	-1.0	0,7	0.8	420	20
6	70	-1.0	0,7	0.8	420	20
7	80	-1.0	0,7	0.8	420	20
8	90	-1.0	0,7	0.8	420	20
9	60	0.0	0,7	0.8	420	20
10	70	0.0	0,7	0.8	420	20
11	80	0.0	0,7	0.8	420	20
12	90	0.0	0,7	0.8	420	20
13	60	1.0	0,7	0.8	420	20
14	70	1.0	0,7	0.8	420	20
15	80	1.0	0,7	0.8	420	20
16	90	1.0	0,7	0.8	420	20
17	60	2.0	0,7	0.8	420	20
18	70	2.0	0,7	0.8	420	20
19	80	2.0	0,7	0.8	420	20
20	90	2.0	0,7	0.8	420	20
21	60	3.0	0,7	0.8	420	20
22	70	3.0	0,7	0.8	420	20
23	80	3.0	0,7	0.8	420	20
24	90	3.0	0,7	0.8	420	20

Table 9.1: FP vs CS experiment. Settings tested to find process window for linear laser cutting with fiber laser. FP and CS are control variables.

Sheet thickness vs cutting speed

Different ST's are used because it is observed that 1mm aluminium can be difficult to cut with the Nd:YAG laser, chapter 8. The ST used are 0.5, 0.7, and 1.0mm because they are available at AAU and to make sure that they are thin enough to be cut with the fiber laser at IPU. The maximum CS is found through an initial experiment, which indicates, that the maximum CS for 1 mm aluminium sheets is 50mm/s. Intervals of 10mm/s are used for the same reasons for the FP vs CS experiment, 9.1.3.

The settings used in the experiment can be seen in table 9.2. The STO for this experiment is held constant at 0.8mm for ST = 0.5mm and ST = 1.0mm and 0.4mm for ST = 0.7mm.

Experiment ID \ CV/WP	CS [mm/s]	FP [mm]	ST [mm]	STO [mm]	OLP [W]	AGP [bar]
25	20	0.0	0,5	0.4	420	20
26	30	0.0	0,5	0.4	420	20
27	40	0.0	0,5	0.4	420	20
28	50	0.0	0,5	0.4	420	20
29	20	0.0	0,7	0.8	420	20
30	30	0.0	0,7	0.8	420	20
31	40	0.0	0,7	0.8	420	20
32	50	0.0	0,7	0.8	420	20
33	20	0.0	1.0	0.4	420	20
34	30	0.0	1.0	0.4	420	20
35	40	0.0	1.0	0.4	420	20
36	50	0.0	1.0	0.4	420	20

Table 9.2: Settings for ST and CS, executed with the fiber laser at IPU.

Data collection

All the results from the FP vs CS and ST vs CS experiments are evaluated for the quality parameters dross, MTE, HAZ, KW and KT, in chapter 10. The method used to measure and evaluate all the experiments can be seen in appendix A.

The heat capacity of the limited area is decisive for how it is affected.

9.2 Assumptions

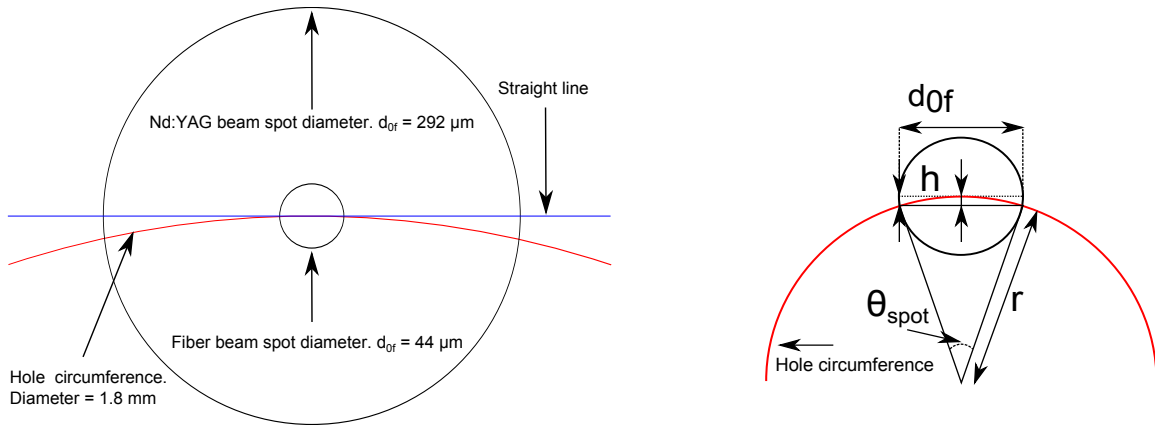
It is assumed that the control variables; STO, AGP and OLP are constant during each experiment. The equipment parameters; assist gas type, nozzle diameter, nozzle design and optical system are also constant, see section 7.1.2.

9.2.1 Approximation of straight cuts

It is chosen that instead of performing experiments of cutting holes, straight lines are cut. This is due to the fact that the XY-table in the IPU setup, section 7.1.2, is not calibrated precise enough to create perfect circular motions. This will affect the quality of the cuts to a high degree, which is not desirable. Calculations of how well an approximation this is, is made by comparing straight cuts to a holes with a diameter of 1.8 mm,. The hole diameter of 1.8 mm is the reference from the speaker grill in chapter 4. Figure 9.5 illustrates this, where a comparison of, how far a section of a hole's circumference is from being straight, in relation to the minimum spot diameter.

The greater the radius of a hole becomes, the smaller the distance, h in equation 9.2, seen on figure 9.5 becomes. The angle θ_{spot} is found in equation 9.1 and is depending on the hole radius and spot diameter. If a hole's radius is infinitely high, the distance, h , becomes zero which is identical to cut a straight line. With this method it can be seen that when the spot diameter increases the approximation to a straight line decreases because h increases, see figure 9.6.

It is found that the ratio for h between the Nd:YAG- and the fiber laser spot is 44. Which means that the fiber laser approximates the straight cut better. Due to the small distance, h for the fiber laser spot



(a) The figure shows a section of the a circle and the Nd:YAG- and fiber laser spot on it. It is clear, that a straight line is approximated significantly better with the fiber laser spot than the Nd:YAG spot. The sizes shown on the figure shows the real ratio between them.

(b) The figure shows where the height, h , between the diameter of the laser spot (the straight line) and the section of a circle circumference is measured. The value of h and θ_{spot} for each laser spot diameter, is shown in table 9.3.

Figure 9.5: Figure and graph used to illustrate how close to a straight line the circular cut looks from the perspective of the spot diameter.

diameter, the assumption of cutting holes, when cutting straight is seen a reasonable approximation.

$$\theta_{spot} = \tan^{-1} \left(\frac{r^2 + r^2 + d_{0f}^2}{2r \cdot r} \right) \cdot \frac{180}{\pi} \quad (9.1)$$

$$h = r \cdot \left(1 - \cos \left(\frac{\theta_{spot}}{2} \right) \right) \quad (9.2)$$

	$d_{0f} [\mu\text{m}]$	$h [\mu\text{m}]$	$\theta_{spot} [^\circ]$
Fiber laser	44	0.27	2.8
Nd:YAG laser	292	11.9	18.7

Tabel 9.3: Comparison on the values and θ_{spot} in relation to a hole circumference.

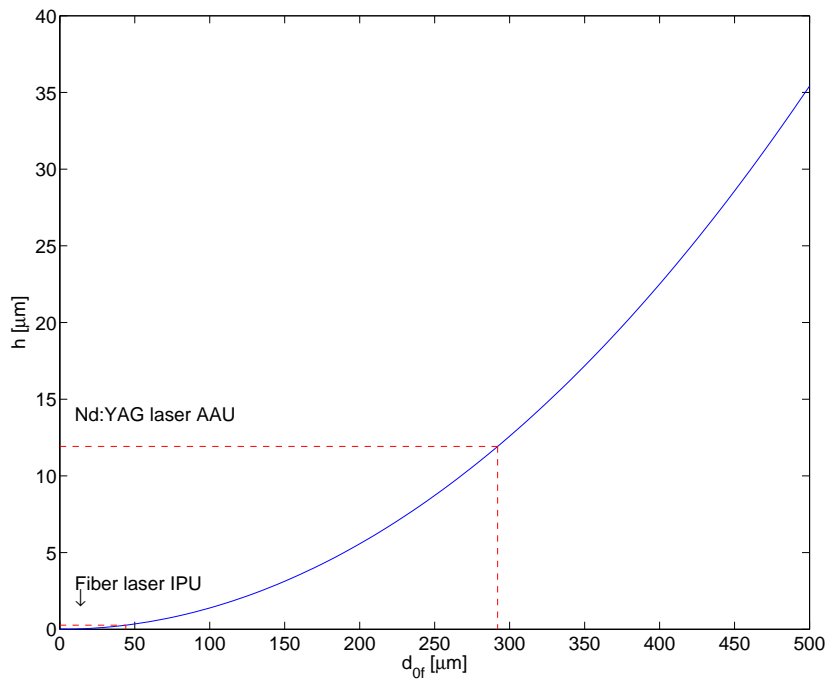


Figure 9.6: The graph shows the distance, h (see figure 9.5b), as a function of the beam spot diameter, compared to a circle with a diameter of 1.8 mm. The distance, h , for the minimum fiber and Nd:YAG laser spot is seen.

9.2.2 Material

It has been chosen to cut in aluminium sheets of the aluminium alloy EN AW-1050A with a thickness of 1 mm. The reason for choosing aluminium alloy 1050A, is that this alloy is the one that is available at AAU and because the aluminium used at B&O is only available in 2mm thick sheets. The alloy elements in the 1050A aluminium alloy is nearly of the same amount of alloy elements as in the B&O alloy with exception of the alloy element Mg. The contents of Mg and Al are also the decisive elements for the mechanical properties of the respective aluminium alloys.

Alloy name	Si	Fe	Cu	Mn	Mg	Cr	Zn	Ti	Others	Al
EN AW-1050A	0.25	0.4	0.05	0.01		0.01	0.07	0.05	0.03	99.5
B&O Alu alloy	0.20	0.20	0.10	0.05	0.8	0.02	0.05	0.03		

Table 9.4: Contents of aluminium alloys, given in percentages, used in this thesis, the EN AW-1050A and the aluminium alloy used at B&O.

Cutting quality experiments -

Results

10

In this chapter the results from the cutting quality experiments are presented. The effects of different settings of the control variables and workpiece parameter are analyzed for the quality parameters; dross, melting of top edge, heat affected zone, kerf width and kerf taper. By evaluating the cutting quality on all the experiments, the optimum settings, of the control variables and workpiece parameter, for obtaining high cut quality, is found.

This chapter is structured in the following way; five sections, one for each quality parameter, are presented. Each section initially describes how the quality parameter belonging to that section is measured. Under each section the results of the two types of experiments, focal position vs cutting speed (FP vs CS) and sheet thickness vs cutting speed (ST vs CS), are presented in their separate subsections. Lastly in each section a conclusion is made based on both types of experiments. The five sections are as follows:

- Dross
- Melting of top edge
- Heat affected zone
- Kerf width
- Kerf taper

In the two types of experiments, FP vs CS and ST vs CS, 24 and 12 experiments are made. Each of those experiments are made with unique settings of the control variables and workpiece parameters and are each given an experiment ID.

For each quality parameter a signal-to-noise ratio (SNR) is calculated for each experiment. An SNR lower than one means that the experiment is influenced more by noise than signal. Likewise, if the mean value of the SNR's of each experiment is lower than one, it means that the experiment type, being FP vs CS or ST vs CS, is influenced more by noise than signal. If this is the case the overall experiment is not further analysed. The SNR is calculated using equation 10.1 and the mean of the SNR's are calculated using equation 10.2 (Montgomery, 2005b).

$$\text{SNR} = \frac{\mu}{s^2} \quad (10.1)$$

Where μ is the mean of the measurements of the quality parameter in each experiment. s^2 is the variance of the measurements of the quality parameter in each experiment.

$$\text{Mean SNR} = \sum_{i=1}^n \text{SNR}_i \quad (10.2)$$

Where SNR_i is the SNR of the i 'th experiment.

Lastly in this chapter an overview of which settings of the control variables and workpiece parameter results in satisfying the requirements of the quality parameters is presented.

NB: In every experiment two systemic errors have influenced the experiments. The first error is a change in the STO due to warping of the sheets in which the experiments are made. The error occur in relation to heating of the material when the experiments are made. The second error occurs in relation to how the sheets are fixated in the XY-table, see 9.3. Because the sheets are fixated in only one side the sheets aren't fixated perfectly horizontally. The change in the STO due to warping and the way the sheets are fixated is estimated to be $\pm 0.2\text{mm}$. The influence of these erros on each quality parameter are evaluated in the quality parameters respective sections.

Experiment 1,2,3,4,8,11 and 12 are not cut through the sheets and are therefore not be included in the results.

10.1 Dross

To measure how much dross there is on each experiment the experiments are cut out of the aluminium sheet as seen in figure 10.1. The cut out experiments are then molded into epoxy and after the epoxy has hardened pictures of the cut kerf seen in profile, see figure 10.2 are taken with a camera through a Leitz Metallovert inverted metallurgic microscope. For each experiment dross is measured **five** times using five different pictures of the same experiment. This is done by sanding down the surface of the epoxy block with a sandpaper, see figure 10.1 and then take a new picture of the experiment. The height between each measurement is approximately 0.2mm.

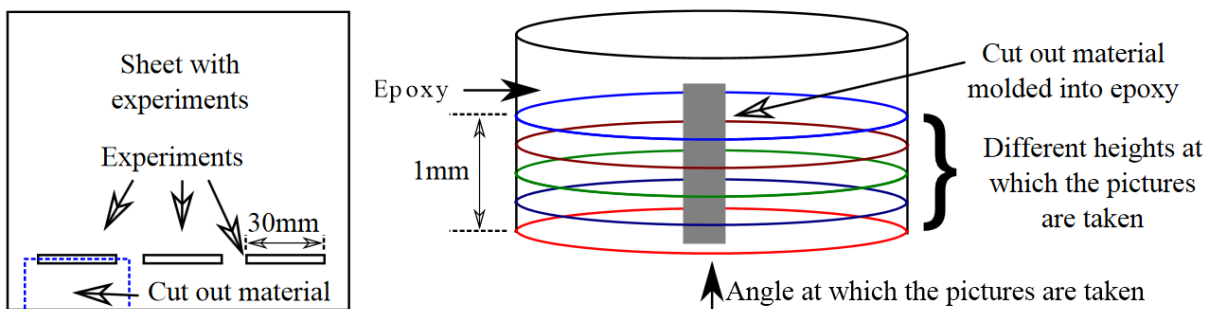


Figure 10.1: To the left a sheet with experiments. The blue dotted line indicates where the experiment is cut out of the sheet. The cut out experiment is molded into epoxy (to the right) so that it can be analyzed. When the epoxy is sanded down, the cut profile can be evaluated in different distances along the cut kerf.

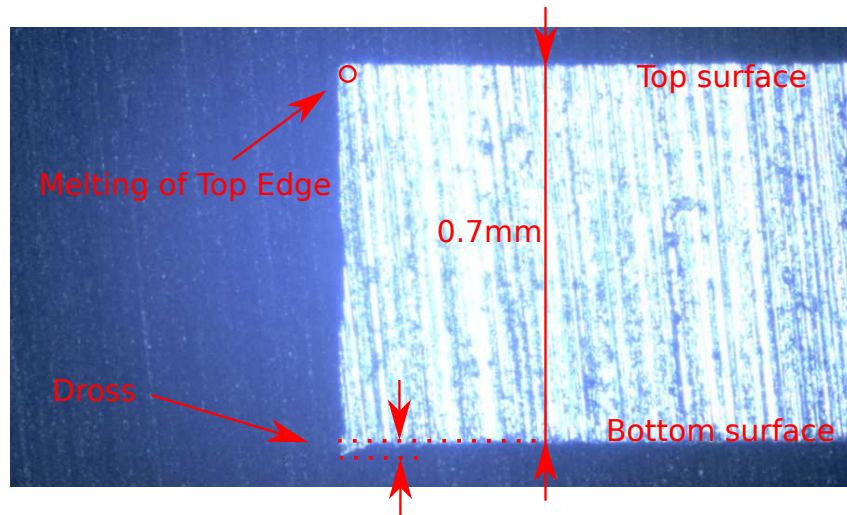


Figure 10.2: The figure shows where dross and MTE are measured on the profile of the laser cut kerfs.

10.1.1 FP vs CS

In table 10.1 the results from the measurements of dross on each experiment is seen. It can be seen that visible dross occur in experiment 6, 7 and 21. For experiment 6 and 7 the FP = -1.0mm, for experiment 21 the FP = 3.0mm. This indicates, that dross occur when the FP is either above or below the top and bottom surface of the sheet respectively. For experiment 5 and 6 the size of the dross has the largest height where CS = 70mm/s and CS = 80mm/s respectively.

Exp. ID	Control variables		Picture no./Dross [μm]					SNR
	CS [$\frac{mm}{s}$]	FP [mm]	1	2	3	4	5	
5	60	-1.0	0	0	0	0	0	-
6	70	-1.0	0	0	0	78	87	0.02
7	80	-1.0	0	0	0	0	48	0.03
9	60	0.0	0	0	0	0	0	-
10	70	0.0	0	0	0	0	0	-
13	60	1.0	0	0	0	0	0	-
14	70	1.0	0	0	0	0	0	-
15	80	1.0	0	0	0	0	0	-
16	90	1.0	0	0	0	0	0	-
17	60	2.0	0	0	0	0	0	-
18	70	2.0	0	0	0	0	0	-
19	80	2.0	0	0	0	0	0	-
20	90	2.0	0	0	0	0	0	-
21	60	3.0	21	18	0	0	0	0.08
22	70	3.0	0	0	0	0	0	-
23	80	3.0	0	0	0	0	0	-
24	90	3.0	0	0	0	0	0	-
Mean SNR								0.04

Tabel 10.1: Results of measuring dross on experiment 1-24. Experiment 1-4 with FP = -2.0mm are not cut through the sheet and can therefore not be measured. Also experiment 8, 11 and 12 are not cut through the sheet making it impossible to measure them.

10.1.2 ST vs CS

In table 10.2 the results from the dross measurements for the three sheet thickness' is seen. Dross occurs in experiment 25, 27, 28, 31, 33 and 34. Among the five measurements of the same cut, dross is mostly seen on experiment 31 and 34.

Exp. ID	Control variables		Picture no./Dross [μm]					SNR
	CS [$\frac{mm}{s}$]	Thickness [mm]	1	2	3	4	5	
25	20	0.5	0	0	5	0	0	0.25
26	30	0.5	0	0	0	0	0	-
27	40	0.5	12	0	0	0	0	0.10
28	50	0.5	0	8	0	0	0	0.16
29	20	0.7	0	0	0	0	0	-
30	30	0.7	0	0	0	0	0	-
31	40	0.7	0	0	16	0	16	0.10
32	50	0.7	0	0	0	0	0	-
33	20	1.0	0	27	0	0	0	0.05
34	30	1.0	17	13	0	0	0	0.11
35	40	1.0	0	0	0	0	0	-
36	50	1.0	0	0	0	0	0	-
Mean SNR								0.13

Table 10.2: Results of measuring dross on experiment 25-36.

10.1.3 Sources of error

For measuring dross the following sources of error are present:

- Caliper tool: the magnitude is approximated to be $\pm 2\mu m$.
- Sanding epoxy blocks: the magnitude is estimated to be negligible.

The sources of error are related to the use of the NI Vision Builder software and are further described in appendix A

10.1.4 Conclusion/analysis

Due to the mean values of the SNR in each type of experiment the two experiment types aren't analysed further with statistical methods.

According to the results of the 36 experiments made the setting of the control variable FP is the most important comparing to the CS and the ST. This conclusion is based on the fact that dross is seen on all ST's but for FP = 1.0 - 2.0mm dross isn't seen.

From section 3.4.4 it is known, that dross is affected by: CS, AGP, assist gas pressure type and FP. This corresponds to the results, but the magnitude of the effect of the control variables is not known. From (Caristan, 2004) it is known, that dross can be reduced in aluminium sheets, by having FP = 0.0mm. This however do not correspond with the results in table 10.2.

For all the cuts assist gas pressure of 20 bar is used. This is a relative high pressure for laser cutting (Caristan, 2004). This entails, that that the molten material is blown away before it solidifies on the bottom of the kerf and becomes dross, which may explain why dross isn't seen more on the cut kerfs.

The influence of the assist gas pressure will not be investigated in this thesis.

Based on the results of the experiments it is concluded that the sources of error described above doesn't have a significant influence on the experiments. Regarding the systematic errors in STO it is unknown how much influence the errors contribute to the height of dross.

When evaluated in relation to the requirement from the case, chapter 4, only experiment 6 and 7 doesn't satisfy the maximum dross height of $44 \mu\text{m}$.

10.2 Melting of top edge

MTE is measured using the same pictures as the ones used for measuring dross. On figure 10.2 it is seen where MTE is evaluated on the cut kerf. Often the top edge on the pictures where MTE is measured is unclear making it difficult to define where the edge is, see figure 10.3. The pictures are therefore manipulated by laying in helplines along the top surface and the cut edge, see experiment 17 in figure 10.3. A reference circle, which has the same radius as the maximum allowed radius according to the definition made in chapter 4, is fitted to the top edge using the helplines. The circle which is fitted must have both helplines as tangents to the circle. If the top edge is outside the reference circle the edge is defined as a sharp edge. Because of the difficulties in measuring a sharp edge, sharp edges will be given the "value" S instead of a radius. If the top edge isn't outside the reference circle the top edge is measured using NI Vision Builder, see appendix A.

The use of the "value" S for the sharp edges implicates that there cannot be calculated an SNR and a mean SNR for each experiment and each experiment type respectively.

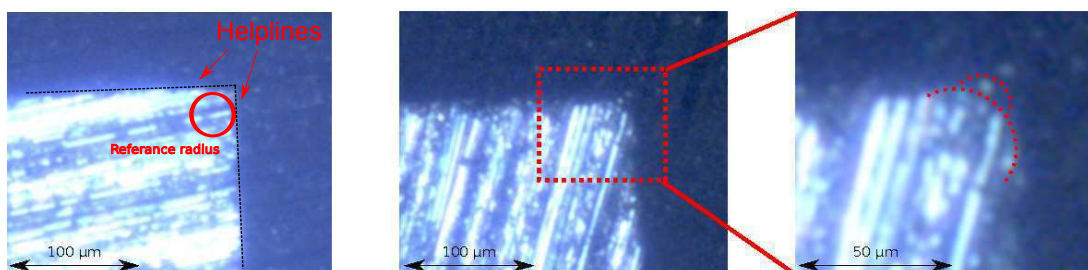


Figure 10.3: On experiment 17 (left) the reference radius is compared to the top edge of the cut. The reference circle is aligned with the vertical and horizontal helpline. Because the top edge is not inside the circle, its radius is smaller than the reference, and the edge is defined as being sharp. On cut 20 (middle and right) it is seen, that the top edge is unclear making it difficult to identify the correct radius of a sharp edge.

10.2.1 FP vs CS

In table 10.3 the measurement of MTE is seen. From the measurements it can be seen that molten edges occur in experiment 5, 16, 23 and 24. For experiment 5 a molten edge is measured on three of the five measurements of the cut, which is the highest number of molten edges in the FP vs CS experiments. As observed for dross it can be seen, that molten edges occur when the FP is either below the bottom surface (-1.0mm) or above the top surface (3.0mm) of the workpiece, with exception of experiment 16. The largest radius of molten edges occur for FP = 3.0mm for CS = 80 and 90mm/s .

Exp. ID	Control variables		Picture no./MTE [μm]				
	CS [$\frac{mm}{s}$]	FP [mm]	1	2	3	4	5
5	60	-1.0	55	S	147	50	S
6	70	-1.0	S	S	S	S	S
7	80	-1.0	S	S	S	S	S
9	60	0.0	S	S	S	S	S
10	70	0.0	S	S	S	S	S
13	60	1.0	S	S	S	S	S
14	70	1.0	S	S	S	S	S
15	80	1.0	S	S	S	S	S
16	90	1.0	S	S	S	47	S
17	60	2.0	S	S	S	S	S
18	70	2.0	S	S	S	S	S
19	80	2.0	S	S	S	S	S
20	90	2.0	S	S	S	S	S
21	60	3.0	S	S	S	S	S
22	70	3.0	S	S	S	S	S
23	80	3.0	S	36	S	S	S
24	90	3.0	114	80	S	S	S

Tabel 10.3: Results of measuring MTE on experiment 1-24.

10.2.2 ST vs CS

For the ST vs CS experiments the results in table 10.4 shows molten edges for experiment 25, 27, 28 and 34. Molten edges occur on ST's of 0.5mm and 1.0mm). The ST where molten edges occur most often is 0.5mm, seen in experiment 25, 27 and 28. The molten edges with the largest radius are also found for a ST of 0.5mm (experiment 5).

Exp. ID	Control variables		Picture no./MTE [μm]				
	CS [$\frac{mm}{s}$]	Thickness [mm]	1	2	3	4	5
25	20	0.5	377	104	S	S	43
26	30	0.5	S	S	S	S	S
27	40	0.5	92	63	51	46	62
28	50	0.5	S	S	S	60	S
29	20	0.7	S	S	S	S	S
30	30	0.7	S	S	S	S	S
31	40	0.7	S	S	S	S	S
32	50	0.7	S	S	S	S	S
33	20	1.0	S	S	S	S	S
34	30	1.0	55	S	S	S	S
35	40	1.0	S	S	S	S	S
36	50	1.0	S	S	S	S	S

Tabel 10.4: Results of measuring MTE in experiment 25-36.

10.2.3 Sources of error

For measuring MTE the following sources of error are present:

- Sanding epoxy blocks: the magnitude is estimated to be negligible on the edges that aren't defined as molten edges.
- Manual circle fitting: as it was described in the beginning of section 10.2, circles are manually fitted on the pictures taken. Based on the picture resolution and zoom level, an approximation is made that the error is $\pm 5\mu m$.

The sources of error are related to the use of the NI Vision Builder software and are further described in appendix A

10.2.4 Conclusion/analysis

For all experiments with FP = 2.0mm and 0.0mm, no molten edges are observed for the FP vs CS experiment. Two molten edges are observed for FP = -1.0mm and 1.0mm. Based on these observations it is difficult to conclude what the influences are of the FP and CS.

For the ST vs CS experiment one measurement for ST = 1.0mm has a molten edge, while nine measurements for ST = 0.5 mm has molten edges and no edges are molten when ST = 0.7mm. This indicates that for thin sheets (ST < 0.7mm) molten edges occur more easily. A possible explanation is that the heat generated in the cut kerf has less thickness to disperse in. This will though not be further analysed in this thesis.

The largest source of error lies in the selection of the edge that defines the fitted circle and thus also the radius measured. A better sanding process will make the surface of the epoxy blocks more smooth. This will entail that better pictures can be taken. Better pictures entail a better possibility to define the sharp edges. By being able to define the sharp edges these can be measured which may give more information on what influences the MTE.

Experiment 5, 16, 23, 24, 25, 27, 28 and 34 does not satisfy the requirements from chapter 4.

10.3 Heat affected zone

For this section FP vs CS and ST vs CS are evaluated in the same section. This is done since none of the 36 experiments shows any HAZ, in this thesis HAZ = color change, along the kerfs, see figure 10.4 for an example.



Figure 10.4: Example of an experiment showing that no HAZ occurs but that spatter (the brownish color) occurs around the piercing point.

When creating the experiments the laser starts by piercing the sheet. When piercing the sheet a brownish curvature around the piercing hole occurs, see figure 10.4 and 10.5. This is not HAZ, but an effect of burned spatter which occurs before the laser beam has pierced through the sheet. This phenomenon occurs because the aluminium at first cannot be ejected downwards because the laser haven't gone through the workpiece. Not before a hole, through the sheet is made, can the molten material be ejected through the

bottom of the cut kerf. As a result of this the aluminium spatter will burn itself onto the surface of the workpiece as a brownish layer of soot.

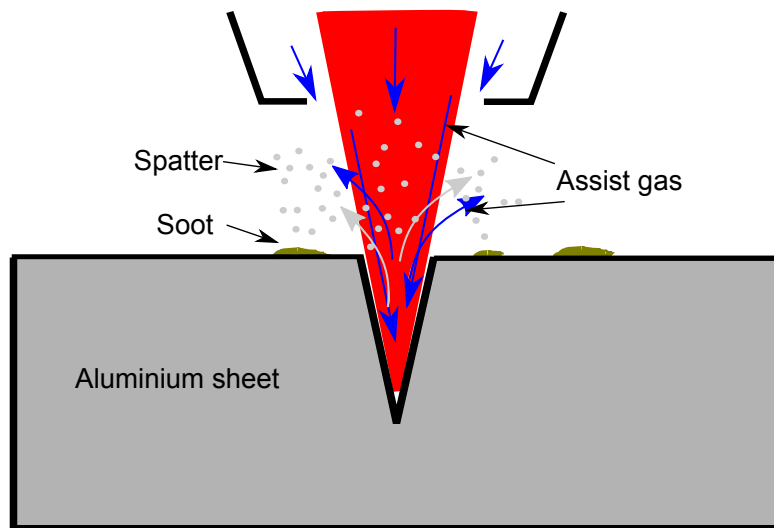


Figure 10.5: Before the workpiece is fully pierced aluminium spatter occurs resulting in a brownish layer of soot on the workpiece.

10.3.1 Conclusion/analysis

Based on the experiments made in this thesis it is concluded that HAZ does not occur in aluminium.

10.4 Kerf width

The kerf width is measured by analysing pictures, of the top and bottom surface of the experiments. The pictures represent a section of the experiments as seen in figure 10.6. The pictures are analyzed using NI Vision Builder. The kerf width is measured at 10 different positions along the picture of the kerf, see figure 10.6. For more information on the method used for analysing the pictures see appendix A

Because of the number of measurements (10 measurements on each experiment) the amount of data is too large to present in the report. Boxplots representing the data are instead used. The boxplots gives a simple overview of how the measurements are distributed. For more information about boxplots see appendix C. Along with the boxplots tables containing the mean, standard deviation, maximum and minimum value of the raw data are presented for both the top and bottom kerf of each experiment. The raw data can be seen on the appendix-DVD in the file "Chapter 10/Raw data/Kerf Width.xlsx".

To analyse which control variables/workpiece parameter has influence on the top and bottom KW, analysis of variance (ANOVA) is made. An ANOVA is made individually for the top kerf and bottom kerf in both the FP vs CS and ST vs CS experiments (in total 4 ANOVA's). The ANOVA method is based on theory explained in appendix C.

10.4.1 FP vs CS

In figure 10.7 the variation in the measurements of the FP vs CS experiments are seen. The boxplot is arranged after the control variable; CS. This entails that the influence of the FP can be seen for each CS.

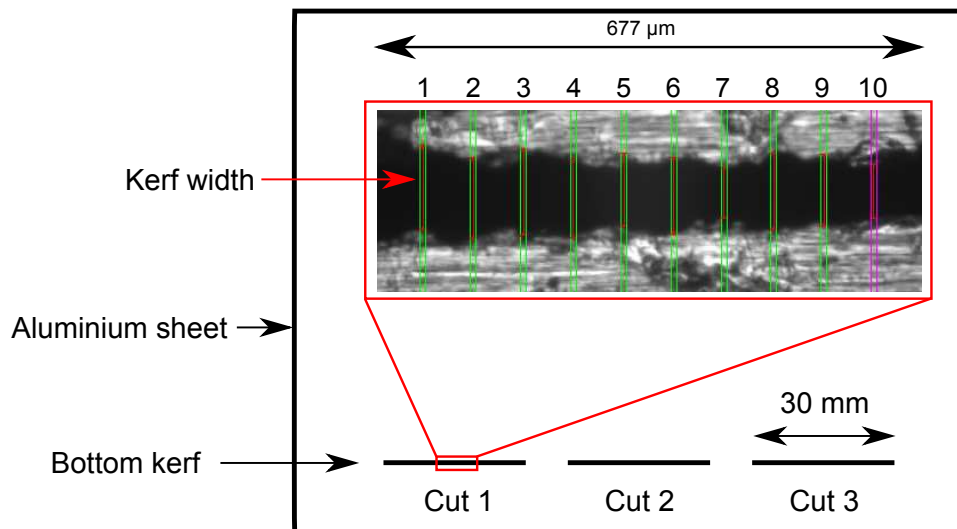


Figure 10.6: Example of 10 measurements of the bottom KW for a cut in a 0.7 mm thick aluminium sheet. The red lines, inside the green boxes, is the found edges.

The blue boxes represents the top KW and the red boxes the bottom KW.

The KW's of the experiments are seen in table 10.5. In table 10.5 the KW's from experiment 5-24, for both top and bottom KW are seen. The mean is found from all measurements of the KW in a single picture (including those measurements which in the boxplot are defined as outliers), the standard deviation, s , is found using equation 10.3. The mean KW is stated with the precision of a whole number, because of the influence from measurement errors, see appendix A. The standard deviation is stated with a precision of one decimal, this way it is comparable with the measurements of the roundness in chapter 4.

$$s = \sqrt{\frac{\sum_{i=1}^n (x_i - \bar{x})^2}{n - 1}} \quad (10.3)$$

Where: x_i is each single measurement of the KW in top or bottom for a specific experiment. \bar{x} is the mean of the measurements. n is the number of measurements for each experiment. (Montgomery, 2005b)

From the boxplots it can be seen, that for all the CS's, the difference between the top and bottom KW is largest at FP = -1.0mm. From the boxplot it can also be seen that as the FP decreases, the KW difference decreases likewise.

It is noticeable, that the bottom box for experiment 12 is only based on three measurements. The matlab tool used for the boxplot, has automatically inserted seven zeroes for the missing measurements explaining why the box looks the way it does.

From the results in table 10.5 it can be seen that there are large deviations in the mean KW when comparing the top and bottom mean KW. This is further illustrated in figure 10.8 where the top and bottom mean KW of the experiments with CS = 60mm/s and CS = 70mm/s. It can be seen that the control variable, having the largest influence on the KW, is the FP. The mean KW in the top is larger than in the bottom for all the experiments when the FP = -1.0mm, 0.0mm and 1.0mm (experiment 5-16).

From table 10.5 it can be seen, that the standard deviation for the top and bottom KW are differs much relative (1.1-15.0 μm) from each other in every experiment. For all the experiments, the top KW has a

¹The mean of the KW at the bottom is only based on measurements at three points in the kerf.

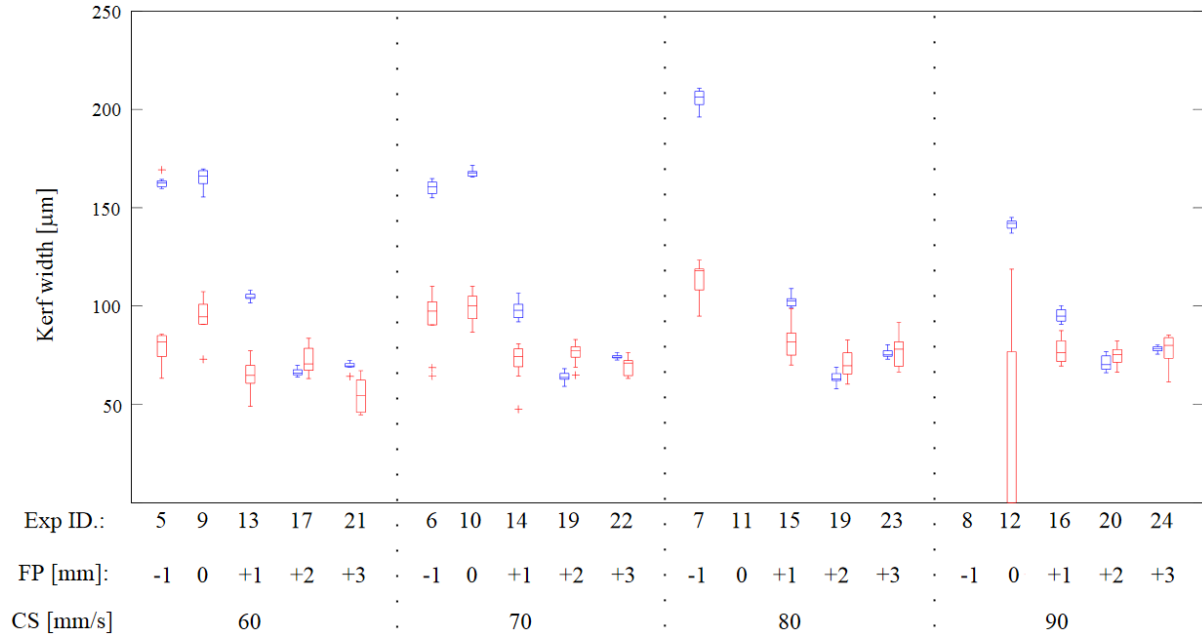


Figure 10.7: Boxplot for FP vs CS experiments. The experiments are arranged after CS first and then FP.

Exp. ID	Control variables		Mean KW [μm]		Std. dev. [μm]		SNR	
	CS [$\frac{\text{mm}}{\text{s}}$]	FP [mm]	Top	Bottom	Top	Bottom	Top	Bottom
5	60	-1.0	163	79	2.7	7.1	24.49	1.73
6	70	-1.0	160	93	3.5	15.0	14.68	0.46
7	80	-1.0	205	114	4.5	8.7	11.14	1.69
9	60	0.0	165	94	4.5	9.1	8.90	1.26
10	70	0.0	168	99	1.9	7.7	51.96	1.84
12 ¹	90	0.0	142	95	2.4	46.8	27.04	0.30
13	60	1.0	105	65	2.1	8.1	25.88	1.10
14	70	1.0	98	72	4.7	10.0	4.91	0.80
15	80	1.0	103	82	2.9	8.7	13.34	1.21
16	90	1.0	95	77	3.2	6.2	10.38	2.14
17	60	2.0	66	72	1.9	6.9	20.30	1.70
18	70	2.0	64	76	2.5	5.6	12.26	2.70
19	80	2.0	63	71	3.5	6.9	5.67	1.62
20	90	2.0	71	70	3.6	4.5	5.93	4.03
21	60	3.0	70	55	2.2	8.6	16.07	0.82
22	70	3.0	74	70	1.1	4.5	64.26	3.79
23	80	3.0	76	77	2.4	8.7	14.54	1.13
24	90	3.0	78	77	1.4	7.8	46.97	1.41
Mean SNR							21.81	1.65

Table 10.5: Results of the FP vs CS experiments.

smaller standard deviation compared to the bottom KW. This is further illustrated on figure 10.9 which illustrates the standard deviation of the top and bottom KW of the experiments with CS = 60mm/s and CS = 70mm/s. The reason for the deviation in the standard deviation can be seen on figure 10.10a when comparing the kerf to figure 10.10b. The two figures 10.10a and 10.10b clearly shows that the kerf in figure 10.10b is much smoother along the length of the cut compared to the kerf in figure 10.10a. The minimum standard deviation among the top KW's is 1.1 μm (experiment 22), and maximum 4.7

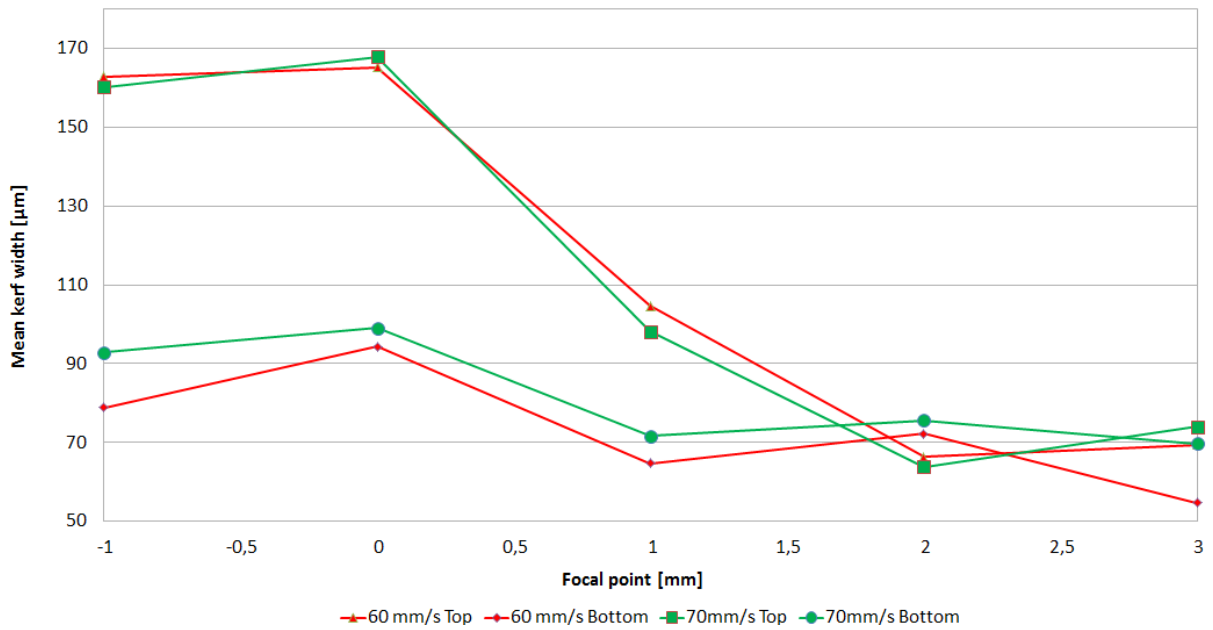


Figure 10.8: The graph shows the mean KW of experiments, with CS = 60mm/s and CS = 70mm/s, as a function of their FP's.

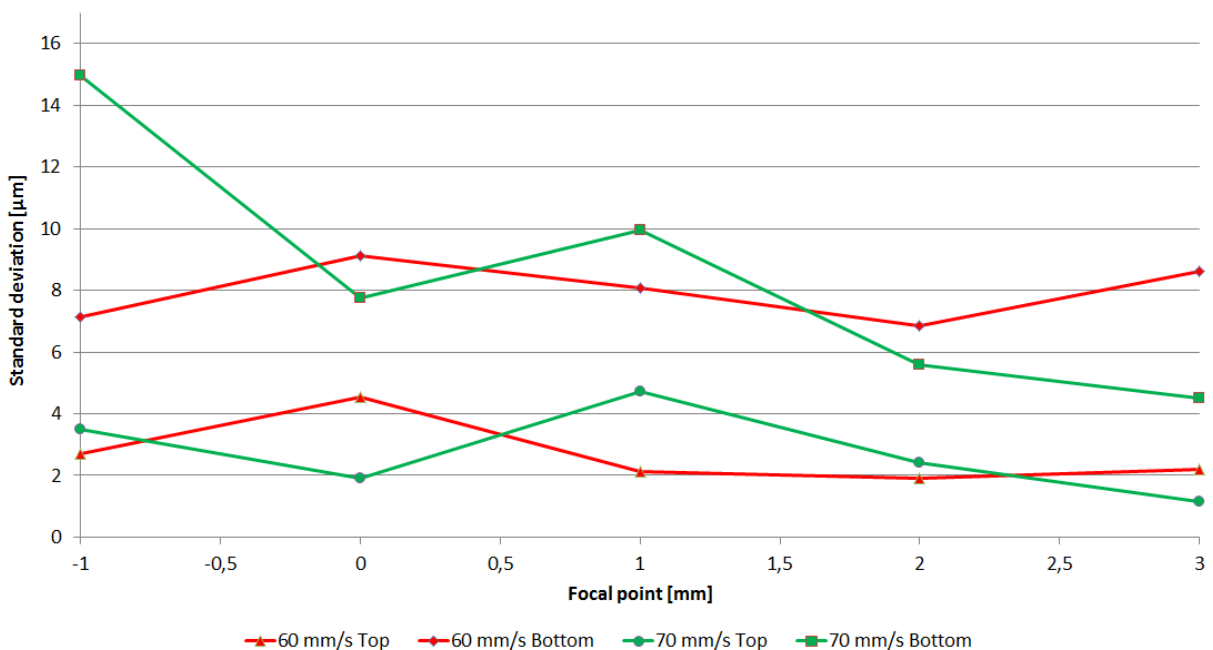


Figure 10.9: The graph shows the standard deviation of the KW in the top and bottom of experiments, with CS = 60mm/s and CS = 70mm/s, as a function their FP's.

μm (experiment 14). The minimum standard deviation among the bottom KW's is $4.5 \mu\text{m}$ (experiment 20 and 22), and maximum $15.0 \mu\text{m}$ (experiment 6). It is difficult to calculate one representative ratio between the standard deviations for all the top and bottom KW's, because of the large deviation in them. The ratio between standard deviation for the top and bottom KW's is approximately 2-6. The top KW with the smallest standard deviation, is found in experiment 22 and 24 which both has FP = 3.0mm.

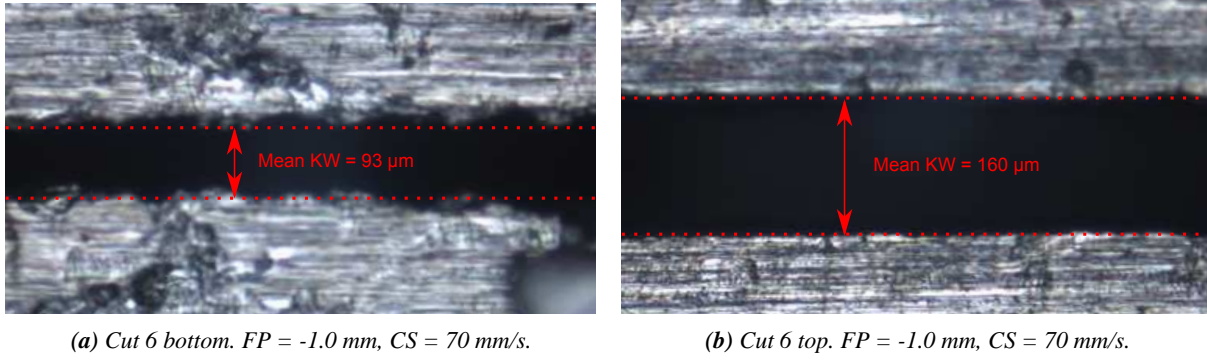


Figure 10.10: Different KW in top and bottom for cut 6. $ST = 0.7 \text{ mm}$

10.4.2 FP vs CS analysis/conclusion

Due to the mean SNR's in table 10.5 two two-way ANOVA's for the FP vs CS experiments, one for the top KW and one for the bottom KW, are performed for experiment 13-24. The experiments where the $FP = -1.0\text{mm}$ and $FP = 0.0\text{mm}$ are not included, since they include experiment 8 and 11 which cannot be measured. For experiment 12 only three measurements is available which is not representative for a mean value. By excluding experiment 1-12 noise from the measured KW's is reduced.

ANOVA

In order for the FP, CS or the interaction between the FP and CS to have a significant influence, their F_0 value must be higher than their respective $F_{0.01}(\text{DoF})$ values.

Table 10.6 shows, that for the top KW, both FP and CS has a significant influence on the KW, see equation 10.4. The FP is the main effect and on the KW with 92.1 % contribution. The error is relatively small because of the small variation in the top KW's. Based on the ANOVA it is clear, that the FP has the most influence on the top KW and ther other effect are negligible.

Source of variation	SS	DoF	MS	F_0	$F_{0.01}(\text{DoF})$	P-value	[%]
Focal point	25185	2	12592.5	1603.24	4.807	0	92.1
Cutting speed	112.3	3	37.4	4.76	3.969	0.0037	0.4
Interaction	1190.6	6	198.4	25.26	2.974	0	4.4
Error	848.3	108	7.9				3.1
Total	27336.1	119					100

Table 10.6: Two-tay ANOVA for the top KW with $FP = 1.0\text{-}3.0\text{mm}$ and $CS = 60\text{-}90\text{mm/s}$.

$$\begin{aligned}
 F_{0FP} &> F_{0.01,2,108} \iff 1603.24 > 4.807 \\
 F_{0CS} &> F_{0.01,3,108} \iff 4.76 > 3.969 \\
 F_{0FP,CS} &> F_{0.01,6,108} \iff 25.26 > 2.974
 \end{aligned}
 \tag{10.4}$$

From table 10.7 and equation 10.5 it can be seen that only the CS has a significant influence on the bottom KW with a 27.6 % contribution. The error makes it clear that there is a great influence from the variance of the bottom KW's. The error within each group has the largest contribution of 51.4 %, for the bottom KW. The FP has, according to the ANOVA, no significant influence on the bottom KW (3.4%).

Source of variation	SS	DoF	MS	F_0	$F_{0.01}(DoF)$	P-value	[%]
Focal point	390.8	2	195.38	3.56	4.807	0.0317	3.4
Cutting speed	3182.1	3	1060.69	19.34	3.969	0	27.6
Interaction	2035.3	6	339.22	6.19	2.974	0	17.7
Error	5921.8	108	54.83				51.4
Total	11529.9	119					100

Tabel 10.7: Two-tay ANOVA for the bottom KW with FP = 1.0-3.0mm and CS = 60-90mm/s.

$$\begin{aligned}
F_{0FP} &> F_{0.01,2,108} \iff 3.56 < 4.807 \\
F_{0CS} &> F_{0.01,3,108} \iff 19.34 > 3.969 \\
F_{0FP,CS} &> F_{0.01,6,108} \iff 6.19 > 2.974
\end{aligned} \tag{10.5}$$

Because of the large variation on the bottom KW, as seen on figure 10.12 the effect from the random error has the largest contribution on the bottom KW for both the FP vs CS experiment. This means that the CS effect on the bottom KW is smaller than the effect from the random error, which is KW variation. It can be concluded, that the variation in the bottom KW makes the bottom unfit to analyze further.

Effect of the FP

The FP's effect is analysed further in relation to the found intensity distribution of the laser beam from section 7.4. This is done with the purpose of understanding the influence of the beam spot intensity on the KW. Because CS has a less significant contribution than the KW variation it is not included. Experiment ID; 14, 18 and 22 are used in this analysis where is constant, CS = 70 mm/s.

The theoretical spot diameters are calculated in the top surface of the sheet. The basic propagation equation, 10.6 is used with the values found from the least-square fit in section 7.4. The z-distance to the top surface is found in equation 10.7 where t is the ST (700 μm). From equation 10.8 the intensity, at a given transverse distance on the beam spot diameter, is calculated. x_0 is the center of the beam and x the transverse distance, see figure 7.4 (Paschotta, 2012).

$$d_z = d_{0f} \left[1 + \left(\frac{2M^2 \lambda z}{\pi d_{0f}^2} \right)^2 \right]^{\frac{1}{2}} \tag{10.6}$$

$$z = \begin{cases} FP - t, & FP > 0 \\ |FP| + t, & FP < 0 \end{cases} \tag{10.7}$$

$$I_x = I_{Max} \cdot e \left(\frac{-2(x-x_0)^2}{(d_{0f}/2)^2} \right) \tag{10.8}$$

FP [mm] (z)	TS, d_z [μm]	Top KW [μm]	I_{avg} [$\frac{kW}{mm^2}$]	I_{max} [$\frac{kW}{mm^2}$]	86% intensity
1.0	45	98	264	528	61
2.0	64	64	131	261	30
3.0	94	74	61	121	14

Tabel 10.8: Calculated spot diameters in the top surface and measured top KW. TS = Top Surface. The 86% intensity is the intensity on the beam spots circumference. The top KW is for 70 mm/s.

When evaluating the KW in relation to the calculated beam spot diameter in the top surface of the 0.7 mm sheet, disagreements are observed. In table 10.8 it can be seen, that the KW for $FP = 3.0$, is smaller, than the beam spot diameter in top surface of the sheet. This indicates, that the KW is not only a function of the beam spot diameter. To understand this phenomenon it is necessary to consider the gaussian intensity distribution of the laser beam. For different FP of the laser beam, the intensity has different distributions, see figure 10.11.

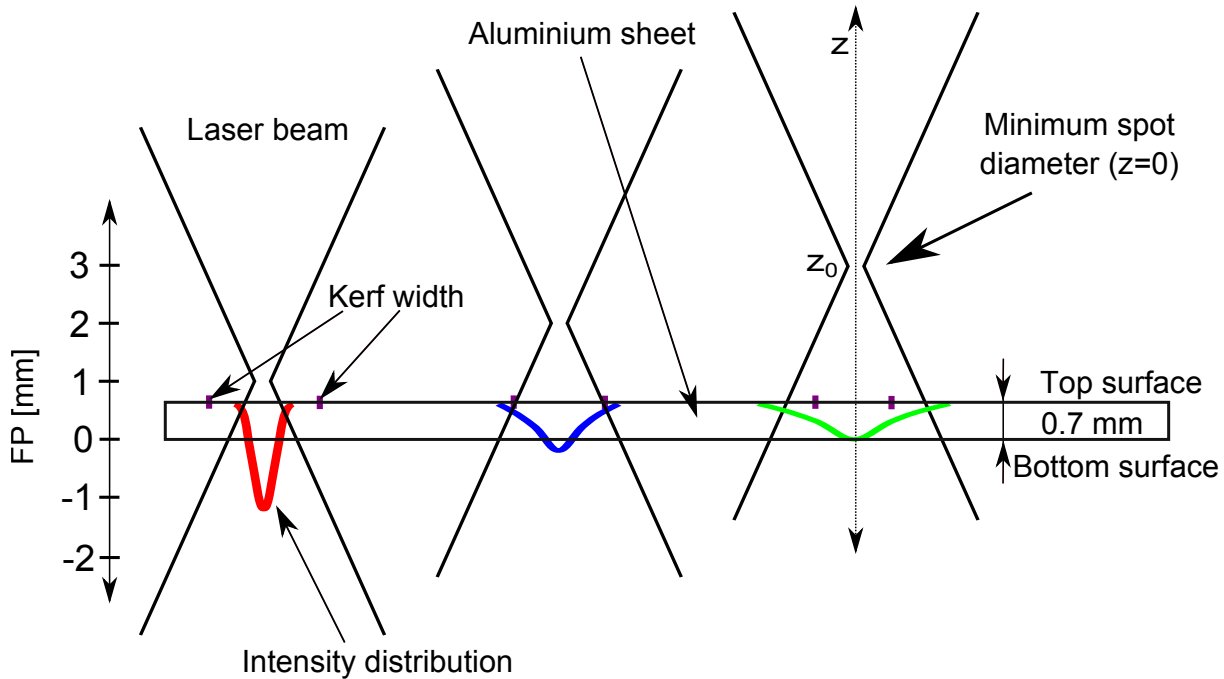


Figure 10.11: The settings for the FP during experiments.

It can be concluded, that both the spot diameter and the intensity distribution has an effect on the KW.

10.4.3 ST vs CS

In figure 10.12 the variation in the measurements of the ST vs CS experiments are seen. In the boxplot the experiments are arranged after the ST first and then CS.

From the boxplot it can be seen that, as it was seen in the FP vs CS experiments, the bottom KW has a larger variance than the top for all the experiments. This corresponds well with the standard deviation seen in table 10.9

From the results in table 10.9 it can be seen that the ST with the largest mean KW in both top and bottom is where $ST = 0.7\text{mm}$. This is further illustrated in figure 10.13. The dispersion of the mean KW in the bottom is highest when the $ST = 1.0\text{mm}$ (from $60\text{-}83\ \mu\text{m}$). On the other hand the dispersion of the mean KW in the top is lowest also when the $ST = 1.0\text{mm}$ (from $127\text{-}132\ \mu\text{m}$).

Regarding the standard deviation of the experiments generally the same tendency is seen as in the FP vs CS experiments meaning that the top KW has a low standard deviation compared to the bottom KW. This is further illustrated in figure 10.14. The minimum standard deviation among the top KW's is $1.4\ \mu\text{m}$ (experiment 29), and the maximum is $4.5\ \mu\text{m}$ (experiment 36). The minimum standard deviation among the bottom KW's is $5.2\ \mu\text{m}$ (experiment 28), whereas the maximum is $15.7\ \mu\text{m}$ (experiment 36).

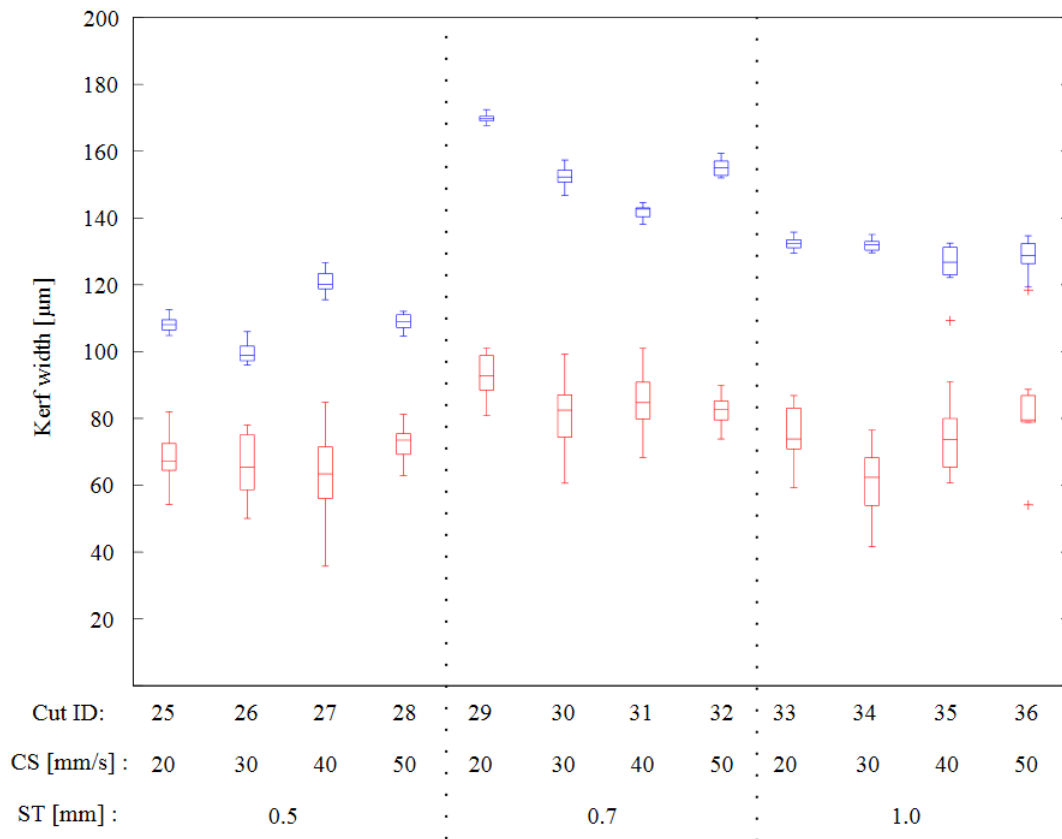


Figure 10.12: Boxplot for ST vs CS experiments. The experiments are arranged after ST first and then CS.

Exp. ID	Control variables		Mean KW [μm]		Std. dev. [μm]		SNR	
	CS [$\frac{\text{mm}}{\text{s}}$]	T [mm]	Top	Bottom	Top	Bottom	Top	Bottom
25	20	0.5	108	68	2.3	8.0	23.16	1.16
26	30	0.5	100	66	3.5	9.2	9.12	0.86
27	40	0.5	121	62	3.3	14.5	12.13	0.33
28	50	0.5	109	73	2.5	5.2	18.76	2.98
29	20	0.7	170	92	1.4	6.5	95.52	2.40
30	30	0.7	151	81	3.0	12.3	19.01	0.59
31	40	0.7	141	82	2.0	8.9	38.05	1.19
32	50	0.7	155	83	2.4	8.9	26.63	3.89
33	20	1.0	132	76	2.1	8.6	34.64	1.14
34	30	1.0	131	60	1.9	10.4	39.58	0.62
35	40	1.0	127	76	3.8	14.9	9.93	0.38
36	50	1.0	128	83	4.5	15.7	7.15	0.37
Mean SNR							27.81	1.33

Tabel 10.9: Results from the ST vs CS experiment.

10.4.4 ST vs CS analysis/conclusion

ANOVA

Due to the mean SNR's in table 10.9 two two-way ANOVA are performed to investigate if either the ST or the CS has a significant influence for the KW on the top and the bottom KW. In order for the ST, CS or the interaction between the ST and CS to have a significant influence on the KW the F_0 value must be

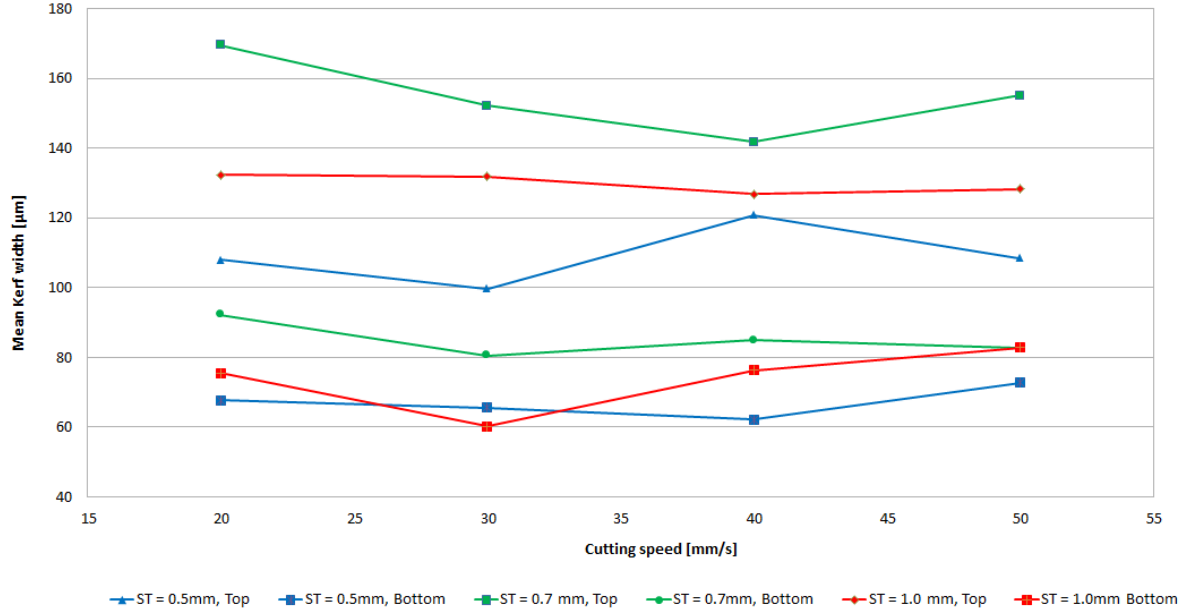


Figure 10.13: The KW as a function of CS for different ST's, 0.5, 0.7 and 1.0 mm.

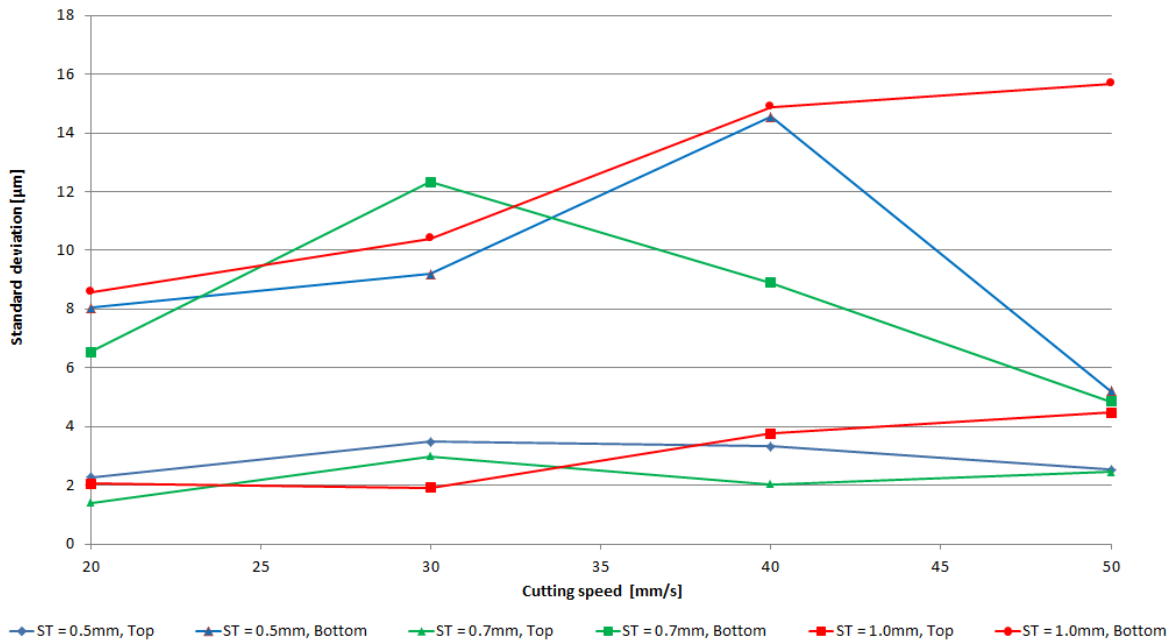


Figure 10.14: The graph shows the standard deviation of the KW in the top and bottom, as a function of CS for different ST's, 0.5, 0.7 and 1.0 mm.

higher than the respective $F_{0.01}(\text{DoF})$ value.

In table 10.10 and equation 10.9 the results of the ANOVA for the top KW is presented. Similarly in table 10.11 and equation 10.10 the results of the ANOVA for the bottom KW is presented.

$$\begin{aligned}
 F_{0ST} &> F_{0.01,2,108} \iff 2529.61 > 4.807 \\
 F_{0CS} &> F_{0.01,3,108} \iff 52.94 > 3.969 \\
 F_{0ST,CS} &> F_{0.01,6,108} \iff 105.04 > 2.974
 \end{aligned}
 \tag{10.9}$$

Source of variation	SS	DoF	MS	F_0	$F_{0.01}(DoF)$	P-value	[%]
Sheet thickness	41298.5	2	20649.3	2529.61	4.807	$1.9 \cdot 10^{-91}$	84.9
Cutting speed	1296.4	3	432.1	52.94	3.969	$3.9 \cdot 10^{-21}$	2.7
Interaction	5144.6	6	857.4	105.04	2.974	$9.4 \cdot 10^{-43}$	10.6
Error	881.6	108	8.2				1.8
Total	48621.1	119					100

Table 10.10: Two-way ANOVA for the top KW with $ST = 0.5, 0.7$ and 1.0mm and $CS = 20\text{-}50\text{mm/s}$.

Source of variation	SS	DoF	MS	F_0	$F_{0.01}(DoF)$	P-value	[%]
Sheet thickness	6674	2	3337.01	30	4.807	0	29.3
Cutting speed	2120	3	706.68	6.35	3.969	0.0005	9.3
Interaction	1985	6	330.84	2.97	2.974	0.01	8.7
Error	12012.9	108	111.23				52.7
Total	22792	119					100

Table 10.11: Two-way ANOVA for the bottom KW with $ST = 0.5, 0.7$ and 1.0mm and $CS = 20\text{-}50\text{mm/s}$.

$$\begin{aligned}
 F_{0ST} &> F_{0.01,2,108} \iff 30 > 4.807 \\
 F_{0CS} &> F_{0.01,3,108} \iff 6.35 > 3.969 \\
 F_{0ST,CS} &> F_{0.01,6,108} \iff 2.97 < 2.974
 \end{aligned}
 \tag{10.10}$$

From equation 10.9 and 10.10 it is found that both the ST and CS have a significant influence on the top and bottom KW. The interaction between the ST and CS also have a significant influence on the top KW. There is however no significant influence from the interaction of the ST and CS for the bottom KW. Table 10.10 shows that for the top KW the ST contributes by 84.9 % on the top KW. On the other hand table 10.11 shows that the ST only contributes 29.3 % to the bottom KW.

It can be seen that the error in sum of squares, in table 10.11, is relatively large and that its effect contributes 52.7 % to the bottom KW. This means that the main reason for variation from the mean KW, comes from variation within the 10 measurements of the bottom KW and not from the ST or CS.

Effect of stand-off distance

As a consequence of having observed that the ST has the largest influence on both the top and bottom KW when not considering error the ST is further analyzed. When considering figure 10.13 it is noticed that the ST of 0.7mm has the largest top and bottom KW.

In chapter 9 it was declared that the STO in the experiments aren't the same for each ST. The STO for $ST = 0.5$ and 1.0 mm are 0.4mm and for $ST = 0.7\text{mm}$ it is 0.8mm. Bearing that in mind this may explain why the KW is larger than the others. From the results of the KW measurements with respect to ST and STO an indication is seen that a larger STO results in larger KW's. Due to a lack of resources the indication is not further studied in this thesis.

10.4.5 Sources of error for both the FP vs CS and ST vs CS experiments

- Caliper tool: The error is approximated to $\pm 1.5\mu\text{m}$.
- Section of measured length of each experiment.

The source of error regarding using the caliper tool to measure the KW arises in relation to using the NI Vision Builder software and is further explained in appendix A.

In relation to selecting the section where the pictures used for the measurements of the KW are taken, a source of error is that the section which is selected varies in each experiment. An effort is made that the pictures are taken in between the start and end of the cuts thereby avoiding errors which may be involved with the start and end of the cuts.

10.4.6 Conclusion for FP vs CS and ST vs CS experiments

In this section it is found, that the top KW is highly depending on the position of the FP and the ST. It is found that the results for the bottom KW's is primarily affected by an error, which is due to the large KW variation. The effect from CV and WP on the bottom KW is negligible. The cutting speed has a significantly influence in the two experiments but can be seen as negligible compared to the other effects.

In appendix C.1 a residual analysis for the four ANOVAs show, that the assumption of normal probability distribution of the residuals is present. This means that the conclusions on the significant effects on the KW can be given high credibility.

It is found that the STO and the intensity distribution of the spot diameter has an influence on the KW. The effects of STO and intensity are not analyzed enough to determine their influence on the KW.

The KW is can not be evaluated in relation to the holes in the speaker grill, because the holes have no kerf. The important information on KW is therefore the standard deviation on the cuts. From chapter 4 it was found that the mean roundness of holes is defined by the maximum and minimum diameter of the hole, see figure 10.15a. The assumption made for the evaluation, is therefore, that the standard deviation for each KW can be separated into two equal standard deviations on each side of the kerf, see figure 10.15b. As a consequence of this, only a quarter of the roundness tolerance is used for the evaluation of the standard deviation. With this assumption, it is found that the following cuts satisfies the requirements with a roundness tolerance of $\pm 4.5\mu m$ on the top KW variances and $\pm 5.25\mu m$ on the bottom KW variances: All the top KWs for experiment 5-36, except experiment 14 and bottom KW experiment 20 and 22.

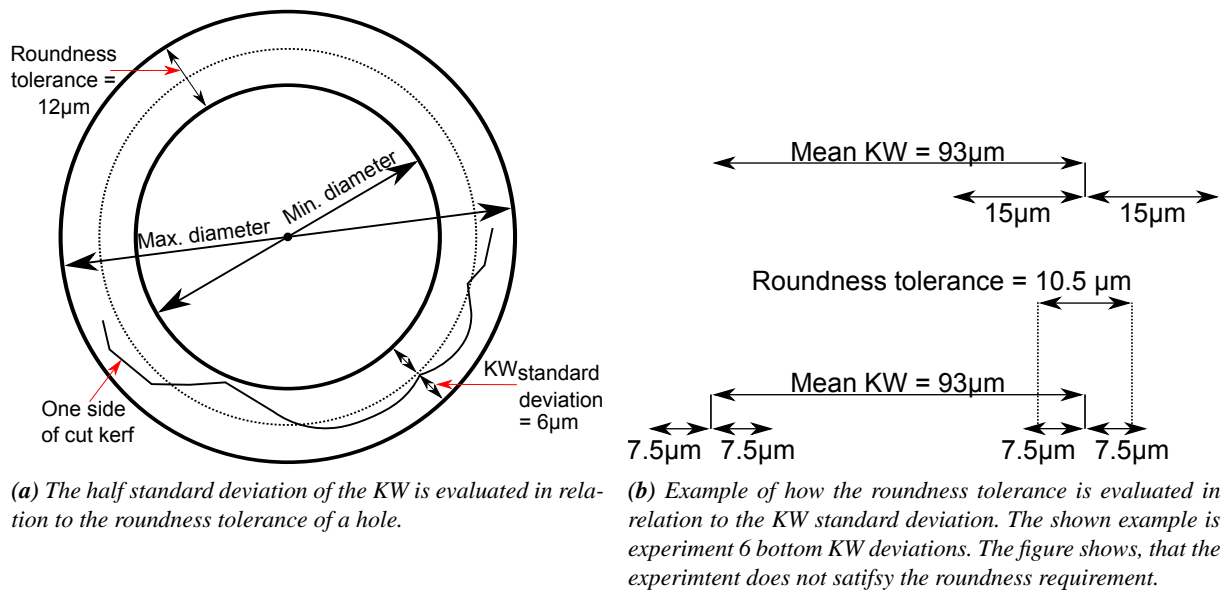


Figure 10.15: The roundness tolerance in relation to the KW standard deviation.

10.5 Kerf taper

The KT is a function of the top and bottom mean KW and the ST. It is therefore a calculated and not measured value. The KT is the angle between the two top and bottom and is calculated using equation 10.11.

$$KT = \tan^{-1} \left(\frac{\frac{\text{top KW} - \text{bottom KW}}{2}}{ST} \right) \cdot \frac{180}{\pi} \quad (10.11)$$

10.5.1 FP vs CS

For calculating the KT for experiment 5-24, the mean KW of the top and bottom of each experiment are used from table 10.5. On figure 10.16 the KT for four different CS's can be seen as a function of the FP. It can be seen, that for the four CS's, the FP has the same effect on the KT. It is clear, that the KT decreases for all the CS's until FP = 2.0mm where the minimum KT is found. The KT starts increasing again from FP = 2.0mm to FP = 3.0mm.

10.5.2 ST vs CS

The KT for the different ST's as a function of the CS is seen on figure 10.17. It can be seen, that the KT does not have any clear tendency as a function of the CS for all three ST's. The ST has the main effect on the KT. The mean KT for the ST's for the four CS's are: ST = 0.5mm: 1.7°, ST = 0.7mm: 2.8° and ST = 1.0mm: 2.3°.

10.5.3 Sources of error for KT

Because KT is found from the KW, the same sources of error are present.

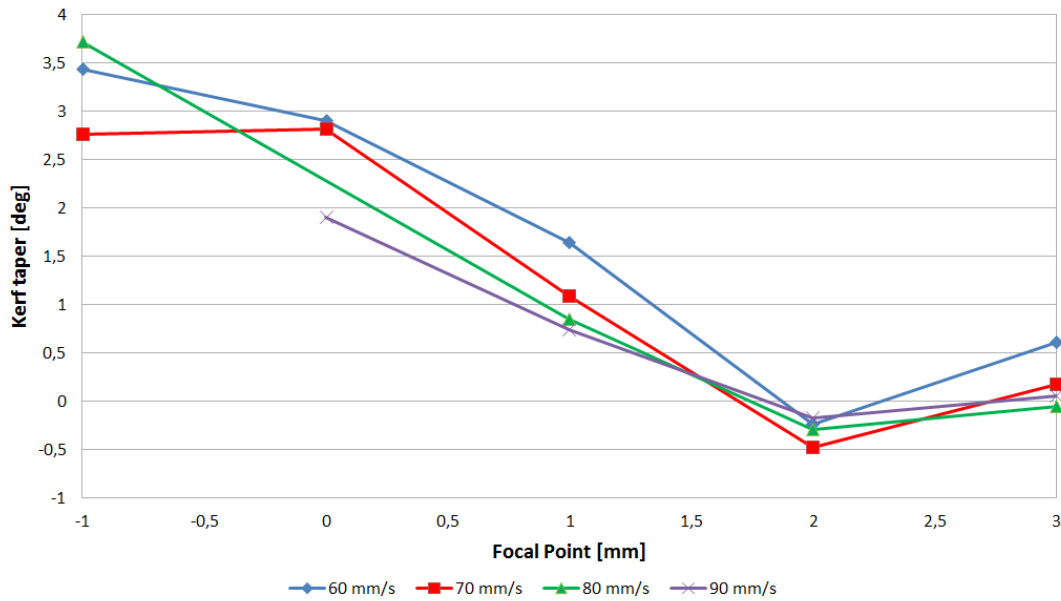


Figure 10.16: The graph shows the KT as a function of the FP for four different CS's.

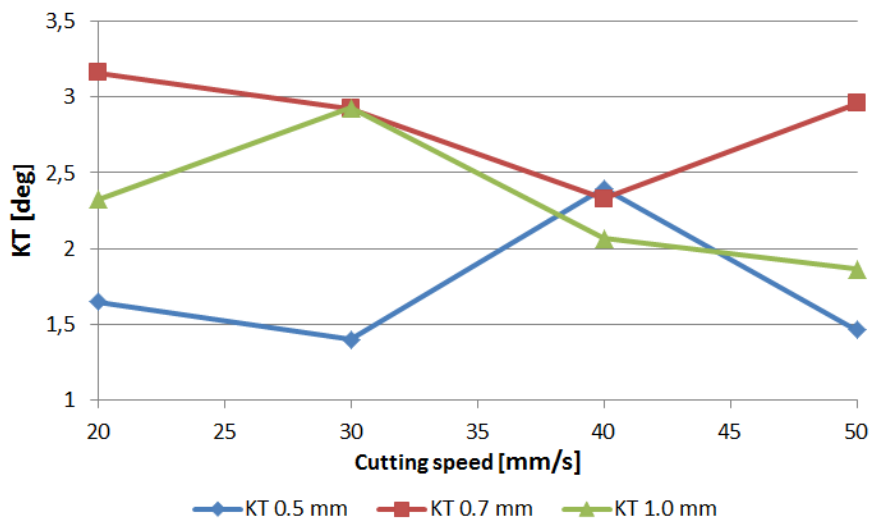


Figure 10.17: The graph shows the KT as a function of the CS for three different ST's.

10.5.4 Conclusion/analysis

From the results it can be concluded, that the FP is decisive for the KT. A decrease in ST shows a tendency for decrease in KT.

From the requirements in chapter 4, the reference for KT is 0.2° . Including the KT standard deviation entails, that the KT must be in the interval of $-0.1 - 0.7^\circ$. Using this interval only cut 16, 21, 22, 23 and 24 are satisfactory. Cut 15, 17 and 20 violates the requirement with an angle on 0.1° , and cut 14 and 15 with an angle on 0.2° and 0.4° .

From section 3.4.7 it is known that an increase in cutting speed will decrease the KT. This corresponds to figure 10.16 for FP = 0.0 and 1.0mm where the cutting speeds decreases the KT. The figure also shows, that the smallest KT is found when FP is above the sheet surface.

From figure 10.17 theory also agrees with the observed, that smaller sheet thickness' entail a smaller KT.

10.6 Overview

When considering all the quality parameters for the FP vs CS experiments as it is visualized in figure 10.18. It shows that only experiment 21 and 22 with the settings: ST = 0.7 mm, FP = 3.0 mm, CS = 70 mm/S satisfies all the requirements from chapter 4.

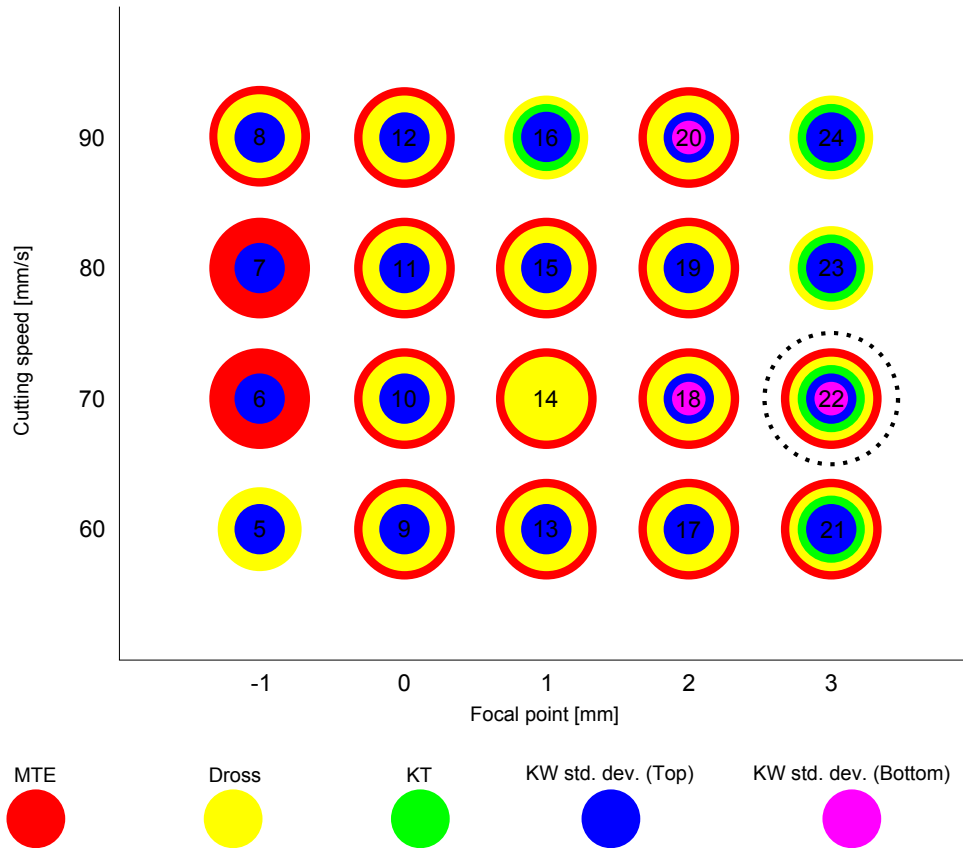


Figure 10.18: The marked quality parameters indicates when the requirements are satisfied for the FP vs CS experiments.

The ST vs CS experiments shows, that none of the experiments (25-36) satisfies all the requirements, see figure 10.19.

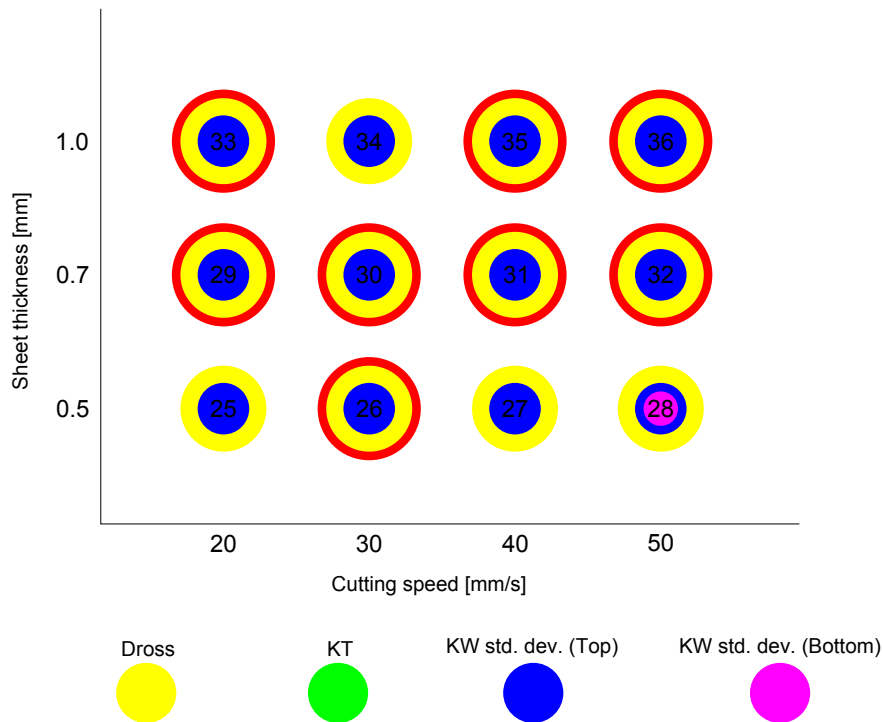


Figure 10.19: The marked quality parameters indicates when the requirements are respected for the ST vs CS experiment.

10.7 Summary

Throughout this chapter the results from the experiments, with respect to the quality parameters dross, MTE, HAZ, KW and KT have been analyzed. It is found, that only experiment 21 and 22 satisfies all the requirements. Indications seen on figure 10.13 shows, that the influence of uncontrollable change in the STO during the experiments, have affected the results of the experiments. The magnitude from this error is not known, but is expected have given rise to a larger variation in the quality parameters.

The used FP interval, that allows the beam to cut through the sheet, is almost the maximum interval which is possible. Is is experienced, that with $FP = -2.0mm$, it is not possible to cut through the sheet. This is because I_{avg} is to small. $FP = 4.0mm$ have not been used in experiments, but from theoretical beam spot diameter calculation, for the sheets top surface, an even lesser I_{avg} is found. Equation 10.6 is used with $z = 3.3mm$. The interval used for the CS is further from the maximum interval, that allows the beam to cut through the 0.7mm sheet. The maximum CS interval is from $0 - 90 < mm/s$, because experiment 8 with $FP = -1mm$ and $CS = 90mm/s$ has not cut through the sheet. This makes it clear why the FP has a higher influence than the CS.

When the considering the calculated Rayleigh length, from section 7.3.5 it is found, that it can not be used as a measure for obtaining parallel KWs (equal in top and bottom). This is seen from experiment 25-36, where $FP = 0.0mm$ and the KT for all the cuts is $\neq 0$. Conclusion on the dept of focus value on $\pm 0.41mm$ can not be made because ST is larger thand 0.41mm for all experiments

The comparison with information on the quality parameters from chapter 3.4 disagrees to some extent with the results. This may be because little of the used litterature is based on experiments with a single mode fiber laser.

High quality laser cutting at

B&O

11

In this chapter it is analyzed how the results of the experiments can be applied in relation to using laser cutting at B&O for processing holes.

From the experiments conducted in this thesis, it is found that it is possible to obtain the desired cutting quality in aluminium sheets with a thickness of 0.7mm. It is also found that the sheet thickness has a significant effect on the quality parameters. As a result of this an assessment of how, the results from the cutting quality experiments, can be applied when using the B&O aluminium alloy (chapter 9) with 2.0mm aluminium sheets, is presented. The assessment is divided into the following three sections:

- Quality parameters
- Assist gas pressure and stand-off distance
- Manufacturing considerations

11.1 Quality parameters

The conclusions on the quality parameters obtained in chapter 10 cannot directly be transferred to B&O and must be evaluated in relation to the aluminium alloy and ST that B&O use.

11.1.1 Dross and MTE

From the results obtained from the experiments in this thesis, it is difficult to give recommendations on how to minimize dross and MTE. This is because both EP's, CV's and WP's have an effect on these quality parameters. The recommendation for B&O is to conduct more experiments where the objective is to minimize dross and MTE.

11.1.2 HAZ

The experiments have shown, that HAZ, in the form of color changes in the workpiece, do not occur for any of the settings of the CV's and WP's. Instead spatter, from the piercing process, is burned onto the surface of the sheets and can create color changes on it. In order to avoid visible spatter on the surface, it is crucial, that the the piercing point is placed at a point where spatter does not affect the final look of the workpiece. It is expected that the amount of spatter will increase with the ST as well as piercing time. This expectation is based on the fact that more material will be in a molten state before it can be ejected out through the bottom of the workpiece. Several solutions to avoid spatter exist, two of them are:

- Spatter can be avoided by controlling the power during piercing. This way a small and precise piercing hole can be created. This is done by decrease the piercing power when the deflection of the laser beam is getting higher. For more information see (Davis, 2012)
- Anti-spatter lotion can be applied on the workpiece surface to avoid adherence of spatter on it. For more information see (GmbH, 2012).

11.1.3 KW

The KW determines the actual diameter of the laser cut holes. It is therefore crucial to know the top and bottom KW in order to obtain the desired hole diameter. In order to obtain which diameter that needs to be specified when cutting a hole of a given diameter the KW must be subtracted from the intended diameter of the hole. The specified diameter is the path that, the center of the laser beam follows, see figure 11.1.

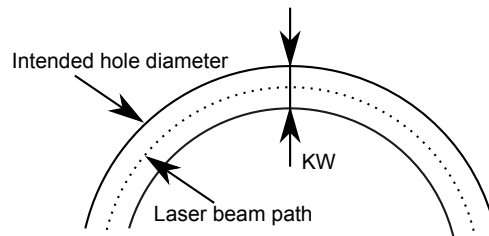


Figure 11.1: The KW must be subtracted from the intended diameter of a hole in order to obtain the desired diameter.

It is difficult to calculate the theoretical KW for a specific aluminium alloy and ST, because it depends on both CV's, EP's and WP's. As a consequence of this, the KW must be measured before the correct KW can be subtracted from the intended hole diameter.

It is found, that the KW increases with ST, which indicates, that with 2mm thick sheets, the KW will increase further. The recommendation to B&O regarding the KW is not to optimize it but rather optimize the other quality parameters along with minimizing the KW deviation and then measure the resulting KW.

KW deviation

It is found that the KW deviation has an influence in the diameter of a laser cut hole. This must be taken into consideration when choosing a positioning system with a specific tolerance. The roundness tolerance is therefore affected by both the KW deviation, accuracy and repeatability tolerance for a given positioning system.

11.1.4 KT

For a constant KT, the difference in the top and bottom hole diameter will increase when the ST increases. From chapter 4 the maximum difference between best fit top and bottom diameter is $20\mu m$. In order to

ensure that the laser cut holes in the top and bottom of the 2.0mm sheet, is within this difference, the KT angle must be approximately 0.3° , see equation 11.1.

$$\text{Maximum KT angle} = \tan^{-1} \left(\frac{\frac{20\mu m}{2}}{2000\mu m} \right) \cdot \frac{180}{\pi} = 0.3^\circ \quad (11.1)$$

From the experiments in this thesis, it is not known if it is possible to obtain a KT angle of 0.3° in 2.0mm aluminium sheets. The recommendation for B&O is to conduct more experiments where the KT is further investigated.

11.2 Assist gas pressure and stand-off distance

Two control variables are set to be constant during the experiments in this thesis, but are known to have an effect on the process, these are:

Assist gas pressure

For industrial use a pressure on 20 bar is relatively high. A high pressure entails, that the total gas use increases as well as the costs. It is therefore recommended to use a lower assist gas pressure to reduce costs. Using a lower gas pressure will have an effect on the quality parameters (Narendra B. Dahotre, 2008). The magnitude of this effect on high quality laser cutting, is not known. More experiments must therefore be made in order to determine this magnitude.

Stand-off distance

A systematic error in stand-off indicates, that it has an influence on the quality parameters. It is therefore crucial for B& that the stand-off distance is controlled with a fine tolerance. For industrial laser-cutting machines, the stand-off distance can be controlled by an automatic height sensor (Narendra B. Dahotre, 2008). To obtain constant stand-off distance, it is necessary to use a sensor. The reason for this is due to the fact the the workpiece will tend to warp as it is cut.

11.3 Manufacturing considerations

From chapter 2 it is known that the currently used drilling process makes four holes each second, when manufacturing the speaker grill from chapter 4. The distance between the holes vary in the interval; 0.7-4.0mm. In the following example is made to illustrate what speed is required in order to compete with the currently used process. In the example a distance of 2.0mm between the holes is used. On figure 11.2 the path of the laser is shown, when cutting four holes in a row and when using an inlet. In equation 11.2 the total distance from the movement of the positioning system is calculated.

In this example a piercing time of each hole of 0.1s is used. Accelerations and deaccelerations are not considered. The estimated cutting speed is calculated in equation 11.3 to approximately 60mm/s. From (B. Adelman, 2011) it is known that CS's of 150mm/s are achievable in aluminium sheets, with a thickness of 1.0mm, with a 500W single mode fiber laser. From (Mounir, 2012) it is known, that for a 2kW single mode fiber laser, CS's of 500mm/s can be achieved in aluminium sheets with a thickness of 1.0mm. Even though (B. Adelman, 2011) and (Mounir, 2012) doesn't have the same requirements

to the quality of the cut, it indicates that a CS of 60mm/s which also results in a good cut quality is achievable.

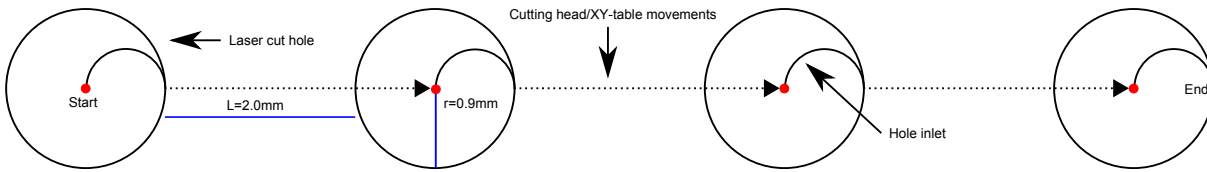


Figure 11.2: Sequence of cutting 4 holes. The circular lines indicate the path where the laser is turned on and the dotted lines indicate the path of the laser where it is turned off.

$$\text{Total distance} = 4 \cdot \left((1.8\text{mm} \cdot \pi) + \left(\frac{0.9\text{mm} \cdot \pi}{2} \right) \right) + 3 \cdot 2 = 34.3\text{mm} \quad (11.2)$$

$$\text{Cutting speed} = \frac{34.3\text{mm}}{0.6\text{s}} \approx 60\text{mm/s} \quad (11.3)$$

Warping in workpieces

As it was mentioned in the section regarding the stand-off distance, the workpieces tend to warp as heat is put into the workpiece. It is known that B&O are interested in being able to laser cut geometries in workpieces that previously have gone through a forming process. In relation to this it is important that reservations regarding warp of the workpieces are made. It is therefore recommended that B&O further investigates how much the workpiece will warp if processed with laser cutting after they have been formed.

Conclusion 12

The general objective of this master thesis is to investigate to which extent laser cutting can be used for hole processing of high quality workpieces in aluminium at B&O.

An analysis of the advantages and disadvantages of using laser cutting compared to a currently used drilling process is made. Based on the analysis it is concluded, that there is a basis for using laser cutting in connection with making holes in high quality workpieces.

Because there aren't a clear definition of what high quality workpieces are, an analysis is made based on a workpiece currently manufactured at B&O. From the analysis a definition of how holes shall be in a high quality workpiece is set up.

On the basis of the problem formulation two types of experiments are conducted wherein different settings of the control variables focal point, cutting speed and sheet thickness are used.

Based on the experiments it is concluded that it is possible to obtain a cutting quality that satisfies the requirements for holes in high quality aluminium workpieces. The settings of the control variables and workpiece parameters which satisfies the requirements are as follows:

- Material: Aluminium EN AW-1050A (99.5%Al)
- Sheet thickness: 0.7mm
- Cutting speed: 60-70mm/s
- Focal point: 3.0mm
- Operating laser power: 420W
- Assist gas pressure: 20bar
- Stand-off distance: 0.8

Even though it is concluded that a combination of settings of the workpiece parameters and control variables result in satisfying the requirements it cannot be concluded if the settings will work for the material that B&O use. This is mainly because it is concluded that the sheet thickness, which in this thesis is 0.5, 0.7 and 1.0mm and at B&O is 2.0mm, have a significant influence on the quality parameters. In order to be able to present the control variables which result in satisfying the requirements more experiments must be conducted.

Discussion 13

Due to the fact that the experiments conducted in this thesis have been made May 10th at IPU in Copenhagen, it has only been possible to conduct laser cutting experiments for one day. Because of this it, has not been possible to correct the obvious errors that have affected the results of the experiments. This is primarily the error in stand-off distance and the large difference in the intervals of the control variables.

From the overall knowledge in this thesis new experiments, with respect to obtaining more information on to which extent laser cutting can be used at B&O, can be conducted. This can be done with one or more of the known optimization methods described in chapter 6.

Regarding the quality parameters it can be discussed if the defined quality parameters from the drilled holes is the best point of reference for high quality laser cutting. The definition is made because B&O doesn't have any definition of the quality of laser cut workpieces. It is recommended that B&O makes a clear definition of the quality parameters if laser cutting shall be used. When doing this, it can be discussed if the perpendicularity and angularity tolerance should be included, since it is a known quality parameter from the thermal cutting standard (Association, 2002). It can further be discussed if this tolerance implicitly can be evaluated through the quality parameter kerf taper. Likewise the quality parameter mean height of the profile have not been evaluated in this thesis. It can be discussed if the parameter implicitly have been analysed through KW deviation.

Because the quality parameters are defined in the magnitude of μm , small impurities in the material, non-uniform assist gas pressure, etc. and measuring errors can affect the results. It can be discussed if the quality parameters should have been stated with a rougher precision than $1\mu m$.

Only two holes from the case is used to define the reference for dross and MTE. More than two holes must be measured in order to obtain more representative reference values.

Abbreviations	
<i>AGP</i>	Assist gas pressure
<i>ANOVA</i>	Analysis of variance
<i>BPP</i>	Beam parameter product
<i>CV</i>	Control variable
<i>CS</i>	Cutting speed
<i>DOF</i>	Depth of focus
<i>DoF</i>	Degree of freedom
<i>EP</i>	Equipment parameter
<i>FP</i>	Focal point
<i>HAZ</i>	Heat affected zone
<i>KW</i>	Kerf width
<i>KT</i>	Kerf taper
<i>KW_{top}</i>	Kerf width in top surface
<i>KW_{bottom}</i>	Kerf width in bottom surface
<i>MHP</i>	Mean height of the profile
<i>MTE</i>	Melting of top edge
<i>Nd : YAG</i>	Neodymium-doped yttrium aluminum garnet
<i>OLP</i>	Operating laser power
<i>PAT</i>	Perpendicularity and angularity tolerance
<i>SNR</i>	Signal-to-noise ratio
<i>ST</i>	Sheet thickness
<i>STO</i>	Stand-off distance
<i>WP</i>	Workpiece parameter

	Variables
c	Specific heat capacity
d_{max}	Max. diameter
d_{min}	Min. diameter
$d_{BestFit}$	Best fitted diameter
$d_{BestFitTop}$	Best fitted diameter on the top surface
$d_{BestFitBottom}$	Best fitted diameter on the bottom surface
d_{0f}	Beam waist diameter
d_k	Core diameter of optical fiber
d_z	Beam diameter at distance z
f	focal length
f_c	collimation length
h	Distance from straight cut to circle
I_{max}	Max. intensity
I_{avg}	Average intensity
M^2	Beam quality factor
MS	Mean square
r	Radius of hole
s	Standard deviation
s^2	Variance
y	Distance from heat source
z_R	Rayleigh length
SNR_i	Signal-to-noise ratio of i 'th experiment
SS	Sum of squares
λ	Wavelength of laser
λ_{tc}	Thermal conductivity
Θ	Beam divergence angle
θ	Ideal beam divergence angle
θ_{spot}	Angle as a function of the spot diameter
μ	Mean
ρ	Density of material

Bibliography

- A. Pihlava, T. Purtonen, A. S. V. K. T. S. (2011). *Quality aspects in remote laser cutting*. Lappeenranta University of Technology.
- A. Stournaras, P. Stavropoulos, K. S. G. C. (2009). *An investigation of quality in CO₂ laser cutting in aluminum*.
- Amit Sharma, V. Y. (2011). *Modelling and optimization of cut quality during pulsed Nd:YAG laser cutting of thin Al-alloy sheet for straight profile*.
- Andreas Ottoa, M. S. (2010). *Towards a Universal Numerical Simulation Model for Laser Material Processing*. Elsevier Science Ltd. Keynote Paper.
- a/s, B. . O. (2011a). *Annual Report 2010-11 Bang & Olufsen concern*. Bang & Olufsen. On Appendix CD: Annual Report 2010-11 Bang & Olufsen concern.
- a/s, B. . O. (2011b). *Interim report, 1 halfyear 2011/12*. Bang & Olufsen. On Appendix CD: Half-year Report 2011- 2012 Bang & Olufsen concern.
- a/s, B. . O. (Used: 31. jan 2012). Bang & Olufsen. URL: <http://www.bang-olufsen.dk>.
- Association, D. S. (2002). *Thermal cutting - Classification of thermal cuts - Geometrical product specification and quality tolerances* (2nd ed.). Linde gas. ISBN: ??
- Avanish Kr. Dubey, V. Y. (2007). *Experimental study of Nd:YAG laser beam machining - An overview*. Elsevier Science Ltd. Journal of Materials Processing Technology.
- Avanish Kumar Dubey, V. Y. (2007a). *Multi-Objective optimisation of laser beam cutting process*.
- Avanish Kumar Dubey, V. Y. (2007b). *Optimization of kerf quality during pulsed laser cutting of aluminium alloy sheet*. Elsevier Science Ltd. Journal of materials processing technology.
- Avanish Kumar Dubey, V. Y. (2007c). *Robust parameter design and multi-objective optimization of laser beam cutting for aluminum alloy sheet*.
- B. Adelman, R. H. (2011). *Fast laser cutting optimization algorithm*.
- Belforte, D. A. (Used: 16. March 2012). *2011 Annual Economic Review and Forecast*. Industrial laser solutions for manufacturing. URL: <http://www.industrial-lasers.com/articles/print/volume-27/issue-1/features/2011-annual-economic-review-and-forecast.html>.
- B.S. Yilbas, S.S. Ahktar, C. C. (2011). *Laser hole cutting into bronze: Thermal stress analysis*. Elsevier Science Ltd. Optics & Laser Technology.
- Caristan, C. L. (2004). *Laser Cutting - Guide for Manufacturing* (1st ed.). Society of Manufacturing Engineers. ISBN: 0-87263-686-0.
- Chong Zhian Syn, Mohzani Mokhtar, C. J. F. Y. H. P. M. (2010). *Approach to prediction of laser cutting quality by employing fuzzy expert system*.
- Coherent (2012). *Understanding Laser Beam Parameters Leads to Better System Performance and Can Save Money*. Coherent. On Appendix CD: Understanding Laser Beam Parameters.
- Davis, D. (Used: 6. june 2012). *No holes in modern laser cutting story*. Thefabricator. URL: <http://www.thefabricator.com/article/lasercutting/no-holes-in-modern-laser-cutting-story>.

BIBLIOGRAPHY

- G. Thawari, J.K. Sarin Sundar, G. S. S. J. (2005). *Influence of process parameters during pulsed Nd:YAG laser cutting of nickel-base superalloys*. Elsevier Science Ltd. Journal of Materials Processing Technology.
- GmbH, P. T. (Used: 10. June 2012). *Laserlotion protec LC20A*. URL: <http://www.protec-austria.com/en/products/anti-spatter-fluids/laserlotion-protec-lc20a-33/>.
- GmbH, T. L. (2004). *Operator's manual D70*. On appendix CD.
- GROUP, L. S. P. (1998). *Industrial LASER Processes - An Introduction*. LASER SYSTEMS PRODUCT GROUP of AMT. On Appendix CD: Industrial LASER Processes An Introduction.
- Hansen, K. S. (2012). *Civil engineer, M.Sc (mech.eng)*.
- James C. Collins, J. I. P. (1996). *Building Your Company's vision*. Harvard Business Review.
- Joachim Berkmanns, M. F. (2003). *FACTS ABOUT Laser cutting*. Prentice Hall, Pearson. On Appendix CD: Facts about laser cutting.
- Johnston, N. (Used: 6. June 2012). *F-distribution*. URL: <http://www.statdistributions.com>.
- Jun Hu, Zhuoxian Zhang, J. L. X. S. (2010). *Simulation and experiment on standoff distance affecting gas flow in laser cutting*. Elsevier Science Ltd. Applied Mathematical Modelling.
- K. Poorhaydari, B. M. Patchett, D. G. I. (2005). *Estimation of cooling rate in the welding of plates with intermediate thickness*. American welding society.
- K. T. Mortensen, D. K. K. (2009). *Bang & Olufsen - En virksomhed i forandring*. Copenhagen Business School. On Appendix CD: kim_thisted_mortensen_og_danny_krath_knudsen.
- Kristiansen, M. (2006). *Proces technology*. AAU. Slides from course on proces technology.
- Kristiansen, M. (2007). *Automation of industrial processes*. AAU. Ph.d.
- Kristiansen, M. (2012). *Associate Professor at Department of Mechanical and Manufacturing Engineering, Aalborg University*. AAU.
- laser Division, T. (Used: 29. february 2012). *Comparison of primary metal cutting processes*. Tesko laser Division. URL: <http://www.teskolaser.com/tips.html>.
- laser GMBH, T. (2006). *Operator's manual*. Trumpf laser GMBH.
- MATWEB (Used: 24. may 2012). MATWEB. URL: <http://www.matweb.com>.
- Montgomery, D. C. (2005a). *Design and Analysis of Experiments* (6st ed.). John Wiley & Sons Inc. ISBN: 978-0-471-48735-7.
- Montgomery, D. C. (2005b). *Statistical Quality Control* (5th ed.). Wiley International. ISBN: 0-471-66122-8.
- Mounir, M. (Used: 1. june 2012). *Why IPGP will Slice the Competition*. The Motley Fool. URL: <http://beta.fool.com/eliteinvesting/2012/06/01/why-ipgp-will-slice-competition/5165/>.
- Narendra B. Dahotre, S. P. H. (2008). *Laser Fabrication and Machining of Materials* (1st ed.). Springer. ISBN: 978-0-387-72344-0.
- Nielsen, H. S. (2010). *GPS Bogen - Geometriske produktspecifikationer pÅ tekniske tegninger* (1st ed.). Erhvervsskolernes Forlag. ISBN: 978-87-7082-110-0.
- Olsen, F. (2010). *Application form - Advanced technology projects 2010, spring*. The Danish National Advanced Technology Foundation. ROBOCUT.
- Paschotta, R. (Used: 14. february 2012). *An Open Access Encyclopedia for Photonics and Laser Technology*. RP Photonics. URL: <http://www.rp-photonics.com/encyclopedia.html>.

- Photonics, I. (Used: 16. March 2012a). IPG Photonics. URL: <http://www.ipgphotonics.com>.
- Photonics, O. (2012b). *High powered water cooled thermal sensors and power pucks*. Ophir Photonics.
- point group, S. (Used: 20. february 2012). *ASTM-beam-diameter*. Spar point group. URL: <https://www.sparpointgroup.com/beam-diameter.aspx>.
- R. Alope, V. Girsh, R. F. S. P. A. M. (1996). *A Model For Prediction of Dimensional Tolerances of Laser Cut Holes in Mild Steel Thin Plates*. Elsevier Science Ltd. Int. J. Math. Tools Manufact. Vol. 37, No. 8, pp. 1069-1078, 1997.
- Shiner, B. (Used: 16. May 2012). *High-power fiber lasers gain market share*. Industrial laser solutions for manufacturing. URL: <http://www.industrial-lasers.com/articles/print/volume-21/issue-2/features/high-power-fiber-lasers-gain-market-share.html>.
- Trumpf (Used: 16. March 2012). *Trumpf*. URL: <http://www.trumpf-laser.com/en/about-trumpf/history/of-the-laser-at-trumpf.html>.
- Wandera, C. (2010). *PERFORMANCE OF HIGH POWER FIBRE LASER CUTTING OF THICK-SECTION STEEL AND MEDIUM-SECTION ALUMINIUM* (1st ed.). Lappeenranta University of Technology, Lappeenranta. ISBN: 978-952-214-973-2.
- William M. Steen, J. M. (2010). *Laser Material Processing* (4th ed.). Springer. ISBN: 978-1-84996-062-5.
- Wollenberger, J. (Used: 20. february 2012). *The challenges of laser cutting: Overcoming some common obstacles*. Thefabricator. URL: <http://www.thefabricator.com/article/lasercutting/the-challenges-of-laser-cutting-overcoming-some-common-obstacles>.
- Yilbas, B. S. (2004). *Laser cutting quality assessment and thermal efficiency analysis*.

Part I

Appendix

Vision Builder Measurements

A

In this appendix the measurements of the quality parameters and dimensional tolerances is documented.

The pictures that shall be measured in order to obtain the results from the experiments:

1. Profile of cut kerf measuring
 - Dross
 - Melting of Top Edge (MTE)
2. Kerf Widths measuring
3. Circular measuring
 - Diameter of holes
 - Diameter of laser beam spots

The above pictures are used for measuring the quality parameters of the laser cut sheets and dimensional tolerances from the holes in the speaker grill. The vision software; NI Vision Builder, is used for all the measurements. The measurements are made from pictures taken with Leica Acquisition Software (LAS) from a camera attached to a Wild M8 Heerbrugg stereomicroscope or a Leitz Metallovert inverted metallurgical microscope. The opensource drawing program; Inkscape, is used to manipulate the pictures taken.

A.1 Dross and MTE

Dross and MTE are measured from the same picture. The picture is taken with zoom 50 and has a resolution of 3132 x 2325 px. The procedure for measuring dross and MTE is:

1. The workpiece is cut with a saw and molded into transparent epoxy, see figure A.1.
2. The molded workpiece is sanded down to where the area of interest is.
3. Pictures of the molded workpieces are taken with one of the microscopes for each cut profile molded in the same block of epoxy.
4. The pictures are imported into Vision Builder and software is calibrated from the ruler on the pictures. The manipulated circles (MTE) and dross is measured. The dross height and radius of molten edges is written to a .txt file.

Dross and MTE are measured from using one side of the cut kerf. The material of the sheet, including the side of the cut kerf, is molded into epoxy. Four or six cut kerfs are molded into the same block of epoxy, depending on the number of cuts from a single sheet. The cut profile is measured from five different pictures of the cut in the epoxy. To obtain the five different pictures the epoxy blocks are sanded down with a sandpaper, see figure A.1. The sandpaper has gritsize of 220. The amount of scratches and flaws as a consequence of the gritsize is not known, but seen as negligible for dross. For MTE the error is though not negligible. Pictures are taken after each sanding process. The height between each measurement is approximately 0.2mm.

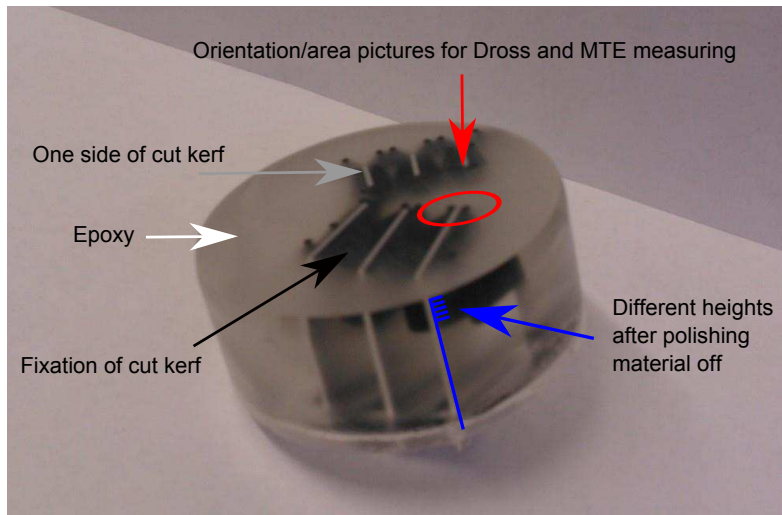
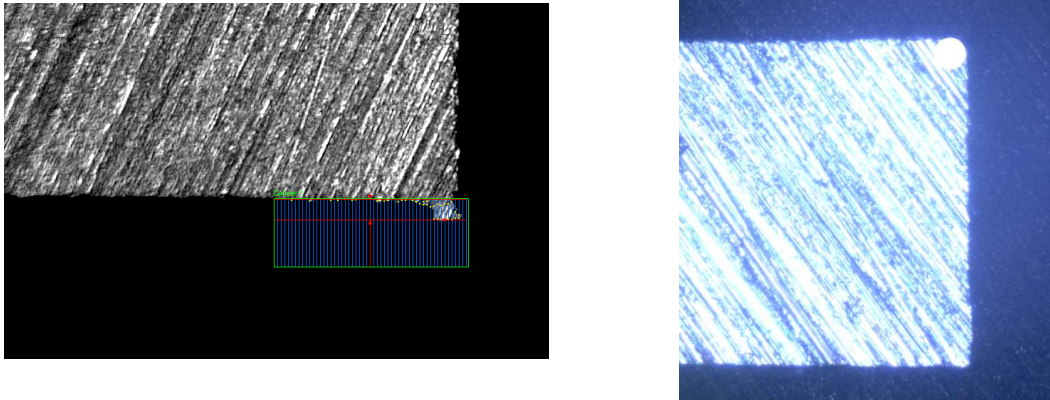


Figure A.1: The sides of the cut kerf molded into epoxy. The different cut kerfs are molded in the block, so they are perpendicular on the plane the pictures are taken from. 5 layers are sanded off.

After obtaining the pictures of the profile, MTE is measured by manipulating the pictures by adding a reference circle to the picture to identify sharp edges and molten edges. The radius of the reference circle corresponds to $35\mu m$. Molten edges are identified from fitting the reference circle to the horizontal and vertical side of the cut. If the top edge is shown, it is given the value S (sharp edge). The others are identified as molten edges. There is drawn a circle in inkscape, which fits the molten edge on the profiles, figure A.2b. This circle is measured with the "find circular edge" tool in Vision Builder, figure A.8a. First a subtraction of colors is made since the "find circular edge" tool is searching for a change in color; from black to white. The edge can thereby be recognized easier by the tool. On the pictures of the holes, the quality parameter, dross is measured using a function called "Caliper", figure A.2a. The caliper tool is moved manually, until the tool recognizes the edges, limiting the dross height.



(a) Measuring dross with the caliper tool

(b) Manipulated profile with circle fitting a molten edge.

Figure A.2: From the profile of the cut both dross and MTE is measured.

A.2 Kerf width

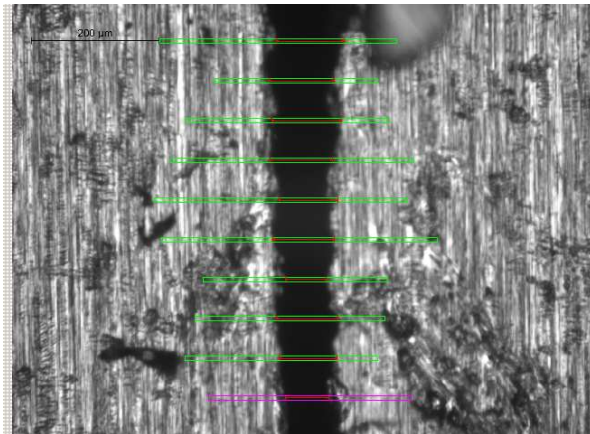
All the pictures of the kerf widths are taken with a zoom 100. The picture resolution is 3132 x 2325 px. The Procedure for measuring the kerf widths is:

- Import picture in NI Vision Builder
- From the first picture, the ratio between pixels and μm is calibrated, by the use of the ruler, see figure A.4. The number of pixels that equals the ruler is specified, by clicking on the starting and ending pixel on the ruler.
- Ten caliper tools are distributed with the same space over the length of the kerf, A.3a.
- Each caliper measurement is evaluated. If the fit is bad, the caliper setting are changed until a reasonable fit is seen, figure A.5, A.6 and A.7.
- This is done for all the available cuts.
- The data from several cuts are written to a .txt file which is used in the further analysis.

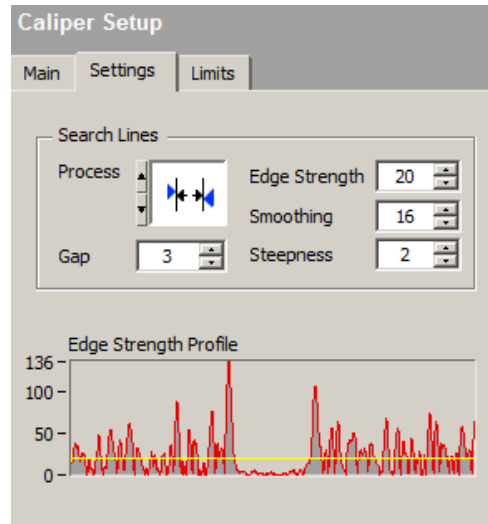
The tool "caliper" locates the edge of the kerf from several points (pixels), figure A.5b. The caliper tool contains a list of settings which influences the distance, the tool measures on the kerf. When locating the distance between two edges, the user specifies the area of interest (green area), figure A.3a.

Five settings of the Caliper tool decides how the tool locates the edges and thereby finds the distance, see figure A.3. The settings are; Gap (between pixels on the edge), Edge strength, Smoothing, Steepness and the chosen height of the area on the kerf width. From changing the setting the tool finds different distances.

In order to take this into consideration the same distance have been measured five times with different settings to find the theoretical error. In table A.1 and A.2 five measurements for the same distance can be seen in respectively bottom and top of the same kerf.



(a) It can be seen how 10 calipers are distributed with the same interval over the whole length of the cut. The height of the picture is 677 μm



(b) The settings of the caliper tool. A histogram of the marked area on the cut kerf is shown in the bottom.

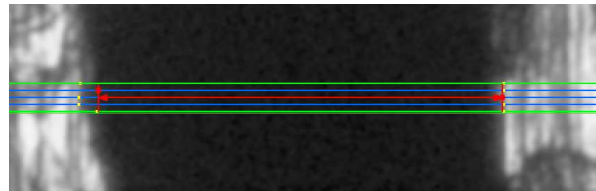
Figure A.3: The use of the caliper tool.



Figure A.4: The ruler from the microscope picture is used to find the pixel μm ratio. The green areas shows the two chosen pixels, which measures the number of pixels used for calculating the ratio. The ruler is 453 pixels.



(a) Exp. 5, bottom. KW = 84.30 μm



(b) Exp. 5, bottom. KW = 85.02 μm

Figure A.5: KW of 84.30 and 85.02 μm measured the same place on the kerf.



(a) Exp. 5, bottom. KW = 85.98 μm



(b) Exp. 5, bottom. KW = 86.81 μm

Figure A.6: KW of 85.98 and 86.81 μm measured the same place on the kerf.



Figure A.7: Exp. 5, bottom. $KW = 87.12 \mu m$.

No.	1	2	3	4	5	Mean	Max. difference
Value	84.30	85.02	85.98	86.81	87.12	85.85	2.82

Table A.1: Five measurements for the same bottom KWs on exp. 5. The settings in the Caliper tool are different for each measurement.

No.	1	2	3	4	5	Mean	Max. difference
Value	159.26	159.97	160.02	161.76	162.35	160.67	3.09

Table A.2: Five measurements for the same distance on exp. 5. The settings in the Caliper tool are different for each measurement.

A.2.1 Error

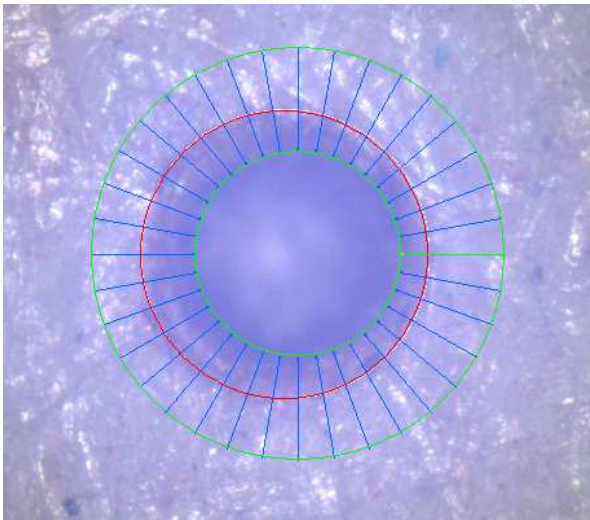
The found mean and max. difference includes a measuring variation ($3 \mu m$) from table A.1 and A.2. The caliper tool recognizes the edges clearly, as seen in the histogram on figure A.3. An error occurs from when different settings of the caliper recognizes different points on the edges, see figure A.5a. The error is approximately $\pm 1.5 \mu m$

The error from the pixel to μm scala is very little. It depends on how well the scala from the Leica software is calibrated, and if the user of Vision Builder clicks on the correct pixel. It is estimated that this error is very little, because the pixels are chosen carefully. $1 \mu m$ equals 2.265 pixels. By choosing 452 instead of 453 px to equal $200 \mu m$ error on 0.2 % occurs.

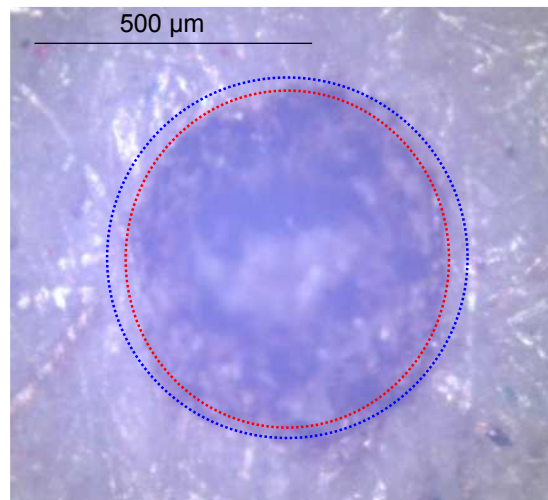
A.3 Holes and beam spot diameter

After obtaining the pictures of the beam spots/holes, the pictures are further manipulated in the drawing program Inkscape to be able to measure the tolerance parameters and beam spots. The manipulation regards drawing a circle, which fits onto the respective diameter, which is to be measured. After the pictures are manipulated in Inkscape they are loaded into the NI Vision Builder software. In the NI Vision Builder software the drawn diameters are measured using a "Find Circular Edge" function. On figure A.8a it can be seen, that the edge from the spot, made with the Nd:YAG laser is unclearly defined. Therefore a white circle has been laid on top of the picture using Inkscape.

The error in measuring beam spots are primarily caused by the beam spots not being round. The magnitude is not known, but expected to be significant. The errors in measuring the hole diameters is estimated to be very small. NI Vision Builder, fits the circle through a set of points. As a consequence of this an error on approximately $0.5 \mu m$ in standard deviation is given from the program.



(a) Finde circular edge tool



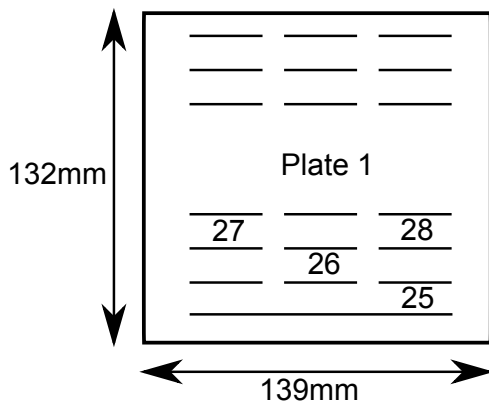
(b) Large error in location the diameter of the spot, due to unclear definition of the spot diameter limits. Different circles can be fitted to the spot circumference.

Figure A.8: Beam spot measurements.

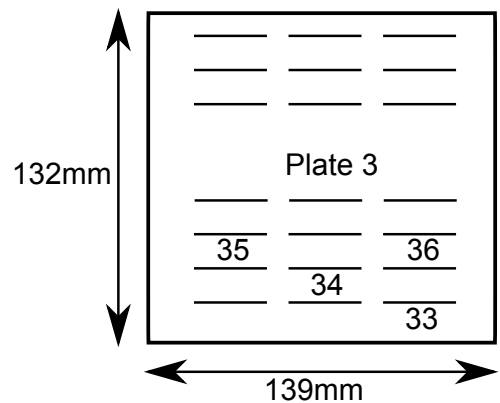
Laser cut sheets **B**

In this appendix figures showing the cuts made in each aluminium sheet and the cuts used in the report are presented.

B.1 Aluminium sheets used in section 9.1

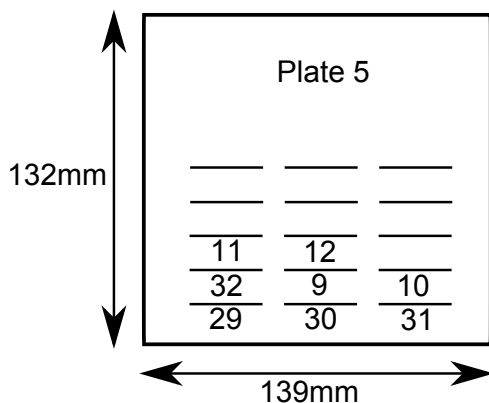


(a) The cuts made in plate 1 indicated by black lines, those used in the report are indicated by a number referring to the experiment ID used in the thesis.

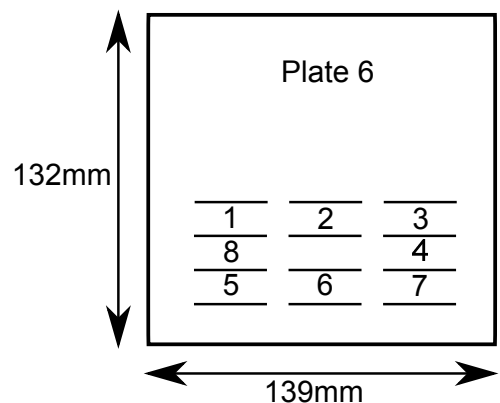


(b) The cuts made in plate 3 indicated by black lines, those used in the report are indicated by a number referring to the experiment ID used in the thesis.

Figure B.1: Cuts/experiments in plate 1 and 3.

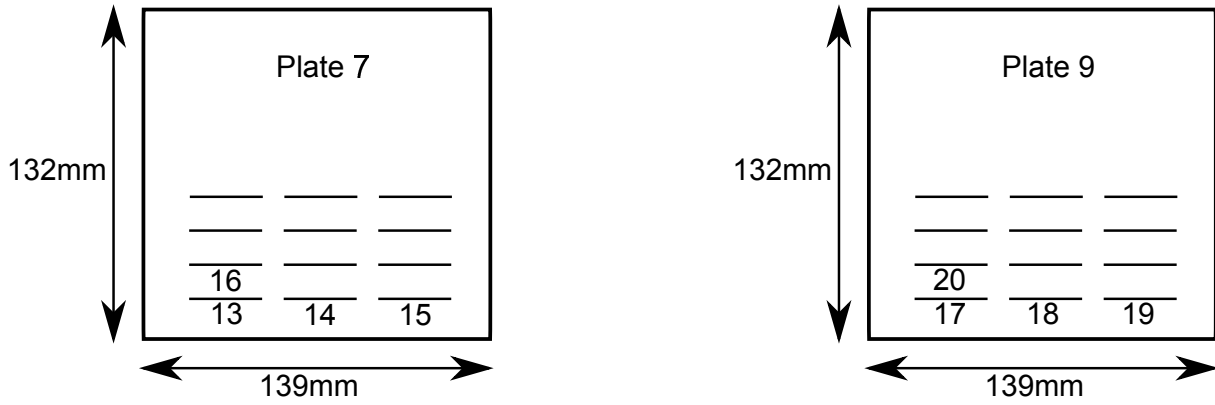


(a) The cuts made in plate 5 indicated by black lines, those used in the report are indicated by a number referring to the experiment ID used in the thesis.



(b) The cuts made in plate 6 indicated by black lines, those used in the report are indicated by a number referring to the experiment ID used in the thesis.

Figure B.2: Cuts/experiments in plate 5 and 6.



(a) The cuts made in plate 7 indicated by black lines, those used in the report are indicated by a number referring to the experiment ID used in the thesis.

(b) The cuts made in plate 9 indicated by black lines, those used in the report are indicated by a number referring to the experiment ID used in the thesis.

Figure B.3: Cuts/experiments in plate 7 and 9.

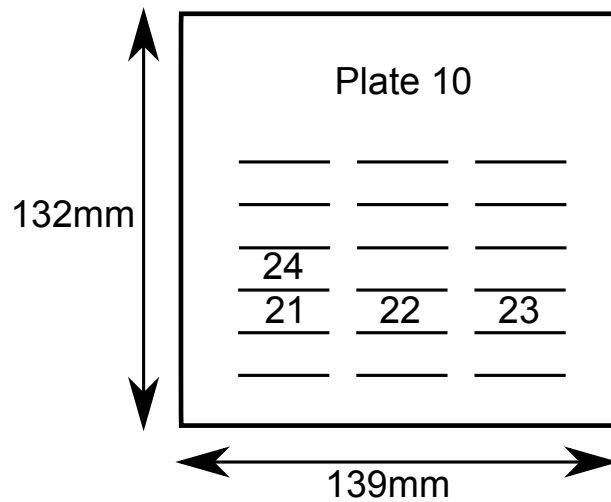


Figure B.4: The cuts made in plate 10 indicated by black lines, those used in the report are indicated by a number referring to the experiment ID used in the thesis.

Analysis of variance

C

In this appenfix the theory of analysis of variance is described. This appendix is inspired by (Montgomery, 2005a)

The purpose of using ANOVA is to determin if the influence from the control variables are significant on the KW. A two-way ANOVA is used for factorial experiments. Through ANOVA the mean KW of the cuts are compared. By doing this it can be determined if there is a significant difference in their respective means as an effect from the control variables or workpiece parameters. To do this it is necessary to define a hypothesis which can be tested. Six hypothesis' are formulated, H_0 and H_1 , see equation C.1, C.2 and C.3. Six hypothesis' are formulated because it is desired to test two control variables and one interaction between them. H_0 is the null hypothesis and H_1 the alternative hypothesis. It is not possible prove the null hypothesis but only to reject or not reject it. The stronger argument is therefore to reject the null hypothesis and thereby prove the alternative hypothesis, than to not reject the null hypothesis.

$$\begin{aligned} H_0 : \tau_1 = \tau_2 = \dots = \tau_i = 0 \\ H_1 : \text{at least one } \tau_i \neq 0 \end{aligned} \quad (C.1)$$

$$\begin{aligned} H_0 : \beta_1 = \beta_2 = \dots = \beta_j = 0 \\ H_1 : \text{at least one } \beta_j \neq 0 \end{aligned} \quad (C.2)$$

$$\begin{aligned} H_0 : (\tau\beta)_{ij} = 0 \text{ for all } i, j \\ H_1 : \text{at least one } (\tau\beta)_{ij} \neq 0 \end{aligned} \quad (C.3)$$

For analysis of variance it is assumed, that the variance between the means is due to variance within a group or between groups. In this ANOVA each group is 10 measurements of the KW for a single cut. Through ANOVA it can thereby be analyzed if the variance is due to:

- Variance between the groups, caused by the control variables or random errors.
- Variance within each group, only caused by random errors.

An effect model is used, which is defined in equation C.4. μ is the overall mean, τ_i is the effect of the i th level of control variabel A, β_j is the effect of the j th level of control variable B, $(\tau\beta)_{ij}$ is the effect of interaction between τ_i and β_j , and ε_{ijk} is a random error. (Montgomery, 2005a).

$$y_{ijk} = \mu + \tau_i + \beta_j + (\tau\beta)_{ij} + \varepsilon_{ijk} \begin{cases} i = 1, 2, \dots, a \\ j = 1, 2, \dots, b \\ k = 1, 2, \dots, n \end{cases} \quad (C.4)$$

In table C.1 a general arrangement for a two-way ANOVA is shown. y_{ijk} is the observed response when control variabel A is at the i th level where $i=1,2,\dots,1$.

		Control variable B				
		1	2	...	b	$y_{i..}$
Control Variable A	1	$y_{111}, y_{112}, \dots, y_{11n}$	$y_{121}, y_{122}, \dots, y_{12n}$		$y_{1b1}, y_{1b2}, \dots, y_{1bn}$	
	2	$y_{211}, y_{212}, \dots, y_{21n}$	$y_{221}, y_{222}, \dots, y_{22n}$		$y_{2b1}, y_{2b2}, \dots, y_{2bn}$	
	⋮					
	a	$y_{a11}, y_{a12}, \dots, y_{a1n}$	$y_{a21}, y_{a22}, \dots, y_{a2n}$		$y_{ab1}, y_{ab2}, \dots, y_{abn}$	
	$y_{.j.}$					$y_{...}$

Table C.1: General arrangement for two-way analysis of variance

In table C.1 and the effect model the following definition applies:

- $y_{i..}$ denote the total of all observations under the i th level of factor A.
- $y_{.j.}$ denote the total of all observations under the j th level of factor B.
- $y_{ij.}$ denote the total of all observations in the ij th cell.
- $y_{...}$ denote the the grand total of all the observations.

The results from ANOVA is set up as in table C.2.

Source O.V.	SS	DoF	MS	F_0	Contribution
A treatments	SS_A	a-1	$MS_A = \frac{SS_A}{(a-1)}$	$F_0 = \frac{MS_A}{MS_E}$	% = $\frac{SS_A}{SS_T}$
B treatments	SS_B	b-1	$MS_B = \frac{SS_B}{(b-1)}$	$F_0 = \frac{MS_B}{MS_E}$	% = $\frac{SS_B}{SS_T}$
Interaction	SS_{AB}	(a-1)(b-1)	$MS_{AB} = \frac{SS_{AB}}{(a-1)(b-1)}$	$F_0 = \frac{MS_{AB}}{MS_E}$	% = $\frac{SS_{AB}}{SS_T}$
Error	SS_E	ab(n-1)	$MS_E = \frac{SS_E}{(ab(n-1))}$		
Total	SS_T	abn-1			

Table C.2: Two-way analysis of variance

SS_T , SS_A and SS_B is found in equation C.5, C.6 and C.7.

$$SS_T = \sum_{i=1}^a \sum_{j=1}^b \sum_{k=1}^n y_{ijk}^2 - \frac{y_{...}^2}{abn} \tag{C.5}$$

$$SS_A = \frac{1}{bn} \sum_{i=1}^a y_{i..}^2 - \frac{y_{...}^2}{abn} \tag{C.6}$$

$$SS_B = \frac{1}{an} \sum_{j=1}^b y_{.j.}^2 - \frac{y_{...}^2}{abn} \tag{C.7}$$

SS_{AB} is found by the use of $SS_{subtotals}$, equation C.8, and found in equation C.9.

$$SS_{subtotals} = \frac{1}{n} \sum_{i=1}^a \sum_{j=1}^b y_{ij.}^2 - \frac{y_{...}^2}{abn} \tag{C.8}$$

$$SS_{AB} = SS_T - SS_{subtotals} - SS_A - SS_B \tag{C.9}$$

The sum of squares errors is found in equation C.10

$$SS_E = SS_T - SS_{subtotals} \quad (C.10)$$

Percentage contribution is found in equation C.11.

$$\begin{aligned} Contribution_A &= \frac{SS_A}{SS_E} \\ Contribution_B &= \frac{SS_B}{SS_E} \\ Contribution_{AB} &= \frac{SS_{AB}}{SS_E} \end{aligned} \quad (C.11)$$

The main assumption when using ANOVA is that the errors ε_{ijk} follows a normal propability distribution. Whith this assumption the relationship F_0 in table C.2 follows a one-sided F distribution with the degrees of freedom, a-1, b-a, (a-1)(b-a) and ab(n-1). The critical region is the upper tail of the F distribution, see figure C.1.

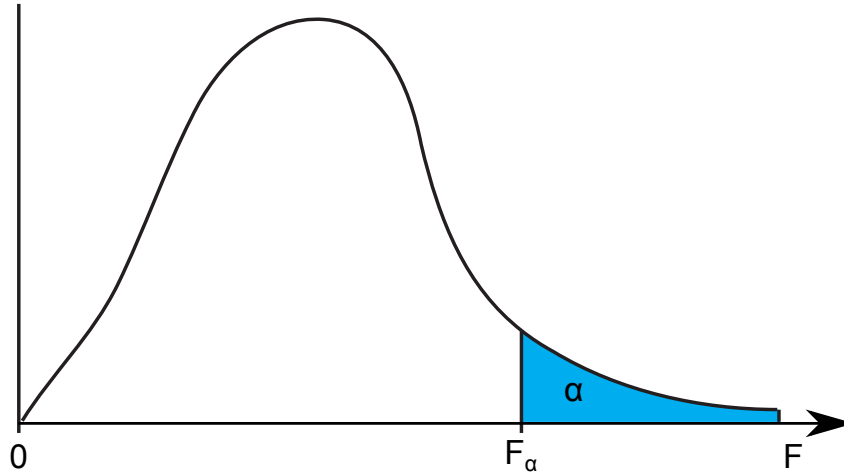


Figure C.1: One-sided F-test. (Johnston, 2012)

$$\begin{aligned} F_{0A} &> F_{\alpha, a-1, ab(n-1)} \\ F_{0B} &> F_{\alpha, b-1, ab(n-1)} \\ F_{0AB} &> F_{\alpha, (a-1)(b-1), ab(n-1)} \end{aligned} \quad (C.12)$$

The level of significance is chosen to be $\alpha = 0.01$. The lower the level of significance, the more the data must diverge from the null hypothesis in order to reject it. More common is an α value on 0.05, which makes 0.01 a more coservative choice (Montgomery, 2005b). This is chosen because it is known, that the measured KW has a rather large variance. F_0 is evaluated as seen in equation C.12. If the calculated F_0 value for a control variable is larger than the F_α value, the H_0 hypothesis can be rejected, which means, that the control variable has a significant influence on the means.

The F-value is not available in tables in literature, but is found from (Johnston, 2012).

C.1 Residual analysis

A residual analysis is made in order to check the adequacy of the models, see equation C.13. It can be seen, that the resisuals follows a normal probability distubruton. Because the residuals fit the tendency

line very close, the models are good.

$$\varepsilon_{ijk} = y_{ijk} - \hat{y}_{ijk} \tag{C.13}$$

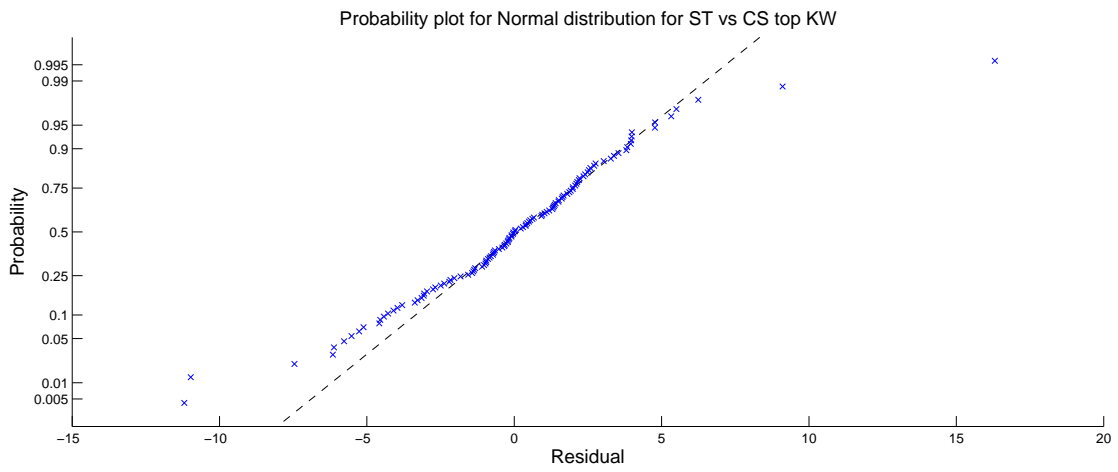


Figure C.2: Normal probability plot of the residuals from the ST vs CS top ANOVA

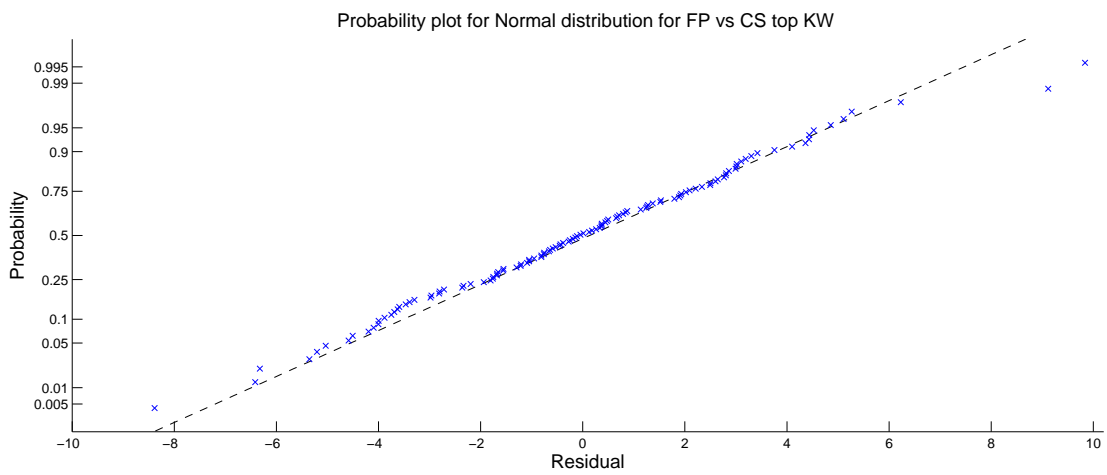


Figure C.3: Normal probability plot of the residuals from the FP vs CS top ANOVA

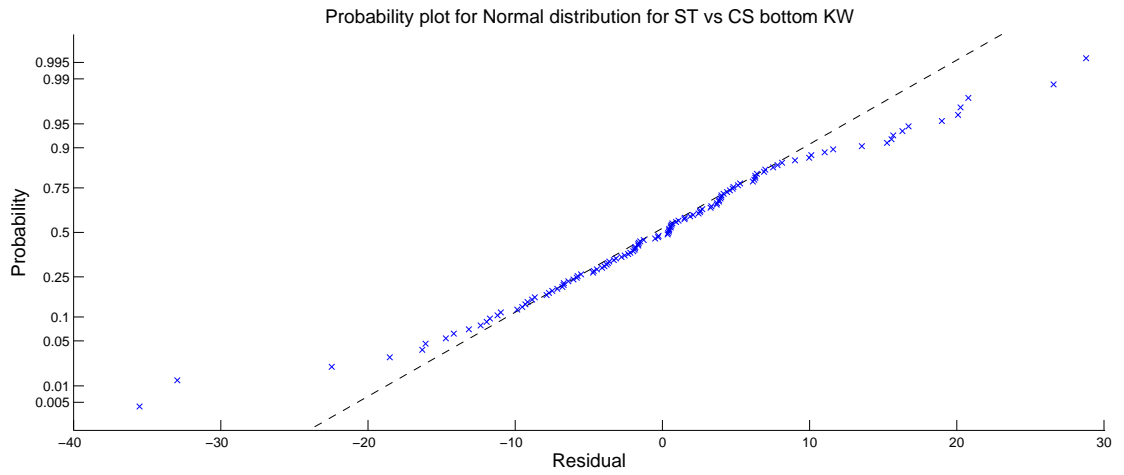


Figure C.4: Normal probability plot of the residuals from the ST vs CS bottom ANOVA

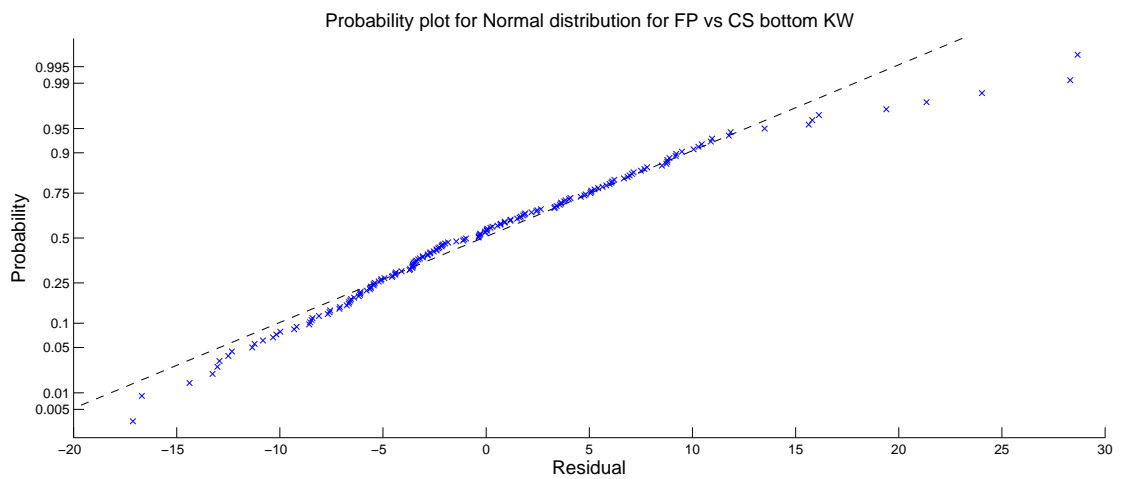


Figure C.5: Normal probability plot of the residuals from the FP vs CS bottom ANOVA

Dansk resumé

Dette kandidatspeciale er lavet i samarbejde med den danske produktionsvirksomhed B&O.

Igennem rapporten bliver det undersøgt i hvilket omfang laser skæring kan erstatte en eksisterende proces brugt i forbindelse med at lave huller i en højttaler grill til biler, produceret i aluminium. Da B&O er en virksomhed som sætter kvalitet højt i forbindelse med deres produkter opstilles krav ud fra en højttaler grill i forbindelse med at skære huller med laser. I kravene indgår kvalitetsparametrene; slagger, smeltning af toppen af skærefladen, den varmepåvirkede zone (som i denne tese er defineret som farveændring i emnet hvori der arbejdes), snitfuge vidde, snitfuge vinkel og rundhed af huller.

Ud fra eksperimenter udført med en 380 W Nd:YAG laser konkluderes det at intensiteten i strålens fokus område er afgørende for at kunne skære i aluminium.

En 400 W single mode fiber laser bruges i forbindelse med at udføre 36 laser skærings forsøg i aluminiumsplader med 0,5, 0,7 og 1,0mm pladetykkelse. Ud fra resultater baseret på de 36 forsøg konkluderes det, at det er muligt, at opnå den ønskede skærekvalitet, som er defineret ud fra kvalitetsparametre.

Det konkluderes at effekten af ændring af kontrolvariablene; fokuspunkt og skæreshastighed har en signifikant indflydelse på kvalitetsparametrene snitfuge bredde og snitfuge vinkel. Der observeres indikationer på at pladetykkelsen og stand-off distancen har indflydelse på resultaterne af forsøgene. Der analyseres ikke videre på disse indikationer på grund af tidsmangel og utilstrækkelig information fra forsøgene. Det er yderligere kompliceret, at konkludere på, hvad der har indflydelse på kvalitetsparametrene slagger og smeltning af toppen af skærefladen. Årsagen til dette er, at det anvendte interval for indstillingerne for forsøgene er for lille. Til gengæld kan det konkluderes at der ikke opstår farveændring i aluminiums emnerne som følge af laser skæringsprocessen.

Det konkluderes at lasere af typen single mode fiber laser har et stort potentiale i forhold til at skære aluminiums emner i høj kvalitet. Dette grunder i dens meget lille strålediameter og kvalitet M^2 . Trods dette kan konklusionerne på resultaterne ikke direkte overføres til B&O's højttaler grill. Dette skyldes bl.a. at de opnåede resultater er påvirket af støj og at der er anvendt for få pladetykkelser til at kunne forudsige om kvalitetsparametrene vil kunne overholdes i 2mm aluminiumsplader. Det vurderes derfor at der skal laves flere forsøg for at kunne svare på dette.

Baseret på de konklusioner og den know-how som er opnået i dette speciale/projekt opstilles anbefalinger til B&O angående det som man skal være opmærksom på i forbindelse med kvaliteten af laserskårte emner.